Università di Pisa

Facoltà di Scienze Matematiche, Fisiche e Naturali

Laurea Magistrale in Biologia Applicata alla Biomedicina

Curriculum Fisiopatologico

Protein Bex1 and Liver Regeneration after Tissue Damage

Relatore:

Prof. Aldo Paolicchi

Relatore esterno:

Prof.ssa Hanne Cathrine Bisgaard

Candidato:

Andrea Giannuzzo

Anno Accademico 2010 - 2011

Index

ABSTRACT

I did my internship for my Master's degree thesis at the Panum Institute, University of Copenhagen, Faculty of Health Sciences, Department of Cellular and Molecular Medicine, after winning an Erasmus Placement scholarship.

Recent studies suggest the involvement of the BEX genes in cancer biology; for example Bex1 (Brain Expressed, X-Linked) is overexpressed in neuroendocrine tumors and is downregulated in glioblastoma cells compared to normal tissue. Genome-wide analysis of epigenetic silencing identifies BEX1 and BEX2 as candidate tumor suppressor genes in malignant glioma. Moreover Bex1 is over-expressed as a result of peripheral axonal damage and some studies also show an altered skeletal muscle regeneration in Bex1 knock out mice; therefore Bex1 could be considered as regeneration-associated gene. It is an adapter molecule involved in p75NTR/NGFR signaling and plays a role in cell cycle progression and neuronal differentiation.

Many aspects of Bex1 are unknown so it is a an exciting field of research. Bex1 is expressed in central nervous system, lung, skeletal muscle, peripheral blood leukocytes, stomach, lymph node, trachea, bone marrow; highly expressed in pituitary, cerebellum, temporal lobe. Our attention was placed on the expression of Bex1 in normal and pathological liver tissues. Our study was focused on defining the mechanism by which Bex1 might regulate proliferation and differentiation of hepatic progenitor cells into the hepatic or cholangiocytic lineages during regeneration after tissue damage and in development of liver cancer.

I used different methods in this project: Real Time-PCR, Immunohistochemistry, immunofluorescence and confocal microscopy, culturing of human hepatocellular carcinoma cell lines, Knock-Down in Huh7 cell line using Dharmacon® Accell® siRNA with subsequent protein harvest, Bradford assay and Western Blot.

The results of Real Time PCR show that there is an up regulation of Bex1 during liver regeneration after all liver diseases compared to donor liver. The immunolocalization in hepatic tissue shows a presence of Bex1 mostly in the bile duct and also in reactive ductular cells (RDCs) and hepatic progenitor cells (HPC).

The knock down of Bex1 in Huh7 cell line shows a doubtful result, because we cobserved a reduction of our protein compared to control, but we expected Bex1 at ~ 23kDa, while we found it at ~ 62kDa. There are maybe three explanations: or the antibody recognizes an isoform of Bex in the cell line, or the protein have not been reduced sufficiently, or modifications of the protein are involved.

For the future my aim is to examine the function of Bex1 as tumor suppressor in hepatocellular carcinoma and the role in signaling pathways regulating apoptosis. This whould likely allow a better understanding of the role that Bex1 plays in liver regeneration.

1 INTRODUCTION

1.1 Brain Expressed X - Linked Gene Family

Bex proteins are expressed from a family of "brain expressed X-linked genes" that are closely linked on the X-chromosome.

The most commonly identified genes in these screens were members of the Bex (Brain expressed X-linked) gene family, rat Bex1 (Rex3), and a novel gene, rat Bex4. After identifying these genes, we then sought to characterize the Bex gene family. Two additional novel Bex genes (human Bex5 and mouse Bex6) were discovered through genomic databases. Bex5 is present in humans and monkeys, but not rodents, while Bex6 exists in mice, but not humans. Bex4 and Bex5 are localized to the X chromosome, are expressed in brain, and are similar in sequence. Bex4 and Bex5 are 54% and 56% identical to human Bex3 (pHGR74, NADE). Mouse Bex6 is on chromosome 16 and is 67% identical to mouse Bex4.

In particular, Bex1 is also known as Rex3, Bex3 is also known as NADE / NGFRAP1 / HGR74, Bex4 is also known as BexL1, and Bex5 is also known as NGFRAP1L1. Ensembl divided the five human Bex genes into two gene families, with Bex1, Bex2, and Bex5 in one family, and Bex3 and Bex4 in the other.
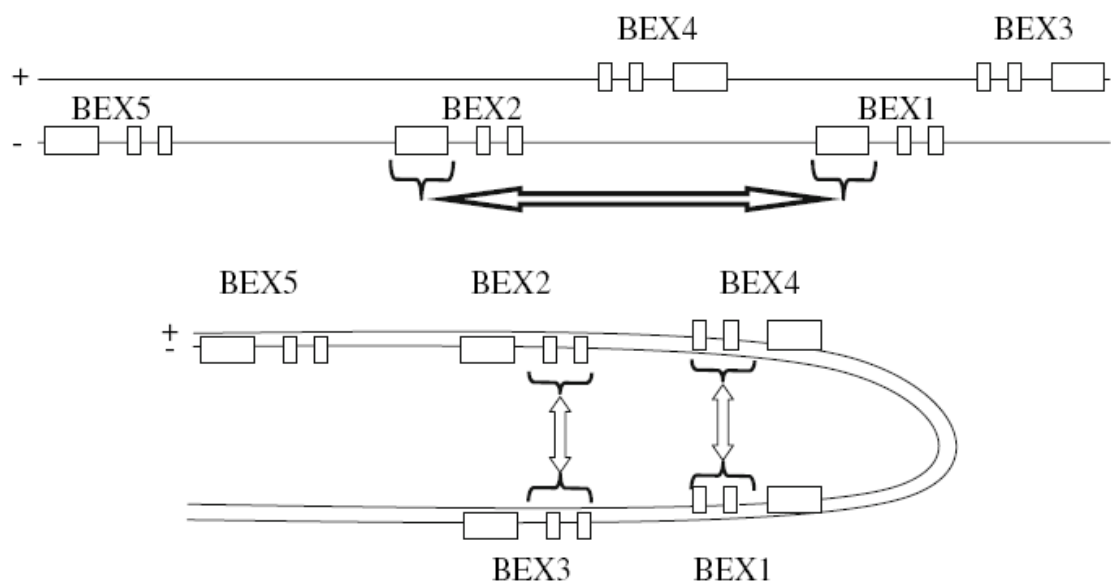
Fig.1 *(Top) The exon–intron gene structure and the chromosomal arrangement of the Bex genes on chromosome X in human. (Bottom) The model of gene conversion explaining the pattern of sequence evolution in Bex. The brackets indicate the portions of Bex involved in gene conversion, and the arrows connect the Bex members involved in gene conversion.*
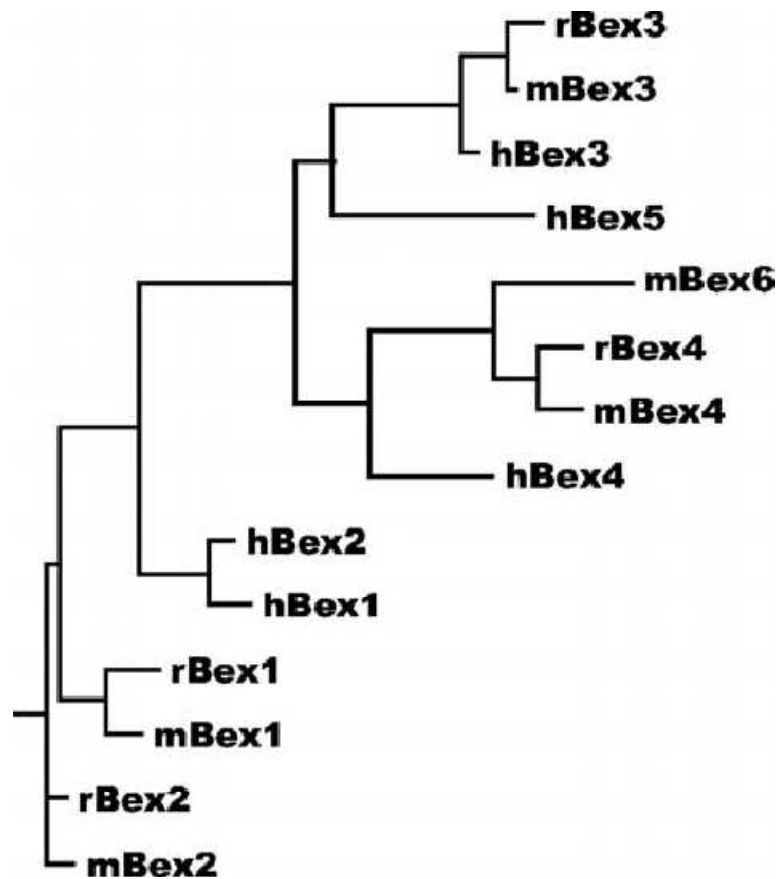
Fig.2 *Phylogenetic tree of the human (h), rat (r), and mouse (m) Bex genes.*

1.2 Discovery and Localization

Functional assays have shown that BEX1 and BEX2 bind and interact with OMP (olfactory marker protein), and the interaction region likely covers amino acid positions 50–75, within which BEX1 and BEX2 show more than 92% identity. Conversely, the corresponding region in BEX3 shows less than 30% identity to BEX1 and BEX2, and therefore BEX3–OMP interaction is unlikely. BEX3 serves as a signaling adapter molecule and interacts with p75NTR to lead to programmed cell death in the presence of NGF (nerve growth factor). BEX1 recently has also been shown to interact with p75NTR and act as a molecular adapter linking neurotrophin signaling to the cell cycle. No functional roles have been assigned to the other members of the Bex family. The candidate sites for positive selection (sites 75, 81, 93, and 110) are mostly located in the tail region of the Bex genes, accounting for one-third of the entire gene. This region corresponds to the regulatory region in BEX3 (site 72–112) that is essential for NGF-dependent

regulation of BEX3-induced apoptosis, suggesting that positive selection has acted on Bex3 after gene duplication and there might have been evolution of a new gene function. As BEX1 can also bind to p75NTR but has not been found to play a role in apoptosis, it is clear that a more detailed functional comparison between BEX1 and BEX3 is needed for a better determination of the specific functional divergence between the two genes.

The BEX members show variation in their subcellular localization. BEX3 is found mainly in cytoplasm and has a nuclear export signal region (amino acid 90–100) that is essential for its export from the nucleus to the cytoplasm. BEX1 however, is found predominantly in the nucleus, and BEX2 and BEX4 can be found in cytoplasm but through passive diffusion. A recent study showed that BEX1 can be found both in nucleus and cytoplasm, and its distribution from the nucleus to the cytoplasm can be
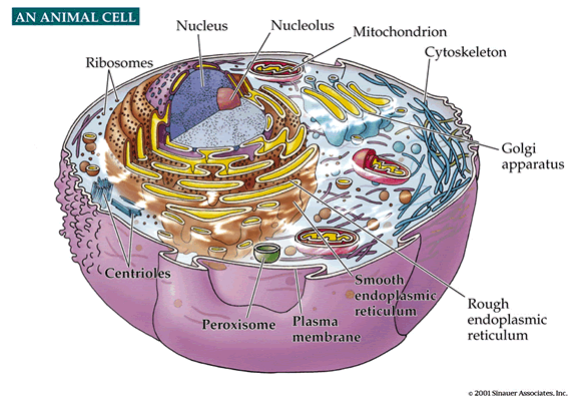
Fig.3 *Eukaryotic Cell*

regulated by NGF. BEX5, similar to BEX3, is found predominantly in cytoplasm, and its nuclear export signal region shows 50% identity to BEX3. Therefore, the phylogenetic relationship of these family members seems to reflect weakly the differentiation or similarity in subcellular localization of these members.

The BEX members show great variation in their expression pattern. Human BEX1 and BEX2 show similar expression patterns within the central nervous system but differ in other tissues, with BEX1 highly expressed in peripheral tissues and BEX2 highly expressed in brain, pancreas, testis, and ovary, and expressed at a low level in other peripheral tissues. BEX3 is widely expressed, with the highest level of expression in liver. BEX4 has a remarkably high expression level in heart, skeletal muscle, liver and kidney. BEX5, similar to BEX3, is also widely expressed, with the highest levels in liver. Compared with the other Bex genes, Bex5 generally tends to be present at lower levels. The duplication–degeneration– complementation model suggests that degeneration of regulatory regions of duplicated genes may actually help to preserve functional copies after gene duplication; the great variation in the expression patterns of these Bex genes

appears to be consistent with this increasingly supported model, which explains why many duplicated genes in the genome remain functional after duplication.

Human Bex gene expression was studied with tissue expression arrays probed with specific oligonucleotides. Human Bex1 and Bex2 have similar expression patterns in the central nervous system with high levels in pituitary, cerebellum, and temporal lobe, and Bex1 is widely expressed outside of the central nervous system with high expression in the liver. Human Bex4 is highly expressed in heart, skeletal muscle, and liver, while Bex3 and Bex5 are more widely expressed. Rat Bex3, rat Bex4, human Bex5, and mouse Bex6 are degraded by the proteasome, while rat Bex1 or Bex2 are not. Rat Bex3 protein can likely bind transition metals through a histidine-rich domain. The Bex gene family members are highly homologous but differ in their expression patterns, subcellular localization, and degradation by the proteasome.

The gene structures are well conserved across family members and among the mammals in that all five members have three exons with the first two exons untranslated. Furthermore, the five members are arranged tandemly on chromosome X with Bex5, Bex1, Bex2 on the negative strand and Bex4, Bex3 on the positive strand, and this physical arrangement remains conserved among species. Sequence analyses indicate that gene conversion has been frequent and ongoing among Bex1-4, occurring in multiple species independently. All gene conversions in different species between Bex1 and Bex4, and between Bex2 and Bex3, appear to be limited to the upstream regions of the third exon, whereas the gene conversions occurred independently in different species between Bex1 and Bex2 and cover only the third exon. Bex5 appears to have little exchange of genetic information with other members, possibly due to its distance from other members. The GC content decreases from 5'-UTR, intron 1, intron 2, coding region, to 3'-UTR, reflecting faithfully the frequency of gene conversion in different regions of the Bex genes. Sequence analyses also suggest that both relaxed selective constraint and positive selection have acted on the Bex members after duplication. In particular, Bex3 shows strong evidence of positive selection and seems to have evolved a new gene function after gene duplication.

To identify additional genes important in dopamine neuron differentiation, a laboratory performed subtractive hybridization screens on the developing ventral

mesencephalon (rat embryonic day 10) compared with dorsal mesencephalon and spinal cord. Of the 480 expressed sequence tag (EST) clones analyzed, the most commonly identified genes, comprising 12% of the ESTs, were members of the Bex (Brain-Expressed X-linked) gene family. The initial description of the Bex genes included three mouse genes sharing high sequence similarity, localization on the X chromosome, and high expression levels in the brain. One of the homologues that was identified was Bex1 (also named Rex3), which was first identified as a gene whose expression decreased after retinoic acid treatment of a mouse teratocarcinoma cell line.

The examination of the chromosomal localization of the Bex genes and their expression in a wide range of human tissues showed that all of the Bex genes are translated, and that their protein products have differences in subcellular localization and degradation.

There was the development and characterization of an antibody to mouse Bex1 protein that cross-reacts with Bex2 (but not Bex3), and its use to determine the cellular distribution of Bex proteins in the murine brain. The specificity of the antiserum was characterized by immunoprecipitation and Western blots of tissue and transfected cell extracts and by immunocytochemical analyses of cells transfected with either Bex1 or Bex2. Antibodies preabsorbed with Bex2 still recognize Bex1, while blocking with Bex1 eliminates all immunoreactivity to both Bex1 and Bex2. Bex immunoreactivity (ir) was primarily localized to neuronal cells within several regions of the brain, including the olfactory epithelium, bulb, peri/paraventricular nuclei, suprachiasmatic nucleus, arcuate nucleus, median eminence, lateral hypothalamic area, thalamus, hippocampus, and cerebellum. RT-PCR and in situ hybridization demonstrated the presence of Bex mRNA in several of these regions.

Fig.4 *Olfactory marker protein*

Double-label immunocytochemistry indicates that Bex-ir is colocalized with OMP in mature olfactory receptor neurons (ORNs) and in the OMP-positive subpopulation of neurons in hypothalamus.
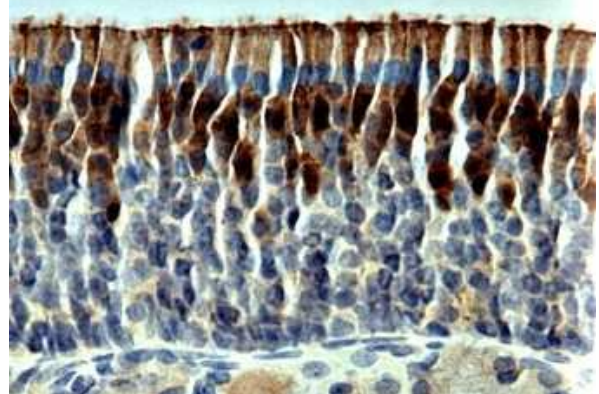
On the basis of the presently characterized distribution of Bex protein in the adult mouse brain, it is tempting to postulate that Bex proteins may participate in the control and integration of various aspects of feeding and regulation of body weight. This independent confirmation of Bex expression in rodent hypothalamus is consistent with the potential involvement of Bex in aspects of feeding or nutrition. Feeding behavior is very complicated and is regulated by several somatomotor and autonomic events in terms of searching for, selecting, eating, and digesting food. This process involves various forebrain circuits related to integration of olfactory and visual information, as well as many brainstem centers that regulate the behaviors of mastication and digestion in many of which we have observed Bex expression.

1.3 Bex1 and p75NTR
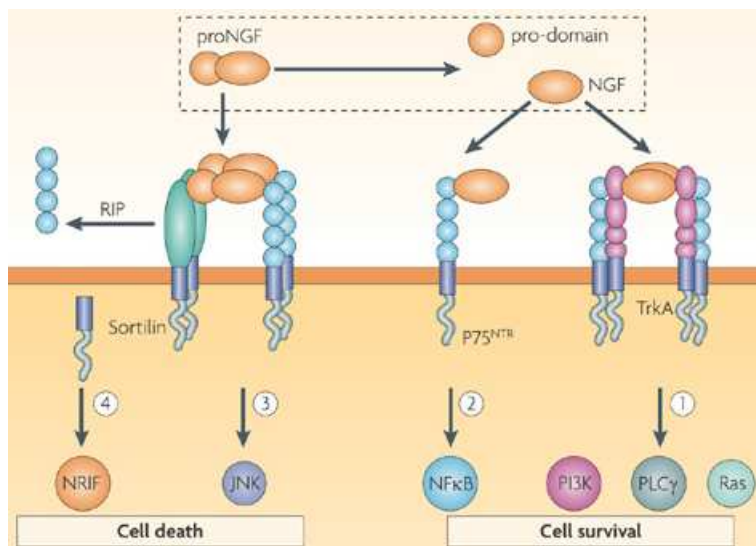
Fig.5 Binding of nerve growth factor

A screening for intracellular interactors of the p75 neurotrophin receptor (p75NTR) identified brain-expressed X-linked 1 (Bex1), a small adaptor-like protein of unknown function. Bex1 levels oscillated during the cell cycle, and preventing the normal cycling and downregulation of Bex1 in PC12 cells sustained cell proliferation under conditions of growth arrest, and inhibited neuronal differentiation in response to nerve growth factor (NGF). In PC12 cells, Bex1 overexpression inhibited the induction of NF-kB activity by NGF without affecting activation of Erk1/2 and AKT, while Bex1 knockdown accelerated neuronal differentiation and potentiated NF-kB activity in response to NGF. Bex1 competed with RIP2 for binding to the p75NTR intracellular domain, and elevating RIP2 levels restored the ability of cells overexpressing Bex1 to differenziate in response to NGF. Together, these data establish Bex1 as a novel link between neurotrophin signaling, the cell cycle, and

neuronal differentiation, and suggest that Bex1 may function by coordinating internal cellular states with the ability of cells to respond to external signals.

Nerve growth factor (NGF) and other members of the neurotrophin family mediate survival, growth and differentiation of neuronal and glial cells by binding to two different types of cell surface receptors, the Trk tyrosine kinases—TrkA, TrkB and TrkC—and the p75 neurotrophin receptor (p75NTR). p75NTR resembles other members of the tumor necrosis factor receptor superfamily in the organization of its extracellular domain and in the presence of a small globular domain in the intracellular region, the so-called death domain. p75NTR signaling can contribute to neurotrophin- mediated survival, differentiation and neurite outgrowth in a variety of neuronal subpopulations. On the other hand, p75NTR can also mediate cell death by neurotrophins, proneurotrophins and various amyloid peptides, as well as inhibit axonal growth and regeneration in its capacity of signaling receptor for myelininhibitory components.

Trk receptors transmit intracellular signals through several of the canonical pathways activated by other receptor tyrosine kinases, including the Ras/MAP kinase and phosphatidylinositol- 3 kinase. In contrast, the signaling mechanisms used by p75NTR have remained elusive. Lacking intrinsic catalytic activity, p75NTR signaling is dependent on the ability of this receptor to interact with components of intracellular signaling pathways. Several different p75NTR interacting molecules, with and without catalytic activity, have been identified to date. Noncatalytic interactors include a series of scaffoldingand adaptor-like molecules, such as caveolin-1, Bex3/NADE and TRAF6; larger proteins containing zinc-finger domains with some degree of nuclear localization, such as NRIF1/2 and SC-1; and members of the MAGE homology domain family, such as NRAGE and necdin, with proposed roles in the regulation of apoptosis. p75NTR interactors with catalytic activity include serine–threonine kinases involved in interleukin and NF-kB signaling, such as IRAK and RIP2; a protein tyrosine phosphatase (FAP-1); and the small GTPase RhoA. How these p75NTR- interacting proteins connect to downstream signaling pathways and cellular responses is less clear, however.

A C-terminal fragment of the rat ortholog of a human protein originally named Bex1 was isolated in a T7 phage display screen for interacting partners of the intracellular domain of p75NTR. Bex1 and Bex2 are very similar in protein

sequence (87% identity), while Bex3/ NADE—a previously characterized interactor of the p75NTR death domain—is only 30% identical to either Bex1 or Bex2 and thus represents a more divergent member of this family. Despite their low similarity, the main region in Bex3/NADE implicated in its interaction with p75NTR was included in the Bex1 cDNA fragment isolated by phage display, suggesting the existence of a conserved p75NTR-binding interface among Bex proteins.

Expression of Bex1, Bex2 and Bex3 mRNAs could be detected by RT–PCR in PC12 cells and primary cultures of embryonic day (E) 14.5 rat dorsal root ganglion (DRG) cells. Only Bex1 and Bex3 mRNAs could be found in Schwann cells isolated from the newborn rat sciatic nerve and in E17.5 hippocampal cultures. mRNAs encoding all three Bex isoforms could also be detected in newborn (P1) cerebral cortex, hippocampus and olfactory bulb. Bex1 mRNA expression could be localized more precisely by in situ hybridization within specific regions of the developing rat embryo. At E13.5, Bex1 mRNA was widely expressed throughout the developing nervous system and in vascular and mesenchymal structures. In particular, prominent Bex1 mRNA expression could be observed in the somitic mesenchyme, heart, aorta, dorsal root ganglia, sympathetic ganglia and the lateral motor columns of the developing spinal cord, all tissues known to express high levels of p75NTR mRNA at this stage. At later stages of brain development, Bex1 mRNA was also observed in structures known to express p75NTR mRNA, including the olfactory bulb, striatum, thalamus, cerebral cortex and hippocampus.

Bex1 expression recovered in arrested cells after prolonged NGF treatment and concomitantly with postmitotic neuronal differentiation, in agreement with the abundant Bex1 expression observed in postmitotic neurons in vivo. In order to examine the regulation of Bex1 levels

Fig.6 *Cell Cycle*
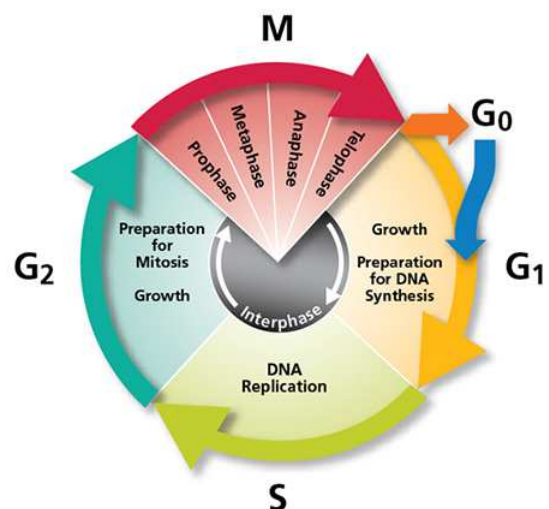
during the cycle, cell cultures were synchronized in G1 by 24 h serum starvation, after which serum was added back to initiate cell cycle re-entry. Bex1 levels were largely restored 12 h after serum re-addition, as the cells entered S phase, and then decreased again 36–48 h thereafter, as cells returned to G1. A second peak

in Bex1 was observed as cells re-entered S phase 72 h after serum addition. Thus, the levels of endogenous Bex1 oscillated during the cell cycle in a pattern that resembled that of p75NTR expression in the membrane of PC12 cells, which had previously been found to be maximal during S phase and lowest during early G1. Serum starvation of PC12 cells did not affect the steady state level of Bex1 mRNA, indicating a posttranscriptional regulation of Bex1 levels. Using the protein synthesis inhibitor cycloheximide, the half-life of Bex1 was estimated at approximately 5 h in exponentially growing cells. Upon serum withdrawal, however, Bex1 declined even more rapidly, falling below detection levels between 30 and 90 min after serum deprivation. Interestingly, this decline could be prevented by treatment with the proteasome inhibitor PS I, confirming that Bex1 levels are regulated by protein degradation.

A motif in the C-terminal portion of the protein (100RERQLS105) matched the consensus site for phosphorylation by the serine threonine kinase AKT (RxRxxS/T). After metabolic labeling of 293 cells with 32P-orthophosphate, incorporation of 32P was observed in wild-type Bex1, but not in a mutant with a Ser105 to Ala substitution, indicating that Ser105 is an endogenous phosphorylation site in this protein. In addition, no phosphorylated Bex1 could be detected after treatment with LY294002, an inhibitor of PI3K, the upstream activator of AKT. Moreover, reduction of endogenous AKT activity by serum withdrawal also attenuated Bex1 phosphorylation. In in vitro kinase assays, wild type, but not mutant, Bex1 was readily phosphorylated by wild-type AKT, while kinase-dead AKT had no effect, indicating that Bex1 is a direct target of AKT in vitro. Using antibodies that recognize a phosphorylated consensus substrate site for AKT, an increase in the phosphorylation of a band corresponding to Bex1 could be observed in PC12 cells treated with NGF, a stimulus that is known to acutely activate AKT in these cells. Bex1S105A was consistently expressed at levels lower than wild-type Bex1 in exponentially growing cells, suggesting a role for Ser105 phosphorylation in regulating the stability of the protein. In agreement with this, treatment with the proteasomal inhibitor PS I produced a significant increase in the levels of Bex1S105A. Using PS I, we could also confirm that the reduced phosphorylation of the S105A mutant observed in 293 cells was not due to its otherwise low level of expression. Taken together, these results indicated that Bex1 can be phosphorylated in Ser105 by AKT, and that this event regulates Bex1

protein turnover. There is not any significant increase in cell death after transient transfection of GFP-Bex1 in PC12 cells, nor in stable PC12 clones overexpressing Bex1. Parental PC12 cells and clones overexpressing Bex1 showed no differences in cell cycle progression during exponential growth. However, upon 24 h serum withdrawal, a larger proportion of cells in clones C4 and E2 were in S phase compared to parental cells, suggesting that Bex1 overexpression may have interfered with cell cycle arrest. Incorporation of BrdU was examined under two growth-arrest conditions, that is, serum withdrawal and NGF treatment. Strikingly, cells overexpressing Bex1 continued proliferating at normal levels under either condition, indicating a failure to exit the cell cycle as a result of deregulated Bex1 expression. Following 5-day treatment with NGF in low serum, clones overexpressing Bex1—as well as transiently transfected cells—failed to differentiate, and showed only incipient signs of neuronal differentiation. Taken together, these results indicated a role for Bex1 in cell cycle progression and neuronal differentiation.

1.4 Bex1 during Skeletal Muscle Regeneration
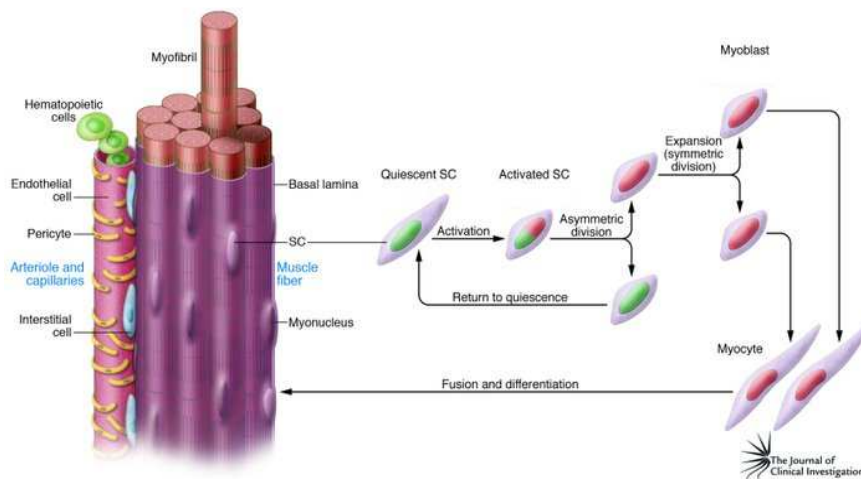
Fig.7 *Skeletal Muscle Regeneration*

Bex1 and Calmodulin (CaM) are up regulated during skeletal muscle regeneration. The study about the role of Bex1 and its interaction with CaM in skeletal muscle regeneration, used Bex1 knock out (Bex1-KO) mice. These mice appeared to develop normally and are fertile, but displayed a functional deficit in exercise performance compared to wild type (WT) mice. After intramuscular injection of cardiotoxin, which causes extensive and reproducible myotrauma followed by recovery, regenerating muscles of Bex1-KO mice exhibited elevated and prolonged cell proliferation, as well as delayed cell differentiation, compared to WT

mice. The results provide the first evidence that Bex1-KO mice show altered muscle regeneration, so the interaction of Bex1 with Ca^{2+}/CaM may be involved in skeletal muscle regeneration.

Skeletal muscle is a very adaptable tissue and can regenerate after injury. The process of skeletal muscle repair is a dramatic response to damage. Regeneration is the result of many biological processes, such as inflammation, angiogenesis, arteriogenesis, and myogenic progenitor cell mediated myogenesis, all of which lead to the reconstitution of functional skeletal muscle tissue. When this controller repair system is impaired, continuous muscle degeneration and regeneration can occur. Such is the case with Duchenne's muscular dystrophy (DMD), the most common form of inherited neuromuscular disorder. Experiments performed using cDNA-based microarrays have identified highly coordinated molecular changes involved in skeletal muscle regeneration following cardiotoxin (CTX)-induced injury, a reproducible method to induce muscle regeneration. Mdx mice possess a mutation in the gene coding dystrophin, the protein that is absent in humans with DMD. Histological findings, such as centrally nucleated fibers, inflammation, and heterogeneity of fiber size, are similar in the skeletal muscle of mdx mice and of patients with DMD. In comparison to controls, many genes are differentially expressed in mdx mouse muscle. Interestingly, the differential expression of Bex1 (Rex3) and Calmodulin (CaM). Expression of Bex1 is transiently elevated at the end of the proliferation state of skeletal muscle regeneration and several studies implicate the Bex1 protein in cell growth and differentiation. To confirm the interaction of Bex1 with CaM, the ability of recombinant Bex1 protein to bind CaM was analyzed by an electrophoretic mobility shift assay in the presence of Ca^{2+}. The interaction of Bex1 and CaM was determined to be Ca^{2+}-dependent. Bex1 expression is elevated following activation of skeletal muscle degeneration and regeneration in response to CTX-induced muscle injury. Bex1 expression was only induced in CTX-treated WT mice, further confirming the specificity of the Bex1-KO. Although mice lacking Bex1 are viable and fertile, their exercise performance measurements were 24% lower than WT mice. This finding is consistent with the report that Bex1 protein is highly expressed in developing muscle, where it is localized in somatic mesenchyme.

The lack of Bex1 in mice may alter normal development of muscle and lead to a reduction in exercise performance. To clarify the role of Bex1 expression in regenerating muscle, the study used markers of myogenesis to characterize Bex1-KO and WT mice after CTX injection.

The virtual absence of Bex1 mRNA in controls and the presence of a small amount of Bex1 transcript 3 days after CTX injection, followed by a dramatic elevation after 5 days. Approximately 5 days after injury, when Bex1 is dramatically induced, myogenic cells withdraw from the cell cycle and either self-
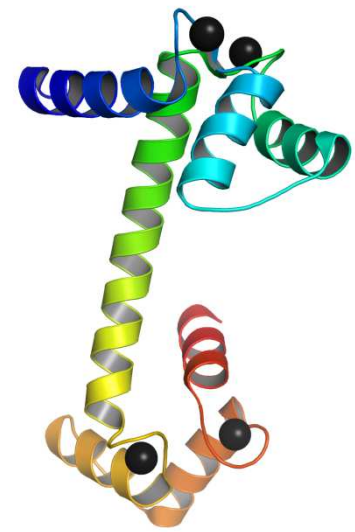
Fig.8 *Calmodulin (CaM)*

renew or form differentiated myotubes that contain central nuclei. At the onset of this differentiation, cell cycle dependent-kinase inhibitors (CDKI) such as p21CIP1, p27KIP1 and p57KIP2, together with myogenin, are induced to prevent cells from reentering the cell division cycle.

Increased expression of CDKIs and myogenin are hallmarks for the initiation of myogenic differentiation. Semi-quantitative RT-PCR was used to determine tran script levels of each gene at 5 days after CTX-injury. The transcript levels of p27, p57, and myogenin were reduced in regenerating muscle of Bex1-KO vs. WT mice by more than 27%, 40%, and 50%, respectively. By contrast, p21 transcript levels were similar between both groups. Even though the mRNA transcript levels of p27 and p57 were reduced in the regenerating muscle of Bex1- KO mice by RT-PCR, it is essential to monitor the level of expressed functional protein. This is particularly important since these proteins were reported to be regulated by ubiquitin-mediated degradation.

There are no expression of p21, p27 and p57 at 1- and 3-days post-injury. However, there was increased expression of these CDKIs at the initial stage of myogenic differentiation at 5-D post injury.

The levels of p27 and p57 proteins were reduced in regenerating muscle of Bex1-KO compared to that of WT mice at 7-D.

The investigations show that Bex1 protein binds CaM in a calcium-dependent manner, Bex1- KO mice exhibit reduced treadmill exercise performance compared to WT mice, and the absence of Bex1 protein in mice results in increased and

prolonged proliferation and delayed differentiation in skeletal muscle post CTX-induced injury. This suggests that Bex1-KO mice should show better muscle function compared to the WT mice.

1.5 Bex1 during Axonal Regeneration
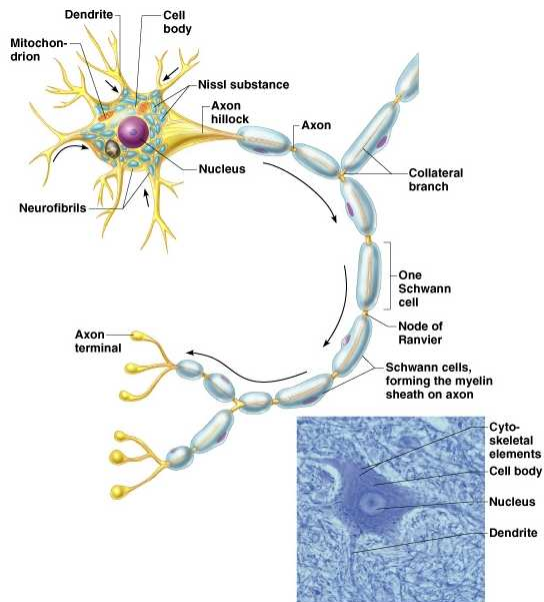
Fig.9 *Motor Neuron (MN)*

Numerous external inhibitory factors inhibit axonal regeneration after injury. In response, neurons express various regeneration-associated genes to overcome this inhibition and increase the intrinsic growth capacity. One recent study showed that the brain expressed X-linked (Bex1) protein was over-expressed as a result of peripheral axonal damage. Bex1 antagonized the axon outgrowth inhibitory effect of myelin-associated glycoprotein. The involvement of Bex1 in axon regeneration was further confirmed in vivo. The study demonstrated that Bex1 knock-out mice showed lower capability for regeneration after peripheral nerve injury than wild-type animals. Wild-type mice could recover from sciatic nerve injury much faster than Bex1 knock-out mice.

The study first analyzed the expression of Bex1 in cultured MNs prepared from E13-14 mice. MNs (motor neurons) were fixed at 3 days in vitro and analyzed by immunofluorescence to determine the subcellular localization of Bex1. Anti-Tau-1 andanti-MAP2 antibodies were used as markers for axons and minor neurites, respectively Bex1 was present in the soma and was detectable in all neurites in a punctate staining pattern. No selective enrichment in axons or minor neurites was apparent.
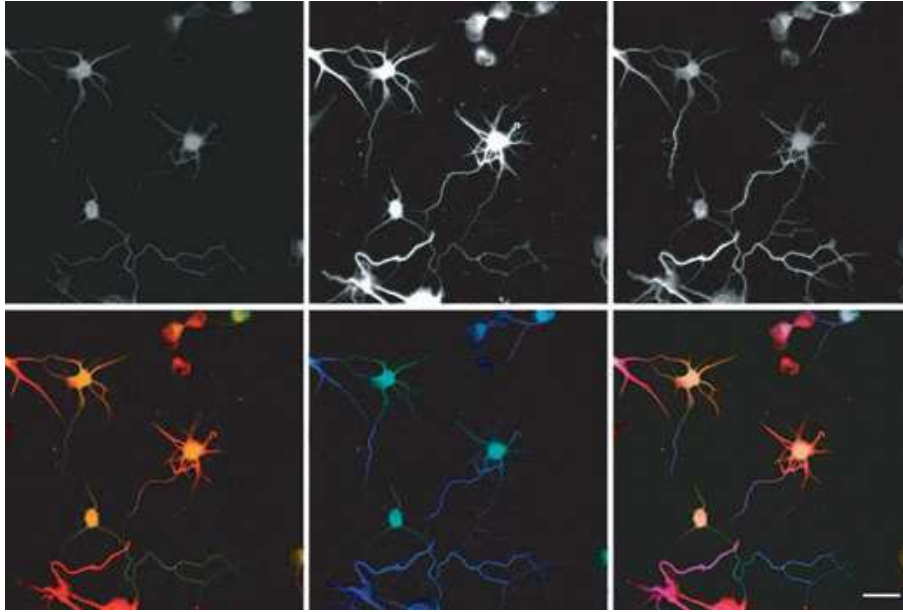
Fig.10 *Bex1 expression in axons. MNs from E13-14 mouse embryos were fixed at 3 days in vitro (DIV) and stained with antibodies specific for Bex1 (green), MAP2 (red) and the Tau-1 antibody (blue). The scale bar is 40 μm.*

The finding that Bex1 expression is up-regulated in the MNs after different types of axonal injury suggests that Bex1 might be involved in the regeneration of damaged axons.
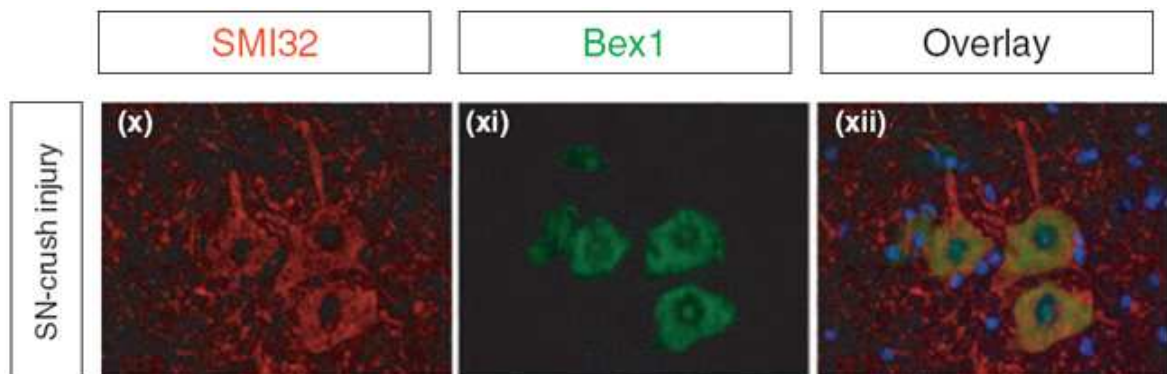
Fig.11 *The expression of Bex1 protein, the tissue sections from lumbar-spinal cord of MPZ-KO and MAG-KO mice and mice subjected to sciatic-nerve crush-injury or demyelination were stained with anti Bex1 (green) and anti-non-phosphorylated neurofilament (SMI32; a marker of neurons) (red) antibodies. 4',6-Diamidino-2-phenylindole dihydrochloride hydrate (blue) was used for nuclear staining. Scale bar is 50 μm.*

These Bex1-KO mice were viable and fertile and indistinguishable from WT littermates and developed normally. The axons and myelin of Bex1-KO peripheral nerves appeared normal. Motor coordination and balance were tested on the rotarod at 8 weeks of age and no deficits were recorded in the knock-out mice.

Most of the motor axons were injured as demonstrated by a significant reduction of 61% in the number of retrogradely labeled MNs in the spinal cords of sciatic nerve-injured mice compared with sham-operated mice 7 days after the nerve crush. These results indicate that the WT mice exhibited more rapid axonal regeneration than the KO mice.

The recovery of motor/sensory function was compared between WT (n = 5) and Bex1-KO (n = 5) mice on 7, 14, 21 and 28 days post-injury, using the Rotarod test to measure the motor coordination and balance, gait analysis with SFI and the toe-pinch reflex analysis. Acute functional deficits compared with baseline performance were observed for both WT and Bex1-KO groups at day 7 [WT = 3.6%, KO = 4%; percentage (%) of mean duration compared with the presurgery control value] and day 14 (WT = 17%, KO = 16%) after injury although there was no significant difference in Rotarod results between Bex1-KO mice and WT littermates at these time-points.

WT performance recovered more rapidly and up to 49 % of baseline at day 21 and 72% of baseline at day 28 whereas Bex1-KO mice showed significantly lower recovery (29% of baseline at day 21 and 59% of baseline at day 21; $p < 0.01$, ANOVA). Although both groups had similar baseline-performance ability before injury and exhibited similar deficits on days 7 and 14 after injury, their performance abilities differed significantly between WT and KO animals on day 21 ($p < 0.01$, ANOVA) and day 28 ($p < 0.01$, ANOVA). The muscle injury recovered within 2 weeks and it seems that the major contribution to the observed difference between WT and Bex1-KO mice after sciatic-nerve injury was related to delayed axonal regeneration rather than muscle regeneration. At 14 days post-injury, the recovery of Bex1-KO mice was significantly less complete than in the WT littermates ($p < 0.01$, ANOVA). Both WT and Bex1- KO mice recovered to the same level after 28 days.

The study demonstrated that mice deficient in Bex1 protein possess a reduced capability to regenerate injured axons than do WT littermates. There are evidences that this effect maybe partially arised from the function of Bex1 on modulation of RhoA activation after injury, which would ultimately result in better axonal growth. However, Bex1 could be also involved in re generation via another mechanism. Bex1 can interact with calmodulin, and it may be involved in the signaling pathway by which receptor-mediated calciumfluxes regulate growth-cone

activity. Bex1 should be considered to be a RAG because may play a role in promoting nerve repair after injury in the PNS. These findings open interesting possibilities for exploring Bex1 function in the control of neuronal regeneration in the CNS.

1.6 Bex1 as Tumor Suppressor

Epigenetic silencing of tumor suppressor genes is a common motif in human cancer. Tumor-associated transcriptional silencing is most frequently described in association with a few common underlying epigenetic mechanisms, such as promoter, histone deacetylation, histone methylation, and other histone modifications, which directly or indirectly alter chromatin structure.

Several recent studies have validated this large-scale approach using DNA methyltransferase and histone deacetylase (HDAC) inhibitors, either alone or in combination, in a variety of human cancers, including pancreatic, colon, prostate, liver, endometrial, blood, and esophageal cancers.

The scope of epigenetic gene silencing in malignant glioma has not been well defined. Malignant glioma, the most aggressive and common brain tumor in adults. Promoter hypermethylation and epigenetic silencing of the DNA repair gene O6-methylguanine-DNA methyltransferase were shown to identify a subset of patients with
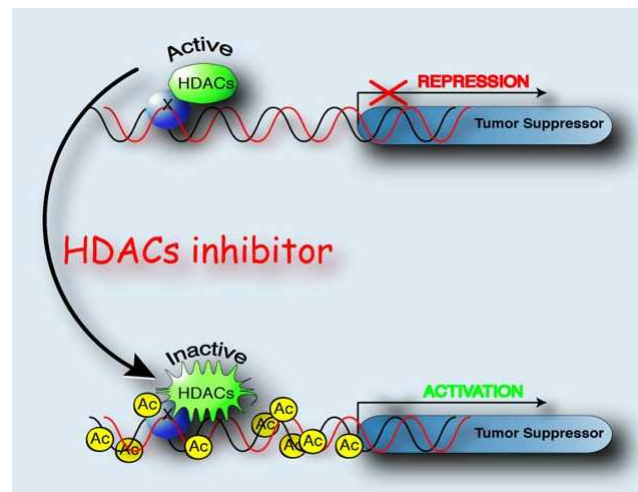
Fig.12 *HDAC inhibition*

markedly improved survival at 2 years in response to combined treatment with chemotherapy and radiation therapy. Several other genes critical for cell proliferation, tumor progression, apoptosis, angiogenesis, and astrocyte motility have also been shown to be silenced in association with promoter hypermethylation in malignant glioma.

Abundant evidence supports a synergistic link between promoter hypermethylation and histone deacetylation in the active suppression of gene transcription. Importantly, several recent reports suggest that pharmacologic inhibition of histone deacetylation alone markedly reverses transcriptional silencing, even in the

absence of promoter hypermethylation. This has led to the hypothesis that histone deacetylation is the primary mechanism that actively modulates epigenetic transcriptional silencing. HDAC inhibitors have subsequently emerged as a powerful new class of chemotherapeutic agents with promising antitumor effects. In immortalized glioma cell lines, HDAC inhibition results in cell cycle arrest and increased apoptosis.

BEX1 and BEX2, both strongly induced by TSA and 5-AzaCin glioma cell lines that were found to be silenced in all glioma tumor specimens when compared with nontumor brain specimens. The Real-Time PCR confirmed the activation of BEX1 and BEX2 in response to TSA and 5-AzaC treatment. Analysis of CpG islands in the promoter region of BEX1 and BEX2 shows that both genes have differentially methylated CpG sites in tumor samples compared with normal brain samples. The increased methylation of the promoter-associated CpG islands correlated with the decreased expression of BEX1 ($P < 0.05$) and BEX2 ($P < 0.05$) in the tumor tissues. The study characterized BEX1 and BEX2 promoter methylation in the T98 and U87 cell lines before and after treatment with TSA and 5-AzaC. BEX1 is densely methylated in both T98 and U87 cells, whereas BEX2 is only methylated in T98 cells.

Using adenoviral transfection constructs, the researchers expressed BEX1 and BEX2 individually in malignant glioma cell lines to determine potential tumor suppressor function. Expression of BEX1 and BEX2 was independently confirmed by real-time PCR. Expression of either BEX1 or BEX2 resulted in a marked decrease in colony formation compared with control transfected cells in both T98 and U87 immortalized cell lines.

There was no increase in apoptotic cells after BEX1 or BEX2 transduction alone as measured by TUNEL staining. After treatment with a subtherapeutic dose of camptothecin and etoposide, two chemotherapeutic agents known to induce apoptosis in glioma cells at higher doses, there was a striking increase in the number of cells undergoing apoptosis in the BEX1 and BEX2 transduced population when compared with control vector-treated cells. Finally, the researchers BEX1- or BEX2-transduced U87 cells in a nude mouse model to measure in vivo tumor growth. There is marked suppression of tumor growth in BEX1- or BEX2-transduced cells when compared with control vectortransduced cells ($P < 0.01$). These results support a tumor suppressor role for both BEX1 and

BEX2 in malignant glioma. Reexpression of either BEX1 or BEX2 suppresses tumor growth and chemosensitizes malignant glioma cells to camptothecin-induced apoptosis.

Epigenetic silencing of tumor suppressor genes in human cancer is widespread, involving signaling pathways controlling angiogenesis, cellular proliferation, migration, apoptosis, and differentiation. Densely methylated DNA is associated with deacetylated histones and compacted chromatin, which is refractory to transcription. Several members of a family of methylbinding domain proteins have been shown to associate with large protein complexes containing HDAC, histone methylase, and chromatin-remodeling enzymes. Promoter methylation as a biomarker for disease detection and prognosis has been validated in prostate, lung, and bladder cancer. Recent reports indicate that many of these methylation markers can be detected in serum and other body fluids with methylation-specific PCR techniques. The correlation of specific epigenetic signatures with disease state, progression, and response to treatment holds great promise for the development of therapeutic advances targeted to genetically stratified patients. The study identified and further characterized the tumor suppressor function of two of these genes, BEX1 and BEX2, in malignant glioma. BEX1 and BEX2 are X-linked uncharacterized cDNAs that have 91% sequence similarity with each other. Proteins coded by both these genes contain the BEX domain. Interestingly, this domain is also present in human p75NTRassociated cell death executor (NADE) protein, which has been implicated in the p75-mediated signal transduction pathway. NADE has been shown to have diverse effects on the central nervous system, including differentiation and apoptosis. BEX1 and BEX2 may play an important role in a novel signaling pathway regulating apoptosis in malignant glioma.

1.7 Architecture of the Liver and Regeneration

1.7.1 Architecture

To understand the molecular basis of hepatogenesis it is first necessary to first consider the structure of the adult liver. In contrast to most complex organs, histological sections through the liver reveal a rather homogeneous landscape of hepatocytes periodically infiltrated with vascular tissue and bile ducts. This somewhat bland histological
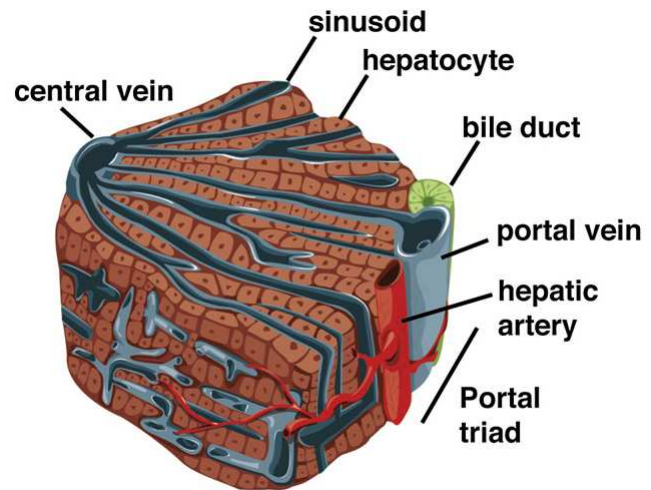
Fig.13 *Overall structure of a portion of a liver*

appearance masks an extremely complex and under appreciated tissue architecture that is crucial for normal hepatic function . The basic architectural unit of the liver is the liver lobule. The lobule consists of plates of hepatocytes lined by sinusoidal capillaries that radiate toward a central efferent vein. Liver lobules are roughly hexagonal with each of six corners demarcated by the presence of a portal triad of vessels consisting of a portal vein, bile duct, and hepatic artery. Both the portal vein and hepatic artery supply blood to the lobule, which flows through a network of sinusoidal capillaries before leaving the lobule through the central vein. Although hepatocytes are the major parenchymal cell type of the liver and account for 78% of liver volume, they function in concert with cholangiocytes (biliary epithelial cells), endothelial cells, sinusoidal endothelial cells, Kupffer cells (resident liver macrophages), pit cells (natural killer cells), and hepatic stellate cells. The hepatocytes, which are polarized epithelial cells, are arranged as cords that are one cell thick in mammals. The basolateral surfaces of the hepatocyte face fenestrated sinusoidal endothelial cells, which facilitates the transfer of endocrine secretions from the hepatocytes into the blood stream. Tight junctions formed between neighboring hepatocytes generate a canaliculus that surrounds each hepatocyte and is responsible for collection of bile acids and bile salts that are transported across the hepatocyte's apical surface. Bile collected by the

canaliculi is carried to the bile ducts within the portal triad and subsequently transported for storage in the gall bladder. The complex arrangement between the polarized hepatocytes with the capillaries and cholangiocytes underlies both endocrine and exocrine functions of the liver. The challenge facing developmental biologists is to understand the molecular events that lead to the generation of each cell type within the liver and to determine how the cells arrange to form the three-dimensional architecture that is so crucial for hepatic function.

1.7.2 Regeneration
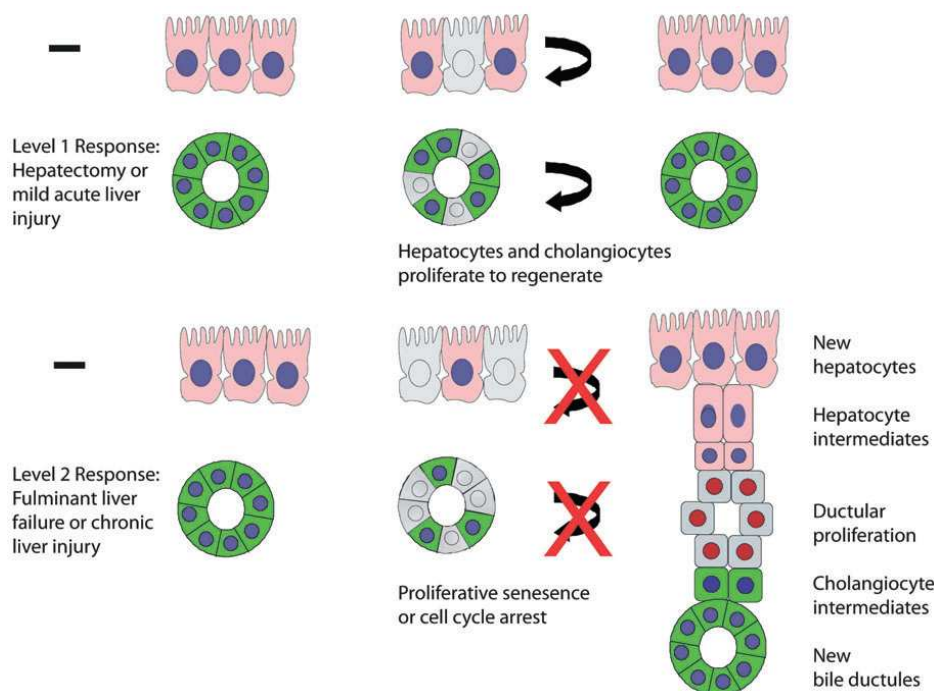
Fig.14 *The two levels of liver regeneration*

The unique ability of the liver to regenerate itself has fascinated biologists for years and has made it the prototype for mammalian organ regeneration. It is now well accepted that there are two physiological forms of regeneration in the liver as responses to different types of liver injury. At the frontline of defense are mature, normally quiescent adult hepatocytes, and in the majority of liver injuries due to drugs, toxins, resection, or acute viral diseases, hepatocytes are the main cell type to proliferate and regenerate the liver. The second layer of defense lies in the reserve progenitor cell population, which is also a quiescent compartment in the liver, but is activated when injury is severe, or when the mature hepatocytes can no longer regenerate the liver due to senescence or arrest. A particularly fascinating point about this process is that the degree of hyperplasia is precisely

controlled by the metabolic needs of the organism, such that the process stops once an appropriate liver to body weight ratio is achieved. PH is reproducible and leads to a proliferative stimulus that is initiated by an inflammatory stimulus, in the absence of significant cell death.

Regeneration of the liver is critical to the survival of mammals and is therefore evolutionarily conserved. Virtually all cellular machinery be activated during regeneration, and that this could realistically entail hundreds of pathways. It is proposed that there is an initial activation of the cytokine cascade in Kupffer cells, which then stimulates growth factor and metabolic pathways in hepatocytes. Other non parenchymal cells (stellate cells, vascular and biliary endothelial cells) proliferate after hepatocytes, presumably responding to yet another set of signals. A great deal of recent work has focused on how pattern recognition receptors and a variety of inflammatory molecules are activated and initiate the cytokine signaling cascade after PH. In brief, involved pathways include (at least) the activation of nuclear factor-kappa B (NF-kB) in Kupffer cells via tumor necrosis factor (TNF), lymphotoxin (from T cells), MyD88 and/or complement components, with downstream secretion of interleukin-6 (IL6). In turn, IL-6 binds its receptor on hepatocytes and leads to activation of the transcription factor signal transducer and activator of transcription 3 (STAT3).15 Fascinating newer work in mice with a hepatocyte-specific deletion of inhibitor-of-kappaB-kinase 2 (IKK2), which normally acts to activate NF-kB, demonstrated earlier and increased NF-kB activation in Kupffer cells, which had intact IKK2, with a concomitant decrease in NF-kB activation in hepatocytes. These animals had more rapid hepatocyte proliferation than control littermates, perhaps via prolonged JNK activation, highlighting both the cross talk between different cell types during liver regeneration and the critical importance of inflammatory stimuli in priming hepatocytes for replication. After cytokines have triggered the G0 to G1 transition, several secondary signals then stimulate progression through the cell cycle. These growth factors are numerous and redundant to a great extent, again highlighting the physiologic importance of liver regeneration to the survival of the animal. Hepatocyte growth factor (HGF) is another key hepatic mitogen active following PH. It is released from the extracellular matrix following PH to bind its receptor, c-Met, on the surface of hepatocytes. Conditional deletion of c-Met in the livers of mice was initially shown to cause either a significant delay in cell cycle entry after PH,or an inability to

survive the procedure. Studies using RNAi against HGF or c-Met in rats supported the former study, showing a suppression of cell proliferation with successful knockdown of this pathway. A family of proteins that appears to function across signaling networks is the matrix metalloproteinase (MMP) family. Through studies of animals genetically modified to lack inhibitors of MMPs (tissue inhibitors of MMPs, or TIMPs), MMPs have been shown to be important in the cleavage and release of growth factors from the extracellular matrix. Specifically, TIMP1 loss of function leads to increased MMP activity after PH, with increases in HGF activity and accelerated cell proliferation. Accordingly, a gain of TIMP1 function lead to a delay in cell proliferation. The metabolic challenges facing the regenerating liver are quite impressive. The liver must continue to regulate systemic Energy levels while meeting its own demands for significant nucleotide and protein synthesis needed for cell division. In fact, some of the most profound phenotypes seen in genetically-modified mice after PH have been demonstrated in those with defects in the phosphoinositide-3 kinase (PI3K) pathway. Important downstream effectors of this pathway include Akt, which activates mTOR and appears to affect cell size specifically and p70 S6 kinase, which regulates the 40S ribosomal protein S6 to control protein synthesis and cell proliferation. The Wnt/beta-catenin pathway has been extensively studied in a myriad of developmental processes in a variety of organs; liver regeneration is no exception. Using reporter mice, some investigators have demonstrated activation of this pathway after PH, while others have suggested that the canonical Wnt pathway is preferentially activated during the proliferation of oval cells (a type of progenitor cell).

Gene expression profiling was recently used to examine the differential proliferative response that occurs after 1/3 (minimal proliferation) versus 2/3 PH (robust proliferation). It was found that even 1/3 PH leads to significant changes in gene expression. Interestingly though, between 4 and 12 h after the two operations, a transcriptional shift seemed to occur, committing hepatocytes toward replication. This transcriptional shift consisted of the activation of genes enriched in transcription regulatory elements for FOXD3, FOXI1, CUX1, ER and E2F-1 at 4 h after 2/3 PH, and their replacement at 12 h by genes enriched in TREs for c-jun, CCAAT box, Myb, Ets-1, Elk-1 and USF, which are associated with DNA replication. These data demonstrate that the liver initially responds to PH with massive changes in gene expression, even if the operation does not result in DNA

replication, and suggest that genomic and epigenomic changes function as a "wake up" call for quiescent hepatocytes to prepare them for the decision to replicate, which occurs 12 h after PH or later.

Additionally, further work in genetically modified mouse models has lead to the discovery of novel and at times unexpected factors that drive hepatocyte proliferation after resection. One such development was the description of the critical role of platelets and platelet-derived serotonin in liver regeneration. In particular, these investigations demonstrated that thrombocytopenic mice (or mice with a variety of functional platelet defects) had a significant impairment in hepatocyte proliferation after PH. Other recent work has focused on the role of the extracellular matrix in determining the appropriate size of the liver at the completion of regeneration, i.e. regulating the termination phase of regeneration. Mice with a hepatocyte-specific loss of integrin-linked kinase subjected to PH, were left with livers an average of 58% larger than their original weights.

When hepatocytes are prevented from proliferating, liver progenitor cells serve as the second line of defense against liver failure. Farber first descrive the presence of a liver progenitor cell population in 1956 when he noted the presence of small cells with high nuclear-cytoplasmic ratio and called them "oval cells". These cells were activated in animal models of liver injury and had bipotential ability to differentiate into hepatocytes and bile duct cells.
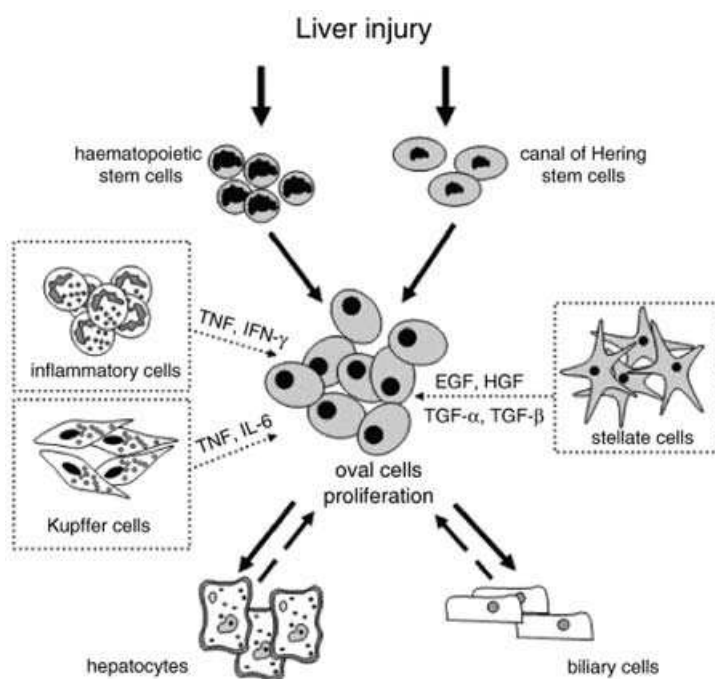
The adult human equivalent of these progenitor cells have been localized to the terminal bile ductules, known as the canals of Hering. This quiescent cell population acts as reserve population to be activated only when the adult hepatocytes are not able to repair and regenerate the injured liver, either due to senescence or cell cycle

Fig.15 Oval cell proliferation

arrest due to liver toxins such as alcohol. Upon activation, these progenitor cells proliferate in the portal zone and are seen as a collection of progenitor cells and cells of intermediate differentiation. The "streaming liver hypothesis" proposes that these cells then migrate toward the central vein in the liver lobules as progressively differentiated daughter hepatocytes. Using mitochondrial DNA mutation tracking, this was demonstrable in the normal human liver as well as in regenerative nodules of liver cirrhosis.

The observation that liver progenitor cells have mixed epithelial and mesenchymal markers and the ease by which mesenchymal stem cells can be converted to hepatocyte-like cells raised the possibility that they may arise from the mesenchymal lineage via mesenchymal to epithelial transition. In light of conflicting evidence, the role of epithelial-mesenchymal transition and vice versa in liver injury and repair remains highly controversial. The role of progenitor cell regeneration in normal liver physiology is still debated. These cells likely have no significant role in dayto- day liver turnover. The progenitor compartment is activated only in severe liver injury, and the belief that it plays an important role in regenerating the injured liver comes from three lines of evidence. First, progenitor cells are present in advanced stages of many human liver diseases in which native hepatocytes are believed to be senescent or inhibited from proliferating, such as alcoholic and non-alcoholic cirrhosis, chronic viral hepatitis, and primary biliary cirrhosis. The presence of these cells directly correlates with both inflammation and the degree of liver injury; patients with higher MELD scores appear to have more progenitor cell activation. Second, studies of chronic viral hepatitis in human patients showed that these progenitor cells are indeed surrounded by hepatocyte-like cells of intermediate differentiation, suggesting ongoing regeneration. Interestingly, although ductular proliferation is also seen after bile duct ligation and in primary biliary cirrhosis, the response in these systems is believed to come from cholangiocytes rather than progenitor cells.

A stem cell environment, or "niche", is believed to maintain the liver progenitor cell in its native state, and allows for regulatory signals to activate it when required. The companion supportive cells in this niche have long been suspected to be mesenchymal cells, such as portal fibroblasts, hepatic stellate cells or vascular endothelial cells.

2 MATERIALS AND METHODS

2.1 RNA Isolation

Obtaining high quality, intact RNA is the first and often the most critical step in performing many fundamental molecular biology experiments, the RNA isolation procedure should include some important steps both before and after the RNA purification.

For cell culture:

The growth media was removed from wells and the cells were washed in PBS and lysed directly by adding 170µl **TRIzol® Reagent**** to each well.

For whole liver tissue:

20-30mg liver tissue were added (fresh or snap frozen in liquid nitrogen and stored at -80°C) to 1ml TRIzol® Reagent in 2ml RNase free Eppendorf tube and homogenized by means of a TissueLyser (Qiagen, Retsch, Germany).

[Lysate solution can be stored at -60 to -70°C for at least one month].

200µl of chloroform per 1ml of Trizol® Reagent were added to the sample. This was centrifuged at 12000 g for 15 minutes at 4°C. The RNA was precipitated from the aqueous phase by vortexing with 500µl isopropyl alcohol (isopropanol/2-propanol/IPA) per 1ml TRIzol® Reagent. After centrifugation at 12000 g for 10 minutes at 4°C, the supernatant was removed and the pellet was washed with 1ml of 75 % ethanol (in RNase-free water) per 1ml TRIzol® Reagent.

[RNA precipitate can be stored at 4°C for up to one week or -20°C for up to one year].

The sample was centrifuged at 7500g for 5 minutes at 4℃ .The RNA was resuspended, incubated in a heat block at 55-60℃ f or 15 minutes and placed on ice.

The RNA concentration was measured on (either a nano or pico depending upon the amount of DNA) <u>Nanodrop ND-1000</u> and evaluate RNA quality on <u>Agilent 2100 Bioanalyser</u>.

**TRIzol® Reagent

TRIzol® Reagent is a ready-to-use reagent, designed to isolate high quality total RNA (as well as DNA and proteins) from cell and tissue samples of human, animal, plant, yeast, or bacterial origin, within one hour. TRIzol® Reagent is a monophasic solution of phenol, guanidine isothiocyanate, and other proprietary components which facilitate the isolation of a variety of RNA species of large or small molecular size. TRIzol® Reagent maintains the integrity of the RNA due to highly effective inhibition of RNase activity while disrupting cells and dissolving cell components during sample homogenization.

.

2.2 RNA Quality

2.2.1 Nanodrop

There are three quality controls that are performed on isolated RNA. One is to determine the quantity of RNA that has been isolated, the second is the purity of RNA that has been isolated and the third is the integrity of the RNA that has been isolated:

- ✓ Measuring the Quantity of RNA using the Nanodrop
- ✓ RNA quality control using the Agilent's 2100 Bioanalyzer

Nanodrop

The Nanodrop is a spectrophotometer that measures 1 µl samples with high accuracy and reproducibility. The full spectrum (220nm-750nm) spectrophotometer utilizes a patented sample retention technology that employs surface tension alone to hold the sample in place. This eliminates the need for cumbersome cuvettes and other sample containment devices and allows for clean up in seconds.

2.2.2 Agilent 2100 Bioanalyzer

Agilent's 2100 Bioanalyzer uses a lab on a chip approach to perform capillary electrophoresis and uses a fluorescent dye that binds to RNA to determine both RNA concentration and integrity. The electrophoretic analysis on the chip is based on traditional gel electrophoresis principles that have been transferred to a chip format.

Charged biomolecules like DNA or RNA are electrophoretically driven by a voltage gradient, similar to slab gel electrophoresis. Because of a constant mass-to-charge ratio and the presence of a sieving polymer matrix, the molecules are separated by size. Smaller fragments are migrating faster than larger ones. Dye molecules intercalate into RNA strands and these complexes are detected by

laser-induced fluorescence. Data is translated into gel-like images (bands) and electropherograms (peaks).

The Bioanalyzer electropherogram of total RNA shows two distinct ribosomal peaks corresponding to either18S and 28S for eukaryotic RNA or 16S and 23S for prokaryotic RNA and a relatively flat baseline between the 5S and 18S ribosomal peaks. In general, when analyzing good quality RNA, the height of the 28S rRNA peak should be at least twice that of the 18S rRNA peak. For perfect quality RNA we indeed find ratios over 2 with the Bioanalyzer. However, almost exclusively RNA isolated from cell culture samples results in 28S/18S ratios larger than 2.

Although the 28S/18S rRNA ratio is a reasonable way to estimate RNA integrity, it is not ideal and in particular in the context of the Bioanalyzer, which does not run under denaturing conditions sometimes the ratios do not reflect the exact level of RNA degradation. Besides the ratio of the 18S to 28S ribosomal RNAs, Agilent has introduced a software algorithm that takes the entire electrophoretic trace into account to help scientists estimate the integrity of total RNA samples. The RNA Integrity Number (RIN) software algorithm allows the classification of total RNA, based on a numbering system from 1 to 10, with 1 being the most degraded and 10 being the most intact.

It is important to realize that we assume that the integrity of the rRNA species provides a good indication for the integrity of the mRNA species, which is most of the time the RNA species that we are interested in. Although this is a reasonable assumption, it is by no means a fact.

For every type of quantitative analysis, performing experiments with RNA with a RIN below 6 should be done with caution. Specially, if one would be using freshly harvested cultured cells or freshly harvested tissue from a laboratory animal, the RIN should be definitely higher that 7.5-8 otherwise there was a problem with the way the RNA extraction procedure was performed.

2.3 Real Time PCR

2.3.1 Introduction

Real-time Polymerase Chain Reaction (PCR) is the ability to monitor the progress of the PCR as it occurs. Data is therefore collected throughout the PCR process, rather than at the end of the PCR. This completely revolutionizes the way one approaches PCR-based quantitation of DNA and RNA. In real-time PCR, reactions are characterized by the point in time during cycling when amplification of a target is first detected rather than the amount of target accumulated after a fixed number of cycles. The higher the starting copy number of the nucleic acid target, the sooner a significant increase in fluorescence is observed. In contrast, an endpoint assay (also called a "plate read assay") measures the amount of accumulated PCR product at the end of the PCR cycle.

TaqMan Gene Expression Assays

In this project we used TaqMan® Gene Expression Assays of Applied Biosystem:

- ✓ **Bex1 ID**: Hs00218464_m1 (_**m** means that an assay whose probe spans an exon-exon junction of the associated genes and will not detect genomic DNA).
- ✓ **Bex2 ID**: Hs00607718_g1 (_**g** means that An assay whose probe spans an exon-exon junction, but the assay may detect genomic DNA if present in the sample).

TaqMan® Gene Expression Assays are biologically informative, pre-formulated gene expression assays used for rapid, reliable detection and quantification of human, mouse and rat mRNA transcripts. These assays have been designed from the annotation of genes from both the public sequence databases and Celera Genomics. Each assay contains pre-formulated primers and TaqMan® probes in a 20X concentration. Each tube supports 250 reactions at a 20 μL reaction volume or 100 reactions at a 50μL reaction volume. The TaqMan® Gene Expression Assays are designed to be used in two-step RT-PCR.

Step Process

1. *An oligonucleotide probe is constructed containing a reporter fluorescent dye on the 5´ end and a quencher dye on the 3´ end. While the probe is intact, the proximity of the quencher dye greatly reduces the* fluorescence emitted by the reporter dye by fluorescence resonance energy transfer (FRET) through space.

2. If the target sequence is present, the probe anneals downstream from one of the primer sites and is cleaved by the 5´ nuclease activity of Taq DNA polymerase as this primer is extended.

3. This cleavage of the probe:

   ➢ Separates the reporter dye from the quencher dye, increasing the reporter dye signal.

   ➢ Removes the probe from the target strand, allowing primer extension to continue to the end of the template strand. Thus, inclusion of the probe does not inhibitthe overall PCR process.

4. Additional reporter dye molecules are cleaved from their respective probes with each cycle, resulting in an increase in fluorescence intensity proportional to the amount of amplicon produced.

One of the most important steps in relative quantitation experimental design is the selection of an appropriate endogenous control. Normalization to an endogenous control (often referred to as a housekeeping gene) allows you to correct results that can be skewed by differing amounts of input nucleic acid template. Any gene shown to be expressed at the same level in all study samples can potentially be used as an endogenous control.

2.3.2 Preliminary Real Time PCR

RNA concentration of the cell lines was analyzed on Nanodrop ND-1000 for cell lines: WRL68, SK-HEP, HEPG2, Chang, HUH7 and human livers: HL28 (healthy), HL42 (paracetamol), HL50 (cyste).

It was reverse transcribed 1 ug RNA from each cell line to cDNA using Applied Biosystems High-Capacity cDNA Reverse Transcription Kit # 4368813 [RT: HL50 (cyste), WRL68].

	X1	X6	÷RT (X3)
10x RT buffer:	2 µl.	12 µl	6 µl
25x dNTP mix (100 mM):	0,8 µl.	4,8 µl	2,4 µl
10x RT Random Primers:	2 µl.	12 µl	6 µl
Multiscribe Revers Trans.:	1 µl.	6 µl	÷
RNase Inhibitor:	1 µl.	6 µl	3 µl
Nuclease Free H$_2$O:	3,2 µl.	19,2 µl	12,6 µl
Total:	**10 µl.**	**60 µl.**	**30 µl.**

10 µl were portioned into each of 5 Biometra tubes, added 1 ug RNA + RNase free H$_2$O (total 10 µl) to each tube and performed reverse transcription on Biometra Thermoblock.

Program 36: **Step 1; 25 ℃, 10 min, Step 2; 37 ℃, 120 min, Step 3; 85 ℃, 5 seconds, Step 4; 4 ℃, ∞.**

It was performed Real Time PCR on ABI 7300.

Bex1:   Master cocktail (x11)

2x TaqMan PCR Master Mix:	25 µl	275 µl
20x **BEX1** TaqMan Gene Expression Assay:	2,5 µl	27,5 µl
RNase free H$_2$O:	19,5 µl	214,5 µl
Total:	47 µl.	517 µl.

Bex2:   Master cocktail (x11)

2x TaqMan PCR Master Mix:	25 µl	275 µl
20x **BEX2** TaqMan Gene Expression Assay:	2,5 µl	27,5 µl
RNase free H$_2$O:	19,5 µl	214,5 µl
Total:	47 µl.	517 µl.

3 µl cDNA were added to each Eppendorf tube and portioned 15 µl into each well of the 96-well PCR plate (running triplicates). Place 96-well plate was placed in ABI 7300, chosen FAM as repoter dye, ROX as passive reference dye. The Real

Time PCR was run with the following parameters: **Step1: 95 ℃ for 10 min repetition = 1, Step 2: 95 ℃ for 0:15 seconds – 6 0 ℃ for 1 min, repetition = 40.**

2.3.3 Real Time PCR Dilution Curves

RNA concentration of the tissue was analyzed [HL42 (paracetamol intoxication of human liver)] on Nanodrop ND-1000 and 1 µg RNA was reverse transcribed to cDNA using Applied Biosystems High-Capacity cDNA Reverse Transcription Kit # 4368813.

	X1	X3
10x RT buffer:	2 µl	6 µl
25x dNTP mix (100 mM):	0,8 µl	2,4 µl
10x RT Random Primers:	2 µl	6 µl
Multiscribe Revers Trans.:	1 µl	3 µl
RNase Inhibitor:	1 µl	3 µl
Nuclease Free H_2O:	3,2 µl	36,89 µl + 2,71 µl RNA
Total:	**10 µl**	**60 µl**

1 ug RNA + RNase free H_2O (total 10 µl) were added to each tube and perform reverse transcription on Biometra Thermoblock.

Dilution

	1	2	3	4	5	6	7	8	9	10	11	12
A (BEX1)	8	8	8	4	4	4	2	2	2	1	1	1
B (BEX1)	0,5	0,5	0,5	0,25	0,25	0,25	0,125	0,125	0,125	0,0625	0,0625	0,0625
C (BEX1)	0,031	0,031	0,031	0,0156	0,0156	0,0156	0,0078	0,0078	0,0078	0,0039	0,0039	0,0039
D (BEX1)	0,002	0,002	0,002	0,001	0,001	0,001	0,0005	0,0005	0,0005	0,0002	0,0002	0,0002
E (BEX2)	8	8	8	4	4	4	2	2	2	1	1	1
F (BEX2)	0,5	0,5	0,5	0,25	0,25	0,25	0,125	0,125	0,125	0,0625	0,0625	0,0625
G (BEX2)	0,031	0,031	0,031	0,0156	0,0156	0,0156	0,0078	0,0078	0,0078	0,0039	0,0039	0,0039
H (BEX2)	0,002	0,002	0,002	0,001	0,001	0,001	0,0005	0,0005	0,0005	0,0002	0,0002	0,0002

Program 36: Step 1; 25 ℃, 10 min, Step 2; 37 ℃, 1 20 min, Step 3; 85 ℃, 5 seconds, Step 4; 4 ℃, ∞.

After reverse transcription it was done the cDNA dilutions with RNase-free H_2O (a total of 16 wells).

cDNA	Dilutions	Most diluted
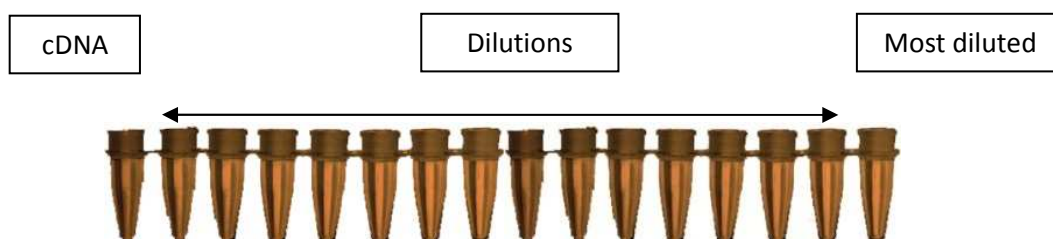
Master Mix (the solutions are sensitive to light)

BEX1

	X1	**X17**
MMx2	25 µl	= 425 µl MMx2
H_2O:	14,5 µl	= 246,5 µl H_2O
20xProbe/Primer:	2,5 µl	= 42,5 µl 20xProbe/Primer
Total.vol. =	**42 µl**	**= 714 µl for 16 samples + 1 for the pipette.**

BEX2

	X1	**X17**
MMx2	25 µl	= 425 µl MMx2
H_2O:	14,5 µl	= 246,5 µl H_2O
20xProbe/Primer:	2,5 µl	= 42,5 µl 20xProbe/Primer
Total.vol. =	**42 µl**	**= 714 µl for 16 samples + 1 for the pipette.**

It was mixed cDNA (8 µl) with Master Mix (42 µl) , started with the most diluted cDNA and proceeded towards the undiluted cDNA. It was transfered 15 µl from the solutions to a 96-well PCR plate, this is done in triplicates. The plate was placed in the Real-Time PCR machine [Applied Biosystems 7300 Real-Time PCR System], programed the software and initiated the run.

2.3.4 Real Time PCR on Liver Tissues

After the Dilution Curves was executed the Real-Time PCR on cDNA of 15 different liver tissues (4 donor livers and 11 diseased livers):

- ✓ Donor Liver HL47
- ✓ Donor Liver HL49
- ✓ Healthy Liver (resection) HL28
- ✓ Healthy Liver HL33
- ✓ Primary Biliary Cirrhosis (PBC) HL26
- ✓ Prymary Biliary Cirrhosis (PBC) HL38
- ✓ Primary Biliary Sclerosis (PBS) HL54
- ✓ Sclerosing Cholangitis HL62
- ✓ Primary Sclerosing Cholangitis (PSC) HL52
- ✓ Adult Ductopeni-Cirrhosis? HL32
- ✓ Alc. Sclerosis-Cirrhosis? HL36
- ✓ Alcoholic Liver Disease HL27
- ✓ Alcoholic Liver Disease HL44
- ✓ Toxic Liver Disease HL43
- ✓ Paracetamol Intoxication HL42

2.4 Immunohistochemistry

2.4.1 Introduction

Fig.16 Protein Bex1 in Donor Liver

Immunohistochemistry (IHC) allows the localization of antigens in tissue sections by the use of labeled antibody as specific reagents through antigen-antibody interactions that are visualized by a marker such as fluorescent dye, enzyme, radioactive element or colloidal gold.

There are numerous immunohistochemistry methods that may be used to localize antigens. The selection of a suitable method should be based on parameters such as the type of specimen under investigation and the degree of sensitivity required.

While using the right antibodies to target the correct antigens and amplify the signal is important for visualization, complete preparation of the sample is critical to maintain cell morphology, tissue architecture and the antigenicity of target epitopes. This requires proper tissue collection, fixation and sectioning. Paraformaldehyde is usually used with fixation. Depending on the purpose and the thickness of the experimental sample, either thin (about 4-40 µm) sections are sliced from the tissue of interest, or if the tissue is not very thick and is penetrable it is used whole. The slicing is usually accomplished through the use of a microtome, and slices are mounted on slides. "Free-floating IHC" uses slices that are not mounted, these slices are normally produced using a vibrating microtome.

Fixation:
Tissue preparation is the cornerstone of immunohistochemistry. To ensure the preservation of tissue architecture and cell morphology, prompt and adequate fixation is essential. However, inappropriate or prolonged fixation may significantly diminish the antibody binding capability.

There is no one universal fixative that is ideal for the demonstration of all antigens. However, in general, many antigens can be successfully demonstrated in formalin-fixed paraffin-embedded tissue sections. The discover and development of antigen retrieval techniques further enhanced the use of formalin as routine fixative for immunohistochemistry in many research laboratories.

For best results, vertebrate tissues (especially neuronal tissues) usually require fixation by transcardial perfusion for optimal tissue preservation. The most common fixatives used for immunohistochemistry are the followings:

a) 4% paraformaldehyde in 0.1M phosphate buffer

b) 2% paraformaldehyde with 0.2% picric acid in 0.1M phosphate buffer

c) PLP fixative: 4% paraformaldehyde, 0.2% periodate and 1.2% lysine in 0.1M phosphate buffer

d) 4% paraformaldehyde with 0.05% glutaraldehyde (TEM immunohistochemistry)

e) 4% formaldehyde in phosphate buffered saline (our fixation)

Some antigens will not survive even moderate amounts of aldehyde fixation. Under this condition, tissues should be rapidly fresh frozen in liquid nitrogen and cut with a cryostat without infiltrating with sucrose. The sections should be kept frozen at -20 C or lower until fixation with cold acetone or alcohol. After fixation, the sections can be processed using standard immunohistochemical staining protocols

Sectioning:

Since its introduction, paraffin wax has remained the most widely used embedding medium for diagnostic histopathology in routine histological laboratories. Accordingly, the largest proportion of material for immunohistochemistry is formalin-fixed, paraffin-embedded. Paraffin sections produce satisfactory results for the demonstration of majority of tissue antigens with the use of antigen retrieval techniques.

Certain cell antigens do not survive routine fixation and paraffin embedding. So the use of frozen sections still remains essential for the demonstration of many

antigens. However, the disadvantage of frozen sections includes poor morphology, poor resolution at higher magnifications, special storage needed, limited retrospective studies and cutting difficulty over paraffin sections.

Vibratome sections have some advantages when doing immunohistochemistry since the tissue is not processed through organic solvents or high heat, which can destroy the antigenicity. In addition, the morphology of tissue sections is not disrupted due to no freezing and thawing needed. Vibratome sections are often used for floating immunostaining, especially for pre-embedding EM immunohistochemistry. The disadvantage of vibratome sections is that the sectioning process is slow and difficult with soft and poorly fixed tissues. In addiction, the chatter marks or vibratome lines are often appeared in the sections.

Whole Mount Preparation:

Small blocks of tissue (less than 5 mm thick) can be processed as whole mounts. The advantage of whole mount preparations is that the results provide three dimensional information about the location of antigens without the need for reconstruction from sections. However, the major limitation of using whole mounts is antibody penetration which may not be complete in the tissue, resulting in uneven staining or false negative staining. So Triton X-100 or saponin treatment are used routinely for whole mount immunohistochemistry to enhance penetration of the antibody.

The antibodies used for specific detection can be polyclonal or monoclonal. Polyclonal antibodies are made by injecting animals with peptide Ag and, after a secondary immune response is stimulated, isolating antibodies from whole serum. Thus, polyclonal antibodies are a heterogeneous mix of antibodies that recognize several epitopes. Monoclonal antibodies show specificity for a single epitope and are therefore considered more specific to the target antigen than polyclonal antibodies. For IHC detection strategies, antibodies are classified as primary or secondary reagents. Primary antibodies are raised against an antigen of interest and are typically unconjugated (unlabelled), while secondary antibodies are raised against immunoglobulins of the primary antibody species. The secondary antibody is usually conjugated to a linker molecule, such as biotin, that then recruits reporter molecules, or the secondary antibody is directly bound to the reporter molecule itself.

Reporter molecules vary based on the nature of the detection method, and the most popular methods of detection are with enzyme- and fluorophore-mediated chromogenic and fluorescent detection, respectively. With chromogenic reporters, an enzyme label is reacted with a substrate to yield an intensely colored product that can be analyzed with an ordinary light microscope. While the list of enzyme substrates is extensive, Alkaline phosphatase (AP) and horseradish peroxidase (HRP) are the two enzymes used most extensively as labels for protein detection. An array of chromogenic, fluorogenic and chemiluminescent substrates is available for use with either enzyme, including DAB or BCIP/NBT, which produce a brown or purple staining, respectively, wherever the enzymes are bound. Reaction with DAB can be enhanced using nickel, producing a deep purple/black staining. Fluorescent reporters are small, organic molecules used for IHC detection and traditionally include FITC, TRITC and AMCA, while commercial derivatives, including the Alexa Fluors and Dylight Fluors, show similar enhanced performance but vary in price. For chromogenic and fluorescent detection methods, densitometric analysis of the signal can provide semi- and fully-quantitative data, respectively, to correlate the level of reporter signal to the level of protein expression or localization.

Fig.17 The <u>direct method</u> of immunohistochemical staining uses one labelled antibody, which binds directly to the antigen being stained for.
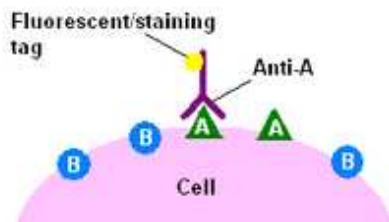
The direct method of immunohistochemical staining uses one labelled antibody, which binds directly to the antigen being stained for.
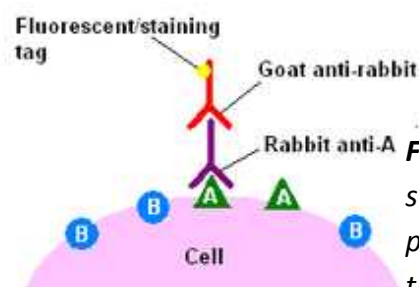

Fig.18 The <u>indirect method</u> of immunohistochemical staining uses one antibody against the antigen being probed for, and a second, labelled, antibody against the first.

The indirect method of immunohistochemical staining uses one antibody against the antigen being probed for, and a second, labeled, antibody against the first.

After immunohistochemical staining of the target antigen, a second stain is often applied to provide contrast that helps the primary stain stand out. Many of these stains show specificity for discrete cellular compartments or antigens, while others will stain the whole cell. Both chromogenic and fluorescent dyes are available for IHC to provide a vast array of reagents to fit every experimental design, and include: hematoxylin, Hoechst stain and DAPI are commonly used.

2.4.2 Antibody Optimization for DAB Histochemistry

Bex1 and CK19 optimization

The sections of human liver (healthy and pathological) were deparafinized, incubated in 3% H_2O_2 / methanol to block endogenous peroxidise activity and rehydrate in ethanol. The sections were boiled in different antigen retrieval buffers for 10min or 10+10min:

- ✓ Do nothing
- ✓ Dako citrate retrieval [*DakoCytomation Target Retrieval Solution, pH6, 10x concentrate, RF S1699*]
- ✓ Dako high pH retrieval [*DakoCytomation Target Retrieval Solution, high pH, 10x concentrate, RF S3307*]
- ✓ Dako pH 9 retrieval [*DakoCytomation Target Retrieval Solution, high pH, 10x concentrate, RF S2367*]

The sections were washed in TBST* and the protein blocked with Serum Free Blocking Medium in a moisture chamber for 20 min at RT *(Protein Block, Serum-Free, Ready-To-Use, Ref X0909, DakoCytomation, Glostrup, Denmark).* The sections were incubated for 1 h at room temperature (RT) or at 4°C overnight, in a moisture chamber, with the primary antibodies diluted in TBSB**. The secondary antibodies were applied for 30min at RT, the sections were incubated in

diaminobenzidine (DAB) for 10 min (exactly) in a moisture chamber, counterstained in Mayers haematoxylin for 7 min or 15min, dehydrated and mounted in Eukitt.

Bex 1 antibody dilutions:

1:100
1:1000
1:1500
1:2000
1:3000
1:15000
1:50000
1:100000
1:150000

Abcam Ab

Margolis Ab

Sections of human liver:

- ✓ Donor Liver HL49
- ✓ Paracetamol Intoxication HL42
- ✓ Primary Biliary Cirrhosis (PBC)
- ✓ Primary Sclerosing Cholangitis (PSC)
- ✓ Large Duct Obstruction (LDO)
- ✓ Steatohepatitis
- ✓ Toxic Hepatitis

CK19 antibody dilutions:

1:50
1:100

Primary antibody:

- Bex1, rabbit, # ab69032, Abcam plc, 330 CambridgeScience Park Cambridge, CB4 0FL, UK
- Polyclonal rabbit anti-Bex1 antibody, Frank L. Margolis Lab, Department of Anatomy and Neurobiology, University of Maryland, School of Medicine, HSF II S203, 20 Penn Street, Baltimore, Maryland 21201.
- CK19, Monoclonal Mouse, Anti-Human Cytokeratin 19, Clone RCK108, Kode nr. M 0888, Dako, Glostrup, Denmark.

Secondary antibody:

- Envision + R system. Labelled Polymer-HRP anti-rabbit. REF K4002. Dakocytomation, 6392 Via Real, Carpinteria, CA 93013, USA.
- Envision + R system. Labelled Polymer-HRP anti-mouse. REF K4000. Dakocytomation, 6392 Via Real, Carpinteria, CA 93013, USA.

Recommended dilutions
ICC/IF: 1/200.
IHC-P: 1/300 - 1/3000. Antigen retrieval is recommended.
IHC-Fr: 1/300 - 1/3000.
WB: 1/300 - 1/3000. This antibody has been tested in Western blot against the recombinant peptide used as an immunogen. We have no data on detection of endogenous protein. Predicted molecular weight: 14 kDa.

Not yet tested in other applications.
Optimal dilutions/concentrations should be determined by the end user.

Cellular localization	Cytoplasmic and Nuclear
Research areas	Neuroscience >> Neurology process >> Neuroregeneration >>Neuroregeneration
	Cancer >> Oncoproteins/suppressors >> Tumor suppressors >> Other
	Neuroscience >> Neurology process >> Neurogenesis
	Signal Transduction >> Adapters >> Cytoplasmic
	Neuroscience >> Neurotransmission >> Intracellular Signaling >> Adapters
Relevance	Bex1 is a signaling adapter molecule involved in p75NTR/NGFR signaling. It is thought to play a role in cell cycle progression and neuronal differentiation. Bex1 inhibits neuronal differentiation in response to nerve growth factor (NGF). Bex1 has also been implicated as a tumor suppressor
	Alternative names Bex1 antibody (ab69032)
Database links	The links below go to external sites and will open in a new browser window

Entrez Gene	55859 (Human)	**SwissProt**	Q9HBH7 (Human)

Raised in	Rabbit
Clonality	Polyclonal
Isotype	IgG
Purity	Whole antiserum
Storage buffer	Preservative: None
	Constituents: Whole serum
Form	Liquid
Concentration	Concentration not determined
Storage instructions	Store at +4°C short term (1-2 weeks). Aliquot and store at -20°C (add glycerol to a final volume of 40% for extra stability). Avoid repeated freeze / thaw cycles.

Information about Bex1 antibody of Frank L. Margolis Lab

Frank L. Margolis Lab
Department of Anatomy & Neurobiology
University of Maryland School of Medicine
HSF II S203
20 Penn Street
Baltimore, Maryland 21201

Background: This is an antibody to Bex1 (<u>B</u>rain <u>ex</u>pressed <u>X</u>-linked

Immunogen: Purified recombinant mouse Bex1 protein

Molecular weight of antigen: ~23kDa

Host: Rabbit #002 4-20-01 and 6/01/01

Supplied as:
It is diluted 1:1 with glycerol (and contains 0.05% sodium azide) to facilitate shipment at ambient temperature

Applications and Suggested Dilutions:
- Western Blotting (WB) (1:20,000 overnight at 4°C)
- Immunofluorescence (1:20K in PBS w/0.2% TX &
  5% horse serum al., overnight at 4°C/1:200K
  in 0.05M KPBS w/ 0.5% TX & 2% BSA, overnight at RT)
- Immunohistochemistry (DAB,1:50,000~100,000, 2days at 4°C)
- Immunoprecipitation (IP) (1ul of Ab/1-5mg of tissue extract)

Storage: Store at -20 °C

Specificity:
Polyclonal rabbit anti-Bex1 antibody is immunospecific for mouse Bex1 and Bex2 but not Bex3 as determined by Western blotting with recombinant mouse Bex1, 2, and Bex3 proteins. An immunoreactive band of about 23-kDa is also detected in lysates from CHO cells that were transfected with Bex1 and Bex2 cDNA and not with empty plasmid. An endogenous anti-Bex1 immuno-band is observed in mouse, rat and the undifferentiated but not in the differentiated F9 cells.

Contact information:
FAX 410-706-2512, Phone 410-706-8913, e-mail FLMOMP@gmail.com

Reference:
1. Koo JH, Manda S, Margolis FL Immunolocalization of Bex protein in the Mouse Brain and Olfactory System. *J Comp Neurol.* 2005 487(1):1-14.
2. Bernstein SL, Koo JH, Slater BJ, Guo Y, Margolis FL. Analysis of optic nerve stroke by retinal Bex expression. *Mol Vis.* 2006 12:147-155.
3. Koo JH, Smiley MA, Lovering RM, Margolis FL. Bex1 knockout mice show altered skeletal muscle regeneration. *Biochem Biophys Res Commun.* 2007 363(2): 405-410.

Creator:
Jae Hyung Koo Ph.D.

D9, differentiated F9 cells
U9, undifferentiated F9 cells
OB, olfactory bulb
CB, cerebellum
CNS, the balance of the brain
from postnatal day 7
BL, Bex1-blocked serum
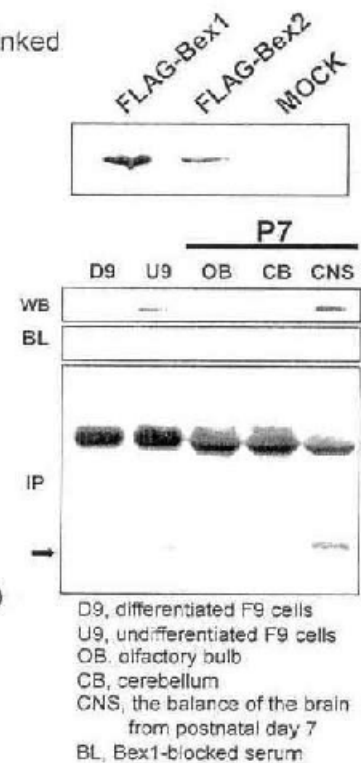
10X TBS (0.5 M TRIS, 1.5 M NaCl), 2 L

121.2 g TRIS

175.2 g NaCl

Dissolve in MQ water. Adjust pH to pH 7.4 for a total volume of 2 liter. When making 1xTBS adjust new solution to pH 7.4

*1xTBS / 1% Triton X-100 (TBST), pH 7.4, 5 L (0.05 M Tris, 0.15 M NaCl, 1% Triton)

500 ml 10 x TBS

50 g Triton X-100

Add MQ water and adjust solution to pH 7.4 for a total volume of 5 liter. Triton x-100 dissolves slowly and foams – therefore start the TBST manufacturing process with dissolving this compound.

**1xTBS / 0.25% BSA (TBSB), pH 7.4

300 ml 1x TBS, pH 7.4

0.75 g BSA

Steril-filtrate and aliquote into 15 ml tubes. Stored by -20 °C.

2.4.3 Antibody Optimization for Immunofluorescence

Frozen sections [HL49 (Donor Liver) and HL54 (Primary Biliary Cirrhosis), 10 µm] were fixed in ice cold acetone (at -20℃) for 20 m in, washed in TBS/1% triton X-100 (TBST) and incubated in humid chamber for 20 min at RT in serum free blocking solution. The primary antibodies were diluted in TBSB or TBSB / 0,2% TX and incubated in a humid chamber for 1 hour at RT. The second antibodies were incubated for 1 hour at RT (it is important to work in the dark). The sections were mounted in DAPI containing mounting medium.

Primary antibodies

- Bex1, rabbit, # ab69032, Abcam plc, 330 CambridgeScience Park Cambridge, CB4 0FL, UK.
  Dilution: 1-100
- Polyclonal rabbit anti-Bex1 antibody, Frank L. Margolis Lab, Department of Anatomy and Neurobiology, University of Maryland, School of Medicine, HSF II S203, 20 Penn Street, Baltimore, Maryland 21201.
  Dilution: 1-2000, 1-20000
- CK7, Monoclonal Mouse, Anti-Human Cytokeratin 7, Clone OV-TL 12/30, Kode nr. M 7018, Glostrup, Denmark.
  Dilution: 1-50

Secondary antibodies

- Alexa Fluor, A11037, 594, goat anti rabbit, Invitrogen, Ltd. 3 Fountain Drive, Inchinnan Business Park, Paisley PA4 9RF, UK
  Dilution: 1-400
- Alexa Fluor, A11029, 488, goat anti mouse, Invitrogen, Ltd. 3 Fountain Drive, Inchinnan Business Park, Paisley PA4 9RF, UK
  Dilution: 1-400

2.4.4 Bex1 and CK19 Detection in Different Liver Tissues

The sections of human liver (healthy and pathological) were deparafinized, incubated in 3% H_2O_2 / methanol to block endogenous peroxidise activity and rehydrated in ethanol. The sections were boiled in <u>Dako pH 9</u> antigen retrieval buffer [*DakoCytomation Target Retrieval Solution, high pH, 10x concentrate, RF S2367*] for <u>10+10min</u>. The sections were washed in TBST and the protein blocked with Serum Free Blocking Medium in a moisture chamber for 20 min at RT *(Protein Block, Serum-Free, Ready-To-Use, Ref X0909, DakoCytomation, Glostrup, Denmark).* The sections were incubated at <u>4°C overnight</u>, in a moisture chamber, with the primary antibodies diluted in TBSB. The secondary antibodies were applied for 30min at RT, the sections were incubated in diaminobenzidine (DAB) for 10 min (exactly) in a moisture chamber, counterstained in Mayers haematoxylin for <u>15min</u>, dehydrated and mounted in Eukitt.

Primary antibody:

- Polyclonal rabbit anti-Bex1 antibody, Frank L. Margolis Lab, Department of Anatomy and Neurobiology, University of Maryland, School of Medicine, HSF II S203, 20 Penn Street, Baltimore, Maryland 21201.
  <u>Dilution: 1-1500</u>
- CK19, Monoclonal Mouse, Anti-Human Cytokeratin 19, Clone RCK108, Kode nr. M 0888, Dako, Glostrup, Denmark.
  <u>Dilution: 1-50</u>

Secondary antibody:

- Envision + R system. Labelled Polymer-HRP anti-rabbit. REF K4002. Dakocytomation, 6392 Via Real, Carpinteria, CA 93013, USA.
- Envision + R system. Labelled Polymer-HRP anti-mouse. REF K4000. Dakocytomation, 6392 Via Real, Carpinteria, CA 93013, USA.

Sections of human liver:

- ✓ Donor Liver
- ✓ Primary Biliary Cirrhosis (PBC)
- ✓ Primary Sclerosing Cholangitis (PSC)
- ✓ Large Duct Obstruction (LDO)
- ✓ Steatohepatitis
- ✓ Toxic Hepatitis
- ✓ Hepatitis B (HBV)
- ✓ Hepatitis C (HCV)

2.5 Maintenance of Cancer Cell Lines

Cell lines:

- ✓ **HUH7** (It is a well differentiated hepatocyte derived cellular carcinoma cell line that was originally taken from a liver tumor in a 57-year-old Japanese male in 1982. The line was established by Nakabayshi, H. and Sato, J.)

- ✓ **HEPG2**
- ✓ **WRL68**
- ✓ **SK-HEP1**

The frozen cells were removed from -80℃ freezer, added media **[DMEM + GlutaMAX (450ml), 10% FBS (50ml), Gentamicin (2.5ml)]** and centrifuged at 1200 RPM for 3 min RT. The pellet was isolated, added media, transfered into the T-25 cell culture flasks and these were put in the incubator at 37℃ with humidified atmosphere of 5% CO_2. The cells were washed with PBS, splitted with Trypsin and put in T-75 flasks.

The cells were trypsinized, counted and diluted in growth media to a plating density of 15-75% confluency (depending upon growth rate of cells and requirements of end point assay). **It was plated 200.000 cells Huh7 cells per well in 2ml media, 2 x 6 well plates, 3 wells / plate**. The cells were incubated at 37℃ with 5% CO_2 overnight.

2.6 Knockdown with siRNA

2.6.1 Introduction

Over the years, gene silencing by RNAi has relied heavily on the use of cationic lipid-based delivery reagents for transfecting cells with small interfering RNAs (siRNAs). In many cases, lipid-based transfection is sufficient and provides efficient levels of gene knockdown. Yet in a significant fraction of cases, cells are either refractory to lipidmediated delivery of siRNAs or aversely sensitive to the presence of lipids.
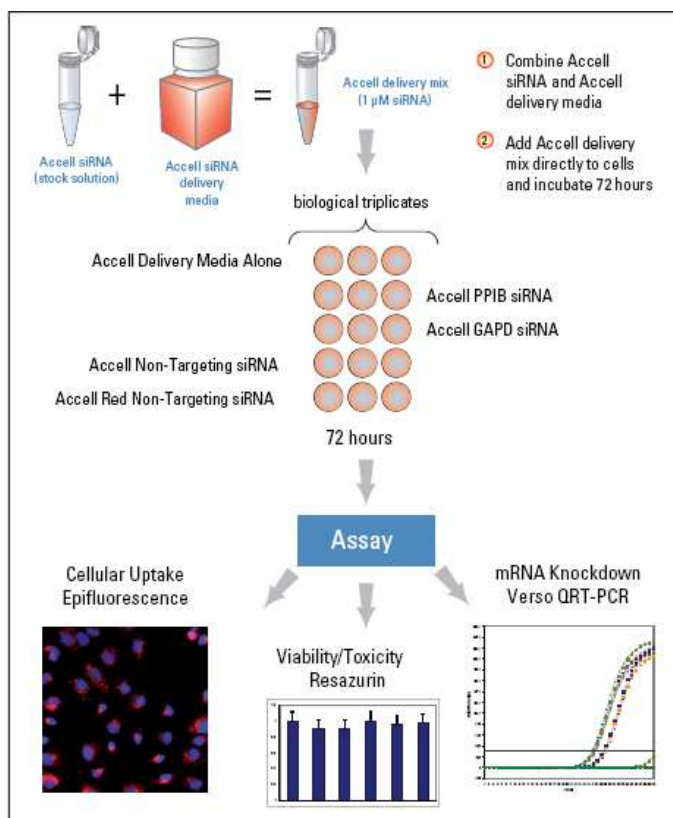
Fig.19 *Experimental workflow for Accell siRNA mediated gene silencing and detection of mRNA knockdown.*

Dharmacon® Accell® siRNA

The Accell siRNA product line represents a recently develope technology that promotes delivery of siRNA independent of viral vectors or lipid-based transfection reagents (also referred to as "passive delivery") to virtually any cell type.

This novel delivery technology permits gene silencing with minimal off-target events (as assessed by genome-wide profiling), has limited repercussions on cell viability, and   triggers a negligible innate immune response. Thus, unlike electroporation, which is historically the first alternative delivery method for cells found to be averse to lipid based transfection reagents, Accell siRNA can be employed without significant effects on cell physiology.

Over the course of investigations, it is often necessary to knock down gene expression for estende periods of time to accurately assess the contribution of a particolar protein to a given biological event. Long-term reduction of gene expression can be problematic, particularly in cases where there are large intracellular reservoirs of the target or the half-life of the protein is drawn out. In some instances, researchers have attempate multiple, consecutive lipid-mediated transfections of siRNAs into cultured cells. Unfortunately, this approach is frequently cytotoxic and can induce brief (24-72 hrs) changes in the state of the innate immune response. To overcome these barriers, DNA-mediated RNAi, commonly exploiting viral delivery platforms, has been adopted. This approach can be successful, but is costly and requie significant development time.

Each experiment should include the following samples in triplicate:

1. Untreated cells (cells growing in Accell medium or any other medium used for Accell siRNA delivery)

2. Positive control siRNA (targeting an endogenous or reporter gene)

3. Negative control siRNA (non-targeting siRNA control)

4. The desired test siRNA

Optimal cell densities will vary with growth characteristics of specific cell types. It is recommended to assess the growth rate of the cells in Accell delivery media prior to carrying out Accell siRNA silencing experiments.

2.6.2 Transfection of Huh7 Cell Line

✓ _Plate 1, 3x well_: - **transfection with siRNA Bex1 SMART Accell (50nm, Thermo Scientific)**
✓ _Plate 2, 3x well_: - **control (no transfection, untreated cells)**

5X siRNA buffer (Cat.# B-002000-UB-100) was diluted to 1X siRNA buffer (100µ + 400µl DEPC-treated Water). 500µl 1x siRNA buffer were added to siRNA BEX1 (50nmol) to have 100 µM siRNA solution. 120µl of this solution were mixed with 12mL Accell delivery media (Cat.# B-005000) with final concentration 1µM Accell siRNA per well in a 6-well plate. The cells were incubated at 37ºC with 5% CO_2 for 72 hours.

2.7 Protein Harvest

Before harvest:

500µL _Buffer A*_ were mixed with 50µL **_Protease inhibitor cocktail (p8340) (Sigma-Aldrich)_**

[It is recommended to use 1:10 every $1x10^8$ cells/mL. There is ca. $8x10^5$ cells/mL in a 10cm dish. For this make a 125x dilution of the cocktail mix (8µL protease inhibitor cocktail + 992µL MilliQ) (stored: -20°C freezer). Of this add 1:10 to Buffer A (50µL cocktail : 500µL Buffer A)].

The cells were washed in PBS, added the solution with 500µL Buffer A* and 50µL Protease inhibitor cocktail (p8340) (Sigma-Aldrich). The scraped cells were freezed – thawed for lysis, centrifugated at 20.000g at 4°C. The supernatant can be store at -20°C.

Protease Inhibitor (in 300 µl)
3 ml PMSF
1.5 µl APO
1.5 µl LEU

*Buffer A:

1ml, 1M Hepes /0,2383g HEPES

0,0757 g KCL

0,0312g MgCl2

11,67g sucrose

20ml 50% glycerol

100µl 100% Triton X-100

1. Add 50ml Milli-Q.
2. pH should be 7,93. (adjusted with 5M HCl and NaOH).
3. Fill up till 100ml with Milli-Q.
4. Aliquot and store at -20°C.

2.8 Bradford Protein Assay

2.8.1 Introduction

The Bradford assay, a colorimetric protein assay, is based on an absorbance shift of the dye Coomassie Brilliant Blue G-250. In the acidic environment of the reagent, protein binds to the Coomassie dye. This results in a spectral shift from the reddish/brown form of the dye (absorbance maximum at 465nm) to the blue form of the dye (absorbance maximum at 610nm). The difference between the two forms of the dye is greatest at 595nm, so that is the optimal wavelength to measure the blue color from the Coomassie dye-protein complex. If desired, the blue color can be measured at any wavelength between 575nm and 615nm. At the two extremes (575nm and 615nm) there is a loss of about 10% in the measured amount of color (absorbance) compared to that obtained at 595nm.

Fig.20 *Coomassie Brilliant Blue*

Coomassie Brilliant Blue G-250 Dye
$C_{47}H_{48}N_3NaO_7S_2$
MW 854.02
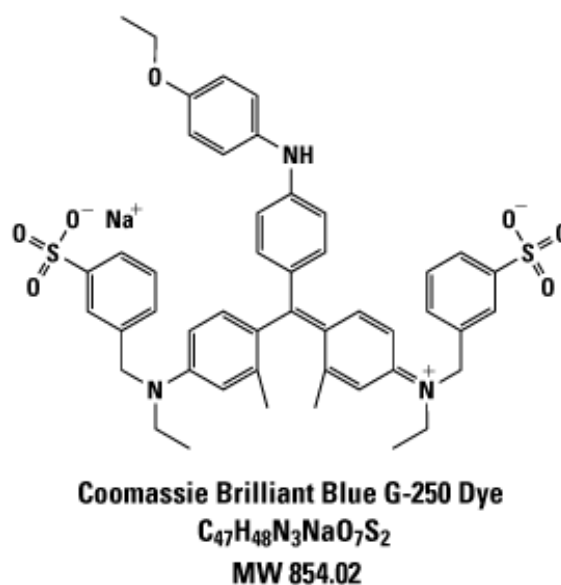
Development of color in Bradford protein assays is associated with the presence of certain basic amino acids (primarily arginine, lysine and histidine) in the protein. Van der Waals forces and hydrophobic interactions also participate in the binding of the dye by protein. The number of Coomassie dye ligands bound to each protein molecule is approximately proportional to the number of positive charges found on the protein. Free amino acids, peptides and low molecular weight proteins do not produce color with Coomassie dye reagents. In general, the mass of a peptide or protein must be at least 3000 daltons to be detectable with this reagent.

Coomassie dye binding assays are the fastest and easiest to perform of all protein assays. The assay is performed at room temperature and no special equipment is

required. Standard and unknown samples are added to tubes containing preformulated Coomassie assay reagent and the resultant blue color is measured at 595nm following a short room temperature incubation. The Coomassie dye-containing protein assays are compatible with most salts, solvents, buffers, thiols, reducing substances and metal chelating agents encountered in protein samples.

The main disadvantage of Coomassie based protein assays is their incompatibility with surfactants at concentrations routinely used to solubilize membrane proteins. In general, the presence of a surfactant in the sample, even at low concentrations, causes precipitation of the reagent. In addition, the Coomassie dye reagent is highly acidic, so proteins with poor acid-solubility cannot be assayed with this reagent.

2.8.2 Protein Concentration Measurement

PIERCE Coomassie Plus – The Better Bradford^{TM} Assay Kit. It was set up a standard set with BSA (2,0 mg/ml) diluted with 1% Buffer A. It was made 3 dilutions 1:100 and 1:300 and 1:1000 with milli-Q.

10 µl protein

400 µl   300 µl

990 µl   800 µl   700 µl   →**Milli-Q**
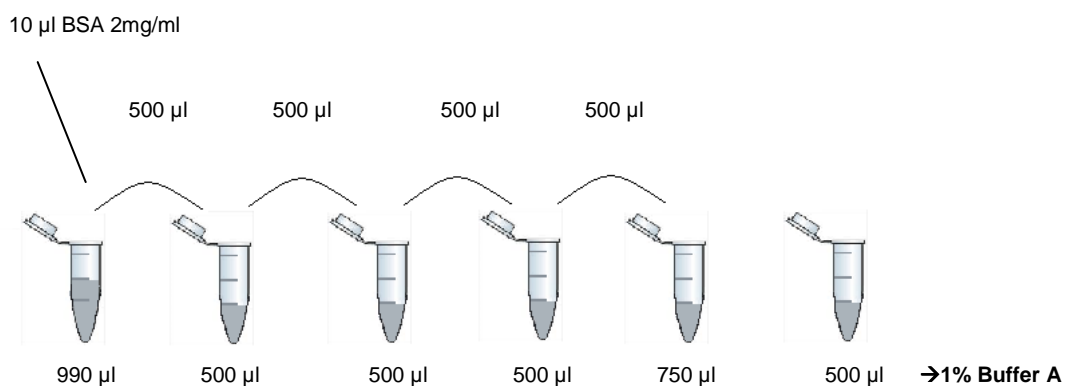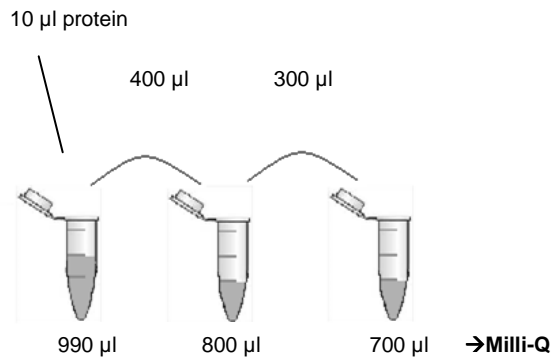
All dilutions were measured in triplo. 150µl was added per well of the BSA standardset and 150 µl of Coomassie Blue Plus reagens (RT) was added to all wells. Absorbance was measured at 595 nm with a spectrophotometer.

2.9 Western Blot

2.9.1 Introduction

The term "blotting" refers to the transfer of biological samples from a gel to a membrane and their subsequent detection on the surface of the membrane. The specificity of the antibody-antigen interaction enables a target protein to be identified in the midst of a complex protein mixture

The first step in a Western blotting procedure is to separate the macromolecules using gel electrophoresis. After electrophoresis, the separated molecules are transferred or blotted onto a second matrix, generally a nitrocellulose or polyvinylidene difluoride (PVDF) membrane. Next, the membrane is blocked to prevent any nonspecific binding of antibodies to the surface of the membrane. Most commonly, the transferred protein is complexed with an enzyme-labeled antibody as a probe. An appropriate substrate is then added to the enzyme and together they produce a detectable product such as a chromogenic precipitate on the membrane for colorimetric detection. The most sensitive detection methods use a chemiluminescent substrate that, when combined with the enzyme, produces light as a byproduct. The light output can be captured using film, a CCD camera or a phosphorimager that is designed for chemiluminescent detection. Alternatively, fluorescently tagged antibodies can be used, which are directly detected with the aid of a fluorescence imaging system. Whatever system is used, the intensity of the signal should correlate with the abundance of the antigen on the membrane.

Detailed procedures for detection of a Western blot vary widely. One common variation involves direct vs. indirect detection. With the direct detection method, the primary antibody that is used to detect an antigen on the blot is labeled with an enzyme or fluorescent dye. This detection method is not widely used as most researchers prefer the indirect detection method for a variety of reasons. In the indirect detection method, a primary antibody is added first to bind to the antigen. This is followed by a labeled secondary antibody that is directed against the primary antibody. Labels include biotin, fluorescent probes such as fluorescein or

rhodamine, and enzyme conjugates such as horseradish peroxidase or alkaline phosphatase. The indirect method offers many advantages over the direct method.

2.9.2 Western Blot Esecution

Product	Cat.nr.	Company
NuPAGE MES SDS Buffer Kit	NP0060	Invitrogen
NuPAGE Transfer Buffer 20x	NP006-1	Invitrogen
NuPAGE Novex Bis-Tris Mini gels 4-12%	NP0323BOX	Invitrogen
Western Lightning® Plus-ECL	NEL103001EA	Perkin Elmer
See Blue Plus2 Pre-stained Marker	LC5925	Invitrogen

Sample preparation

	Huh7+Bex1	Huh7 (Control)
Sample (12µg)	6,6µl*	9,1µl
4x Sample buffer(kit)	3,75µl	3,75µl
10x Reducing Agent (kit)	1,5µl	1,5µl
H₂O	3,15µl	0,65µl

*protein concentration Huh7+Bex1 [1,82mg/ml], Huh7(control)[1,32mg/ml]

Gel preparetion

In the XCell SureLock™ Mini-Cell system(Invitrogen) was put the MES running Buffer(1x) [40ml 20x running buffer(kit) plus 760ml H_2O] plus antioxidant. The comb was removed and the wells were rinsed with running buffer. The samples and 5µl of **M**arker were loaded and in the rest of wells were filled with 3,75µl sample buffer + 11,25µl H_2O. The gel was run at 200V for 50 min.

Gel load: **M**   **H_2O**   **H_2O**   **H_2O**   **Bex1**   **Control**   **M**

The 2 sponge pads, 4 filterpapers and the nitrocellulose membrane were pre wetted in 1x transfer buffer*.

> ***1x Transfer Buffer:***
> - 25ml 20x transfer buffer(kit)
> - 0,5 ml antioxidant (kit)
> - 50 ml methanol (for 1 gel)
> - 424,5 ml H_2O

Set up the Xcell II Blot Module (Invitrogen) [Blot Sandwich]

The wells were cut off and with the pre-soaked filterpapers, the 2 sponge pads, the membrane was formed the Blot Sandwich and the gel is closest to the cathode plate (see figure below).

-Sponge pad
-Sponge pad

-Filter paper
-Membrane
-Gel
-Filter paper

-Sponge pad
-Sponge pad

Cathode Core (-)

The gel membrane sandwich and blotting pads were positioned in the cathode core of the XCell II™ Blot Module to fit horizontally across the bottom of the unit. The sandwich was covered with transfer buffer and 600ml of deionized H$_2$O was added to the lower chamber. It was blotted at 30V for 1 hour (start with 220mA and end with 180 mA).

[The membrane can be stored from this time on wrapped in plastic foil at 4ºC]

Immunodetection

[Bex1 antibody (Margolis, **~23kDa**), *host:* rabbit. 1:20000 WB]

The membrane was blocked 1 hour in 20ml 5% skimmed milk powder in TBST, incubated membrane 1 hour with the primary antibody (anti-Bex1:   diluted 1:20000 in TBS-T, 0,5µl in 10ml) and 1 hour with the secondary antibody (rabbit anti Ab HRP diluted 1:5000 in TBS-T , 1µl in 5ml).

Detection with Western Lightning Plus-ECL

The Luminol Reagent was mixed 1:1with the oxidizing reagent (500µl +500µl), the membrane - protein was faced down on the mixture and wrapped in cling film. Pictures were taken with LAS 1000 with Chemiluminescence (high intensity exposure, start with 1-5 seconds and longer depending on detection).

3 RESULTS

3.1 Nanodrop Results

	ng/µl (Nanodrop)	Take out (µl) (1000/nanodrop ng)	add water RNA free to 10 µl	total volume µl
WRL68	333,9	2,99	7,01	10
SK-HEP1	340,01	2,94	7,06	10
Chang	365,6	2,74	7,26	10
HEPG2	333,3	3,00	7,00	10
HUH7	338,4	2,96	7,04	10
HL50	634,8	1,58	8,42	10

Table 1

	ng/ul (Nanodrop)	260/280	260/230
HL42	1107	1,91	0,76

Table 2

3.2 Agilent 2100 Bioanalyzer Results

Fig.21
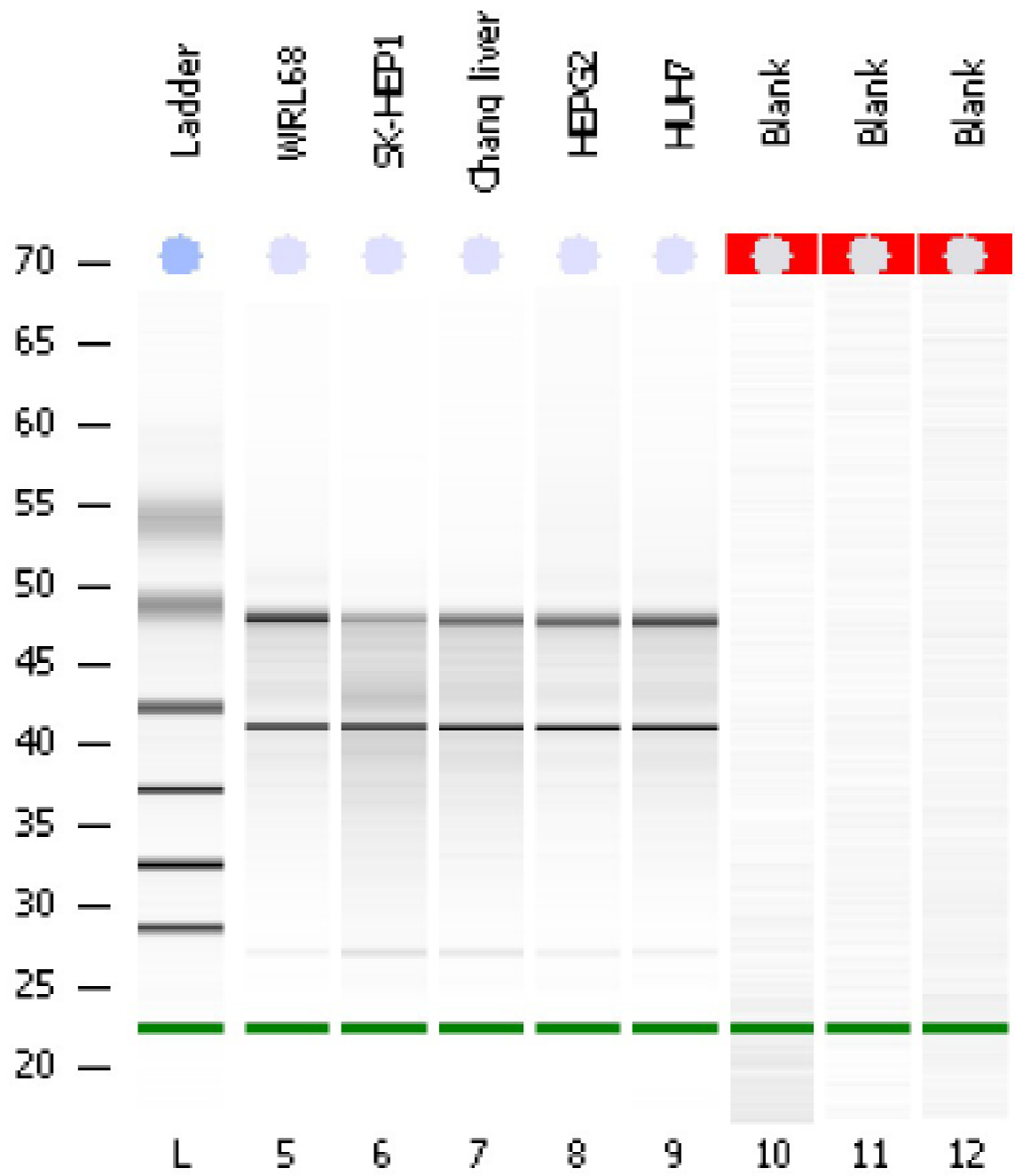
Chart1
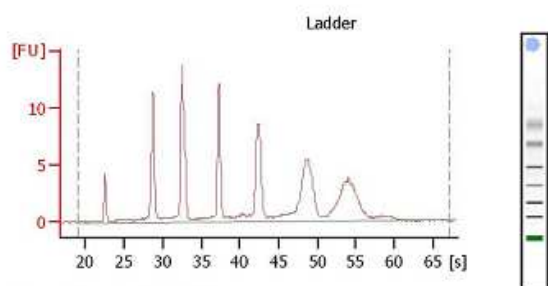
Ladder

Overall Results for Ladder

RNA Area:	131,9
RNA Concentration:	150 ng/µl
Result Flagging Color:	
Result Flagging Label:	All Other Samples
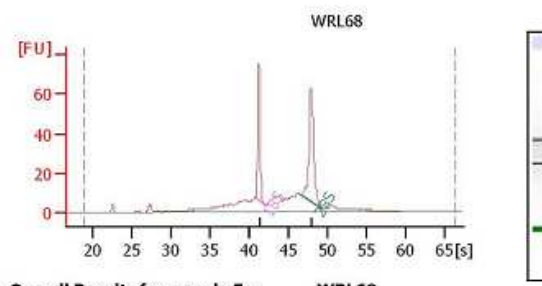
WRL68

Overall Results for sample 5 : **WRL68**

RNA Area:	359,7
RNA Concentration:	409 ng/µl
rRNA Ratio [28s / 18s]:	1,5
RNA Integrity Number (RIN):	7.7 (B.02.07)
Result Flagging Color:	
Result Flagging Label:	RIN: 7.70

Fragment table for sample 5 : **WRL68**

Name	Start Time [s]	End Time [s]	Area	% of total Area
18S	40,86	42,06	53,6	14,9
28S	46,49	49,34	80,0	22,2
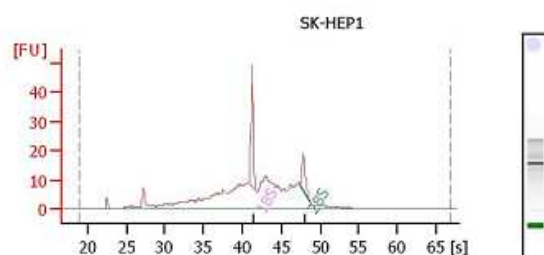
SK-HEP1

Overall Results for sample 6 : **SK-HEP1**

RNA Area:	344,7
RNA Concentration:	392 ng/µl
rRNA Ratio [28s / 18s]:	0,5
RNA Integrity Number (RIN):	5.4 (B.02.07)
Result Flagging Color:	
Result Flagging Label:	RIN: 5.40

Fragment table for sample 6 : **SK-HEP1**

Name	Start Time [s]	End Time [s]	Area	% of total Area
18S	40,88	41,90	31,0	9,0
28S	47,42	48,73	14,1	4,1
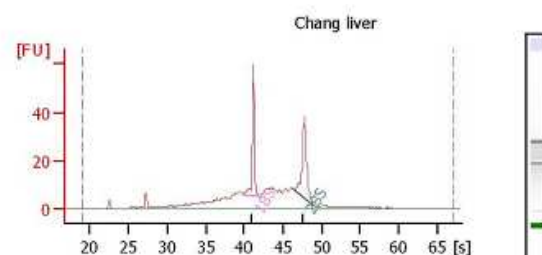
Chang liver

Overall Results for sample 7 : **Chang liver**

RNA Area:	340,4
RNA Concentration:	387 ng/µl
rRNA Ratio [28s / 18s]:	1,1
RNA Integrity Number (RIN):	7.1 (B.02.07)
Result Flagging Color:	
Result Flagging Label:	RIN: 7.10

Fragment table for sample 7 : **Chang liver**

Name	Start Time [s]	End Time [s]	Area	% of total Area
18S	39,94	41,98	44,9	13,2
28S	46,46	48,99	48,1	14,1
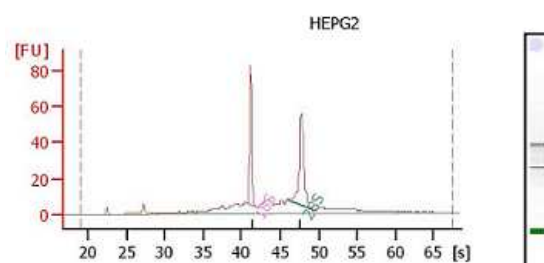
HEPG2

Overall Results for sample 8 : **HEPG2**

RNA Area:	360,6
RNA Concentration:	410 ng/µl
rRNA Ratio [28s / 18s]:	1,2
RNA Integrity Number (RIN):	7.9 (B.02.07)
Result Flagging Color:	
Result Flagging Label:	RIN: 7.90

Fragment table for sample 8 : **HEPG2**

Name	Start Time [s]	End Time [s]	Area	% of total Area
18S	40,79	42,02	60,8	16,9
28S	46,13	49,11	75,0	20,8
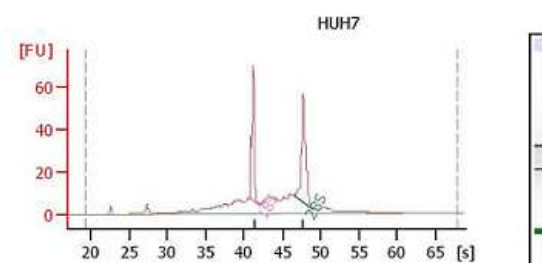
HUH7

Overall Results for sample 9 : **HUH7**

RNA Area:	372,5
RNA Concentration:	424 ng/µl
rRNA Ratio [28s / 18s]:	1,4
RNA Integrity Number (RIN):	7.3 (B.02.07)
Result Flagging Color:	
Result Flagging Label:	RIN: 7.30

Fragment table for sample 9 : **HUH7**

Name	Start Time [s]	End Time [s]	Area	% of total Area
18S	40,82	42,00	49,4	13,3
28S	46,48	48,99	68,9	18,5

Overall Results for sample 10 : __Blank__

RNA Area:	0,4
RNA Concentration:	0 ng/µl
rRNA Ratio [28s / 18s]:	0,0
RNA Integrity Number (RIN):	N/A (B.02.07)
Result Flagging Color:	
Result Flagging Label:	RIN N/A

Overall Results for sample 11 : __Blank__

RNA Area:	5,6
RNA Concentration:	6 ng/µl
rRNA Ratio [28s / 18s]:	0,0
RNA Integrity Number (RIN):	N/A (B.02.07)
Result Flagging Color:	
Result Flagging Label:	RIN N/A

Overall Results for sample 12 : __Blank__

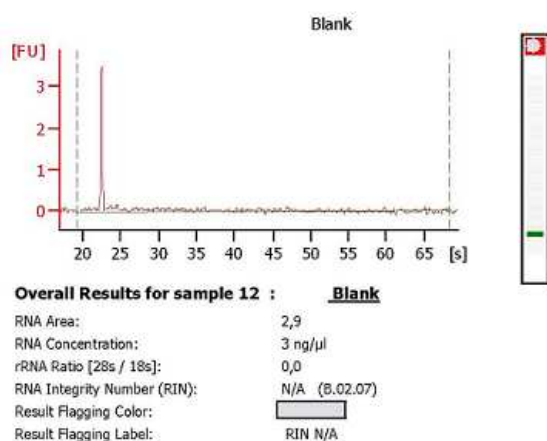|	
RNA Area:	2,9
RNA Concentration:	3 ng/µl
rRNA Ratio [28s / 18s]:	0,0
RNA Integrity Number (RIN):	N/A (B.02.07)
Result Flagging Color:	
Result Flagging Label:	RIN N/A

Chart 2

Standard Curve

3.3 Preliminary Real Time PCR Results

Table 4

Document Name: BEX1-BEX2	07/04/2011	

Document Name: BEX1-BEX2   07/04/2011
Plate Type: Absolute Quantification
User: ICMM8011
Document Information
Operator: ICMM8011
Run Date: Friday   April 08   2011 12:48:13
Last Modified: Friday   April 08   2011 14:10:21
Instrument Type: Applied Biosystems 7300 Real-Time PCR System
Comments:
SDS v1.3.1

Baseline: 3-15

Threshold: 0,2

Thermal Cycler Profile

Stage		Repetitions	Temperature	Time	Ramp Rate	Auto Increment
	1	1	95.0 °C	10:00	Auto	
	2	40	95.0 °C	00:15	Auto	
			60.0 °C	01:00	Auto	

Standard 7300 Mode
Data Collection : Stage 2 Step 1
PCR Volume: 15 µL

Well	Sample Name	Detector	Task	Ct	StdDev Ct
A1	WRL68 Bex1	Bex1 Human	Unknown	35.39	0.324
A2	WRL68 Bex1	Bex1 Human	Unknown	34.91	0.324
A3	WRL68 Bex1	Bex1 Human	Unknown	34.77	0.324
A4	SK-HEP Bex1	Bex1 Human	Unknown	33.03	0.054
A5	SK-HEP Bex1	Bex1 Human	Unknown	33.12	0.054
A6	SK-HEP Bex1	Bex1 Human	Unknown	33.12	0.054
A7	HEPG2 Bex1	Bex1 Human	Unknown	20.76	0.060
A8	HEPG2 Bex1	Bex1 Human	Unknown	20.79	0.060
A9	HEPG2 Bex1	Bex1 Human	Unknown	20.88	0.060
A10	Chang Bex1	Bex1 Human	Unknown	35.87	0.363
A11	Chang Bex1	Bex1 Human	Unknown	35.36	0.363
A12	Chang Bex1	Bex1 Human	Unknown	35.16	0.363
B1	HUH7 Bex1	Bex1 Human	Unknown	23.20	0.045
B2	HUH7 Bex1	Bex1 Human	Unknown	23.27	0.045
B3	HUH7 Bex1	Bex1 Human	Unknown	23.18	0.045
B4	HL28 Bex1	Bex1 Human	Unknown	29.08	0.037
B5	HL28 Bex1	Bex1 Human	Unknown	29.08	0.037
B6	HL28 Bex1	Bex1 Human	Unknown	29.14	0.037
B7	HL42 Bex1	Bex1 Human	Unknown	26.13	0.025
B8	HL42 Bex1	Bex1 Human	Unknown	26.13	0.025
B9	HL42 Bex1	Bex1 Human	Unknown	26.09	0.025
B10	HL50 Bex1	Bex1 Human	Unknown	28.55	0.189
B11	HL50 Bex1	Bex1 Human	Unknown	28.24	0.189
B12	HL50 Bex1	Bex1 Human	Unknown	28.21	0.189
C1	RT WRL68 Bex1	Bex1 Human	Unknown	Undetermined	
C2	RT WRL68 Bex1	Bex1 Human	Unknown	Undetermined	
C3	RT WRL68 Bex1	Bex1 Human	Unknown	Undetermined	
C4	RT HL50 Bex1	Bex1 Human	Unknown	Undetermined	
C5	RT HL50 Bex1	Bex1 Human	Unknown	Undetermined	
C6	RT HL50 Bex1	Bex1 Human	Unknown	Undetermined	

Chart 3

Delta Rn vs Cycle

Delta Rn

Cycle Number
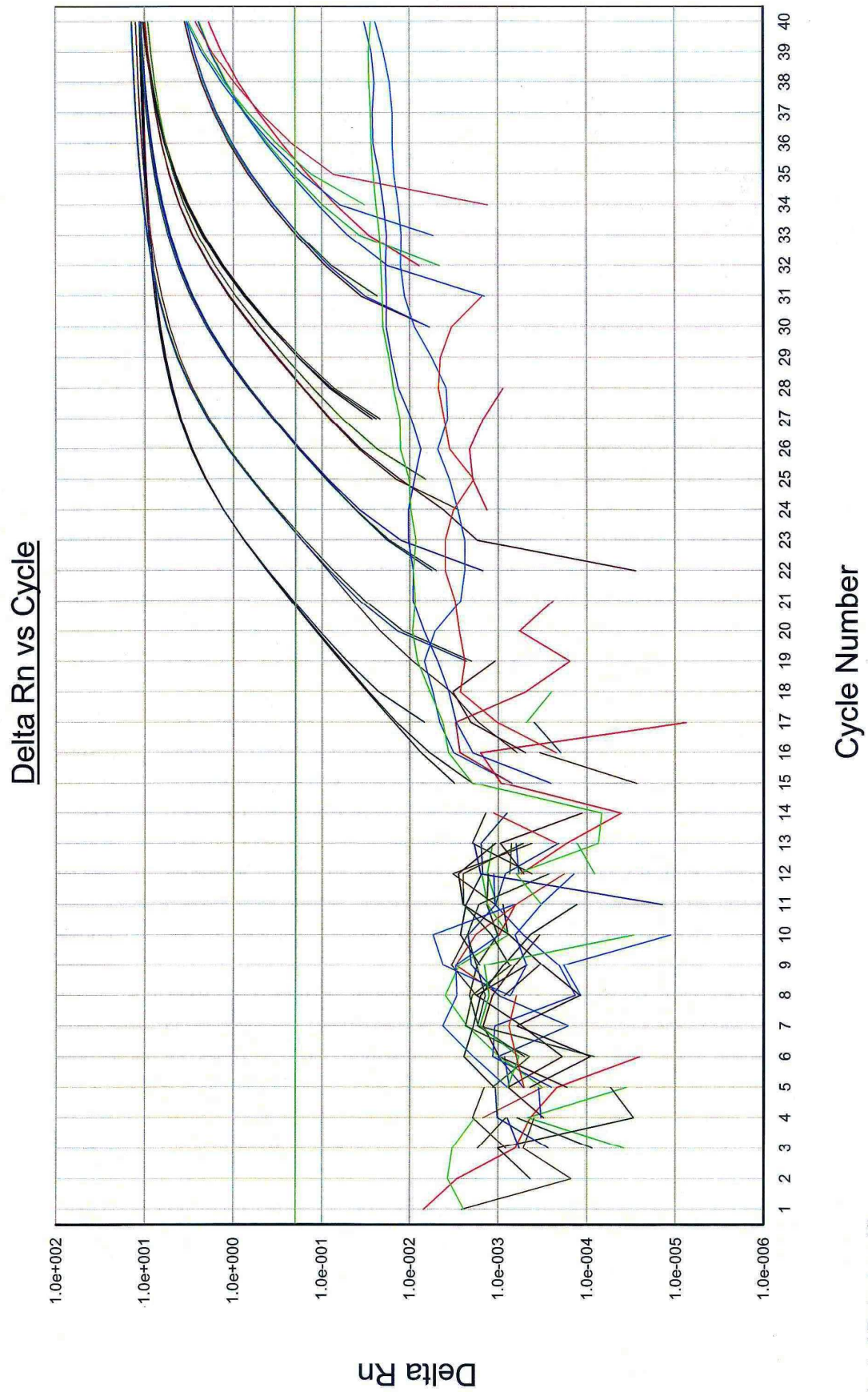
Selected Detector: All

Well(s): A1-C6

Document: BEX1-BEX2,07-04-2011 (Absolute Quantification)

Table 5

Plate Type: Absolute Quantification
User: ICMM8011

Document Information

Operator: ICMM8011
Run Date: Friday   April 08   2011 12:48:13
Last Modified: Friday   April 08   2011 14:10:21
Instrument Type: Applied Biosystems 7300 Real-Time PCR System

Comments:
SDS v1.3.1

Thermal Cycler Profile

Stage	Repetitions	Temperature	Time	Ramp Rate	Auto Increment
1	1	95.0 °C	10:00	Auto	
2	40	95.0 °C	00:15	Auto	
		60.0 °C	01:00	Auto	

Standard 7300 Mode
Data Collection : Stage 2 Step 1
PCR Volume: 15 µL

Well	Sample Name	Detector	Task	Ct	StdDev Ct
D1	WRL68 Bex2	Bex2 Human	Unknown	27.42	0.126
D2	WRL68 Bex2	Bex2 Human	Unknown	27.35	0.126
D3	WRL68 Bex2	Bex2 Human	Unknown	27.18	0.126
D4	SK-HEP Bex2	Bex2 Human	Unknown	25.24	0.038
D5	SK-HEP Bex2	Bex2 Human	Unknown	25.19	0.038
D6	SK-HEP Bex2	Bex2 Human	Unknown	25.16	0.038
D7	HEPG2 Bex2	Bex2 Human	Unknown	27.45	0.025
D8	HEPG2 Bex2	Bex2 Human	Unknown	27.45	0.025
D9	HEPG2 Bex2	Bex2 Human	Unknown	27.49	0.025
D10	Chang Bex2	Bex2 Human	Unknown	29.38	0.179
D11	Chang Bex2	Bex2 Human	Unknown	29.22	0.179
D12	Chang Bex2	Bex2 Human	Unknown	29.58	0.179
E1	HUH7 Bex2	Bex2 Human	Unknown	25.43	0.034
E2	HUH7 Bex2	Bex2 Human	Unknown	25.43	0.034
E3	HUH7 Bex2	Bex2 Human	Unknown	25.37	0.034
E4	HL28 Bex2	Bex2 Human	Unknown	33.73	0.623
E5	HL28 Bex2	Bex2 Human	Unknown	32.57	0.623
E6	HL28 Bex2	Bex2 Human	Unknown	32.77	0.623
E7	HL42 Bex2	Bex2 Human	Unknown	27.72	0.150
E8	HL42 Bex2	Bex2 Human	Unknown	27.45	0.150
E9	HL42 Bex2	Bex2 Human	Unknown	27.48	0.150
E10	HL50 Bex2	Bex2 Human	Unknown	26.40	0.099
E11	HL50 Bex2	Bex2 Human	Unknown	26.55	0.099
E12	HL50 Bex2	Bex2 Human	Unknown	26.37	0.099
F1	RT WRL68 Bex2	Bex2 Human	Unknown	Undetermined	
F2	RT WRL68 Bex2	Bex2 Human	Unknown	Undetermined	
F3	RT WRL68 Bex2	Bex2 Human	Unknown	Undetermined	
F4	RT HL50 Bex2	Bex2 Human	Unknown	Undetermined	
F5	RT HL50 Bex2	Bex2 Human	Unknown	Undetermined	
F6	RT HL50 Bex2	Bex2 Human	Unknown	Undetermined	

Baseline: 3-15

Threshold: 0,1

Chart 4

Delta Rn vs Cycle

Delta Rn
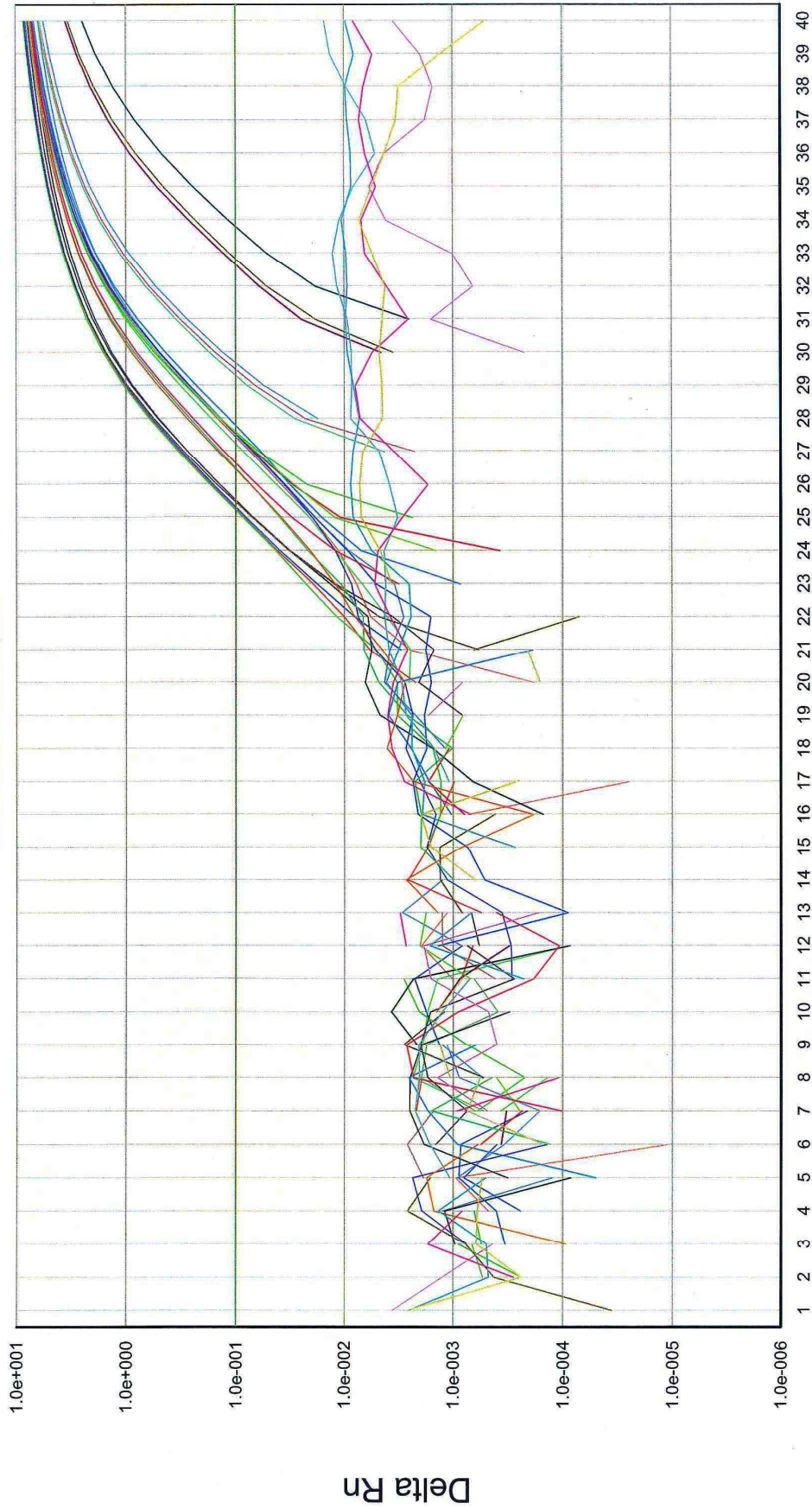
Cycle Number

Selected Detector: All
Well(s): D1-F6
Document: BEX1-BEX2,07-04-2011 (Absolute Quantification)

3.4 Results of Real Time PCR Dilution Curves

Table 6

Document Name: Bex1Bex2 dilution curves HL42 Andrea12042011
Plate Type: Absolute Quantification
User: ICMM8011
Document Information
Operator: ICMM8011

Run Date: Tuesday	April 12	2011 14:17:56	
Last Modified: Tuesday	April 12	2011 15:40:35	

Baseline: 3-15

Threshold: 0,05

Instrument Type: Applied Biosystems 7300 Real-Time PCR System
Comments:
SDS v1.3.1
Thermal Cycler Profile

Stage	Repetitions	Temperature	Time	Ramp Rate	Auto Increment
1	1	95.0 °C	10:00	Auto	
2	40	95.0 °C	00:15	Auto	
		60.0 °C	01:00	Auto	

Standard 7300 Mode
Data Collection : Stage 2 Step 1
PCR Volume: 15 µL

Well	Sample Name	Detector	Task	Ct	StdDev Ct
A1	8 Bex1	Bex1 Human	Unknown	21.24	0.187
A2	8 Bex1	Bex1 Human	Unknown	21.61	0.187
A3	8 Bex1	Bex1 Human	Unknown	21.41	0.187
A4	4 Bex1	Bex1 Human	Unknown	22.52	0.058
A5	4 Bex1	Bex1 Human	Unknown	22.63	0.058
A6	4 Bex1	Bex1 Human	Unknown	22.55	0.058
A7	2 Bex1	Bex1 Human	Unknown	23.68	0.068
A8	2 Bex1	Bex1 Human	Unknown	23.54	0.068
A9	2 Bex1	Bex1 Human	Unknown	23.59	0.068
A10	1 Bex1	Bex1 Human	Unknown	24.56	0.137
A11	1 Bex1	Bex1 Human	Unknown	24.53	0.137
A12	1 Bex1	Bex1 Human	Unknown	24.78	0.137
B1	0.5 Bex1	Bex1 Human	Unknown	25.97	0.326
B2	0.5 Bex1	Bex1 Human	Unknown	25.38	0.326
B3	0.5 Bex1	Bex1 Human	Unknown	25.44	0.326
B4	0.25 Bex1	Bex1 Human	Unknown	26.64	0.143
B5	0.25 Bex1	Bex1 Human	Unknown	26.91	0.143
B6	0.25 Bex1	Bex1 Human	Unknown	26.86	0.143
B7	0.125 Bex1	Bex1 Human	Unknown	27.38	0.232
B8	0.125 Bex1	Bex1 Human	Unknown	27.84	0.232
B9	0.125 Bex1	Bex1 Human	Unknown	27.54	0.232
B10	0.0625 Bex1	Bex1 Human	Unknown	27.81	0.472
B11	0.0625 Bex1	Bex1 Human	Unknown	28.42	0.472
B12	0.0625 Bex1	Bex1 Human	Unknown	27.49	0.472
C1	0.03125 Bex1	Bex1 Human	Unknown	30.74	0.700
C2	0.03125 Bex1	Bex1 Human	Unknown	29.68	0.700
C3	0.03125 Bex1	Bex1 Human	Unknown	29.42	0.700
C4	0.0156 Bex1	Bex1 Human	Unknown	31.34	0.014
C5	0.0156 Bex1	Bex1 Human	Unknown	31.36	0.014
C6	0.0156 Bex1	Bex1 Human	Unknown	31.33	0.014
C7	0.0078 Bex1	Bex1 Human	Unknown	32.93	0.048
C8	0.0078 Bex1	Bex1 Human	Unknown	32.97	0.048
C9	0.0078 Bex1	Bex1 Human	Unknown	32.87	0.048

C10	0.0039 Bex1	Bex1 Human	Unknown	32.42	1.118
C11	0.0039 Bex1	Bex1 Human	Unknown	33.08	1.118
C12	0.0039 Bex1	Bex1 Human	Unknown	34.60	1.118
D1	0.00195 Bex1	Bex1 Human	Unknown	34.76	0.799
D2	0.00195 Bex1	Bex1 Human	Unknown	33.98	0.799
D3	0.00195 Bex1	Bex1 Human	Unknown	33.17	0.799
D4	0.00098 Bex1	Bex1 Human	Unknown	35.21	
D5	0.00098 Bex1	Bex1 Human	Unknown	Undetermined	
D6	0.00098 Bex1	Bex1 Human	Unknown	Undetermined	
D7	0.0005 Bex1	Bex1 Human	Unknown	Undetermined	
D8	0.0005 Bex1	Bex1 Human	Unknown	Undetermined	
D9	0.0005 Bex1	Bex1 Human	Unknown	Undetermined	
D10	0.00024 Bex1	Bex1 Human	Unknown	36.47	0.413
D11	0.00024 Bex1	Bex1 Human	Unknown	Undetermined	

Dilution Curve Bex1:

Chart 5

Log ul cDNA vs. Ct

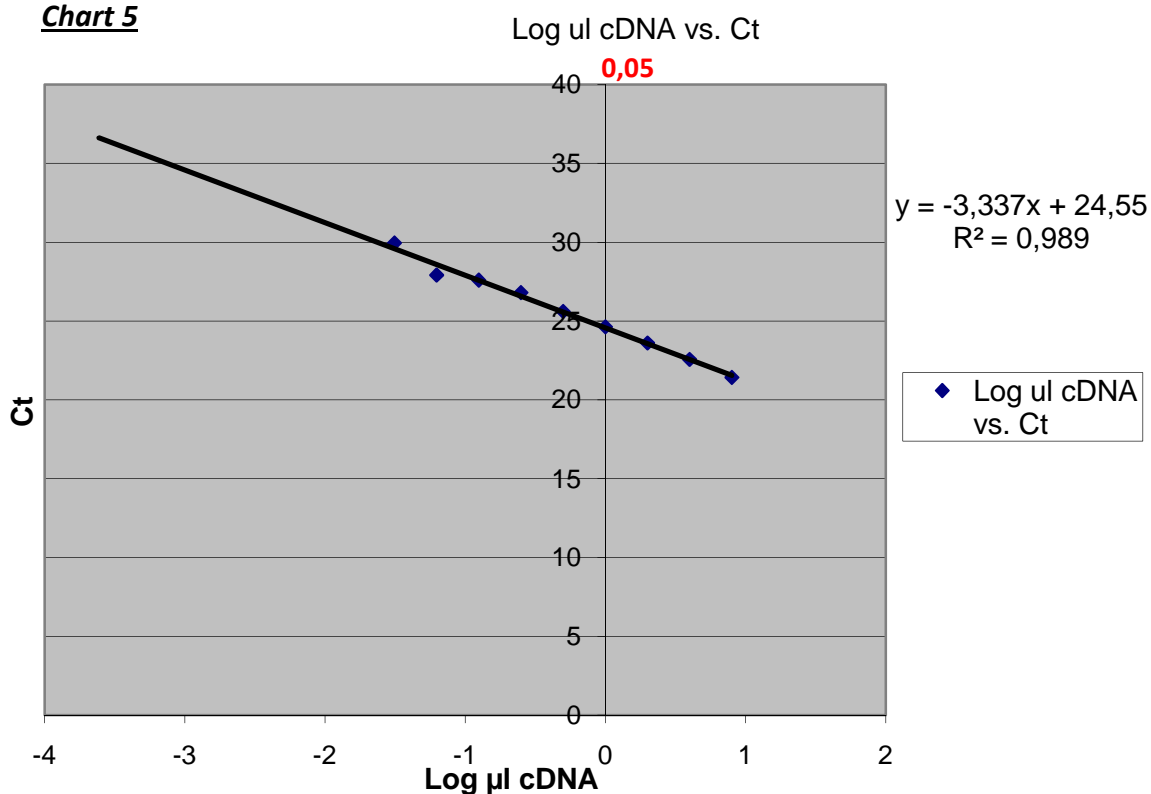$y = -3{,}337x + 24{,}55$
$R^2 = 0{,}989$

Table 7

Document Name: Bex1Bex2 dilution curves HL42 Andrea12042011
Plate Type: Absolute Quantification
User: ICMM8011
Document Information
Operator: ICMM8011

Baseline: 3-15	
Threshold: 0,1	

Run Date: Tuesday   April 12   2011 14:17:56
Last Modified: Tuesday   April 12   2011 15:40:35
Instrument Type: Applied Biosystems 7300 Real-Time PCR System
Comments:
SDS v1.3.1
Thermal Cycler Profile

Stage	Repetitions	Temperature	Time	Ramp Rate	Auto Increment
1	1	95.0 °C	10:00	Auto	
2	40	95.0 °C	00:15	Auto	
		60.0 °C	01:00	Auto	

Standard 7300 Mode
Data Collection : Stage 2 Step 1
PCR Volume: 15 µL

Well	Sample Name	Detector	Task	Ct	StdDev Ct
E1	8 Bex2	Bex2 Human	Unknown	27.65	0.356
E2	8 Bex2	Bex2 Human	Unknown	27.26	0.356
E3	8 Bex2	Bex2 Human	Unknown	26.94	0.356
E4	4 Bex2	Bex2 Human	Unknown	27.02	0.171
E5	4 Bex2	Bex2 Human	Unknown	26.87	0.171
E6	4 Bex2	Bex2 Human	Unknown	26.67	0.171
E7	2 Bex2	Bex2 Human	Unknown	28.22	0.109
E8	2 Bex2	Bex2 Human	Unknown	28.02	0.109
E9	2 Bex2	Bex2 Human	Unknown	28.06	0.109
E10	1 Bex2	Bex2 Human	Unknown	28.96	0.040
E11	1 Bex2	Bex2 Human	Unknown	28.96	0.040
E12	1 Bex2	Bex2 Human	Unknown	29.03	0.040
F1	0.5 Bex2	Bex2 Human	Unknown	30.23	0.136
F2	0.5 Bex2	Bex2 Human	Unknown	30.45	0.136
F3	0.5 Bex2	Bex2 Human	Unknown	30.21	0.136
F4	0.25 Bex2	Bex2 Human	Unknown	31.57	0.143
F5	0.25 Bex2	Bex2 Human	Unknown	31.29	0.143
F6	0.25 Bex2	Bex2 Human	Unknown	31.38	0.143
F7	0.125 Bex2	Bex2 Human	Unknown	32.28	0.144
F8	0.125 Bex2	Bex2 Human	Unknown	32.01	0.144
F9	0.125 Bex2	Bex2 Human	Unknown	32.24	0.144
F10	0.0625 Bex2	Bex2 Human	Unknown	33.32	0.228
F11	0.0625 Bex2	Bex2 Human	Unknown	33.43	0.228
F12	0.0625 Bex2	Bex2 Human	Unknown	32.99	0.228
G1	0.03125 Bex2	Bex2 Human	Unknown	34.20	0.033
G2	0.03125 Bex2	Bex2 Human	Unknown	34.26	0.033
G3	0.03125 Bex2	Bex2 Human	Unknown	34.21	0.033
G4	0.01563 Bex2	Bex2 Human	Unknown	35.19	0.380
G5	0.01563 Bex2	Bex2 Human	Unknown	35.32	0.380
G6	0.01563 Bex2	Bex2 Human	Unknown	34.60	0.380
G7	0.0078 Bex2	Bex2 Human	Unknown	36.11	0.635
G8	0.0078 Bex2	Bex2 Human	Unknown	36.13	0.635
G9	0.0078 Bex2	Bex2 Human	Unknown	37.22	0.635

G10	0.00391 Bex2	Bex2 Human	Unknown	38.18	0.834
G11	0.00391 Bex2	Bex2 Human	Unknown	Undetermined	
G12	0.00391 Bex2	Bex2 Human	Unknown	39.36	0.834
H1	0.00195 Bex2	Bex2 Human	Unknown	Undetermined	
H2	0.00195 Bex2	Bex2 Human	Unknown	38.16	1.035
H3	0.00195 Bex2	Bex2 Human	Unknown	39.62	1.035
H4	0.00098 Bex2	Bex2 Human	Unknown	37.75	0.911
H5	0.00098 Bex2	Bex2 Human	Unknown	Undetermined	
H6	0.00098 Bex2	Bex2 Human	Unknown	39.04	0.911
H7	0.0005 Bex2	Bex2 Human	Unknown	Undetermined	
H8	0.0005 Bex2	Bex2 Human	Unknown	38.76	
H9	0.0005 Bex2	Bex2 Human	Unknown	Undetermined	
H10	0.00024 Bex2	Bex2 Human	Unknown	Undetermined	
H11	0.00024 Bex2	Bex2 Human	Unknown	Undetermined	
H12	0.00024 Bex2	Bex2 Human	Unknown	Undetermined	

Dilution Curve Bex2:

Chart 6

Log ul cDNA vs. Ct

0.1

$y = -3,317x + 29,18$
$R^2 = 0,997$

3.5 Real Time PCR Results

Table 8

Document Name: Bex1Bex2   Human livers   13-04-2011
Plate Type: Absolute Quantification
User: ICMM8011
Document Information
Operator: ICMM8011

	Baseline: 3-15
	Threshold: 0,05

		2011
Run Date: Wednesday	April 13	14:06:55
		2011
Last Modified: Wednesday	April 13	15:29:16

Instrument Type: Applied Biosystems 7300 Real-Time PCR System
Comments:
SDS v1.3.1
Thermal Cycler Profile

Stage	Repetitions	Temperature	Time	Ramp Rate	Auto Increment
1	1	95.0 ⁻C	10:00	Auto	
2	40	95.0 ⁻C	00:15	Auto	
		60.0 ⁻C	01:00	Auto	

Standard 7300 Mode
Data Collection : Stage 2 Step 1
PCR Volume: 15 ·L

Well	Sample Name	Detector	Task	Ct	StdDev Ct
A1	HL26 Bex1	Bex1 Human	Unknown	27.59	0.030
A2	HL26 Bex1	Bex1 Human	Unknown	27.62	0.030
A3	HL26 Bex1	Bex1 Human	Unknown	27.56	0.030
A4	HL27 Bex1	Bex1 Human	Unknown	25.52	0.140
A5	HL27 Bex1	Bex1 Human	Unknown	25.25	0.140
A6	HL27 Bex1	Bex1 Human	Unknown	25.33	0.140
A7	HL28 Bex1	Bex1 Human	Unknown	28.28	0.144
A8	HL28 Bex1	Bex1 Human	Unknown	28.05	0.144
A9	HL28 Bex1	Bex1 Human	Unknown	28.32	0.144
A10	HL32 Bex1	Bex1 Human	Unknown	26.04	0.257
A11	HL32 Bex1	Bex1 Human	Unknown	26.33	0.257
A12	HL32 Bex1	Bex1 Human	Unknown	26.55	0.257
B1	HL33 Bex1	Bex1 Human	Unknown	28.28	0.126
B2	HL33 Bex1	Bex1 Human	Unknown	28.12	0.126
B3	HL33 Bex1	Bex1 Human	Unknown	28.03	0.126
B4	HL36 Bex1	Bex1 Human	Unknown	27.51	0.273
B5	HL36 Bex1	Bex1 Human	Unknown	27.22	0.273
B6	HL36 Bex1	Bex1 Human	Unknown	26.96	0.273
B7	HL38 Bex1	Bex1 Human	Unknown	27.45	0.156
B8	HL38 Bex1	Bex1 Human	Unknown	27.76	0.156
B9	HL38 Bex1	Bex1 Human	Unknown	27.66	0.156
B10	HL42 Bex1	Bex1 Human	Unknown	25.10	0.253
B11	HL42 Bex1	Bex1 Human	Unknown	24.66	0.253
B12	HL42 Bex1	Bex1 Human	Unknown	24.66	0.253
C1	HL43 Bex1	Bex1 Human	Unknown	28.33	0.671
C2	HL43 Bex1	Bex1 Human	Unknown	27.28	0.671
C3	HL43 Bex1	Bex1 Human	Unknown	27.07	0.671
C4	HL44 Bex1	Bex1 Human	Unknown	28.05	0.296

Well	Sample Name	Detector	Task	Ct	StdDev Ct
C5	HL44 Bex1	Bex1 Human	Unknown	27.85	0.296
C6	HL44 Bex1	Bex1 Human	Unknown	27.47	0.296
C7	HL47 Bex1	Bex1 Human	Unknown	29.03	0.133
C8	HL47 Bex1	Bex1 Human	Unknown	29.25	0.133
C9	HL47 Bex1	Bex1 Human	Unknown	29.02	0.133
C10	HL49 Bex1	Bex1 Human	Unknown	29.59	0.359
C11	HL49 Bex1	Bex1 Human	Unknown	28.88	0.359
C12	HL49 Bex1	Bex1 Human	Unknown	29.19	0.359
D1	HL52 Bex1	Bex1 Human	Unknown	26.87	0.053
D2	HL52 Bex1	Bex1 Human	Unknown	26.79	0.053
D3	HL52 Bex1	Bex1 Human	Unknown	26.76	0.053
D4	HL54 Bex1	Bex1 Human	Unknown	25.37	0.091
D5	HL54 Bex1	Bex1 Human	Unknown	25.19	0.091
D6	HL54 Bex1	Bex1 Human	Unknown	25.25	0.091
D7	HL62 Bex1	Bex1 Human	Unknown	28.18	0.054
D8	HL62 Bex1	Bex1 Human	Unknown	28.07	0.054
D9	HL62 Bex1	Bex1 Human	Unknown	28.13	0.054
D10	Minus RT Bex1	Bex1 Human	Unknown	Undetermined	
D11	Minus RT Bex1	Bex1 Human	Unknown	Undetermined	
D12	Minus RT Bex1	Bex1 Human	Unknown	Undetermined	

Table 9

Document Name: Bex1Bex2   Human livers   13-04-2011
Plate Type: Absolute Quantification
User: ICMM8011
Document Information
Operator: ICMM8011

		Baseline: 3-15
		Threshold: 0,1

Run Date: Wednesday   April 13   2011
                                            14:06:55
Last Modified: Wednesday   April 13   2011
                                            15:29:16
Instrument Type: Applied Biosystems 7300 Real-Time PCR System
Comments:
SDS v1.3.1
Thermal Cycler Profile

Stage		Repetitions	Temperature	Time	Ramp Rate	Auto Increment
	1	1	95.0 −C	10:00	Auto	
	2	40	95.0 −C	00:15	Auto	
			60.0 −C	01:00	Auto	

Standard 7300 Mode
Data Collection : Stage 2 Step 1
PCR Volume: 15 μL

Well	Sample Name	Detector	Task	Ct	StdDev Ct
E1	HL26 Bex2	Bex2 Human	Unknown	31.25	0.210
E2	HL26 Bex2	Bex2 Human	Unknown	30.83	0.210
E3	HL26 Bex2	Bex2 Human	Unknown	31.07	0.210
E4	HL27 Bex2	Bex2 Human	Unknown	30.11	0.082
E5	HL27 Bex2	Bex2 Human	Unknown	30.19	0.082
E6	HL27 Bex2	Bex2 Human	Unknown	30.02	0.082

E7	HL28 Bex2	Bex2 Human	Unknown	35.08	0.546
E8	HL28 Bex2	Bex2 Human	Unknown	34.18	0.546
E9	HL28 Bex2	Bex2 Human	Unknown	34.09	0.546
E10	HL32 Bex2	Bex2 Human	Unknown	30.19	0.076
E11	HL32 Bex2	Bex2 Human	Unknown	30.34	0.076
E12	HL32 Bex2	Bex2 Human	Unknown	30.23	0.076
F1	HL33 Bex2	Bex2 Human	Unknown	32.08	0.268
F2	HL33 Bex2	Bex2 Human	Unknown	31.55	0.268
F3	HL33 Bex2	Bex2 Human	Unknown	31.72	0.268
F4	HL36 Bex2	Bex2 Human	Unknown	30.20	0.079
F5	HL36 Bex2	Bex2 Human	Unknown	30.36	0.079
F6	HL36 Bex2	Bex2 Human	Unknown	30.27	0.079
F7	HL38 Bex2	Bex2 Human	Unknown	30.93	0.288
F8	HL38 Bex2	Bex2 Human	Unknown	30.36	0.288
F9	HL38 Bex2	Bex2 Human	Unknown	30.53	0.288
F10	HL42 Bex2	Bex2 Human	Unknown	29.52	0.098
F11	HL42 Bex2	Bex2 Human	Unknown	29.33	0.098
F12	HL42 Bex2	Bex2 Human	Unknown	29.38	0.098
G1	HL43 Bex2	Bex2 Human	Unknown	30.08	0.211
G2	HL43 Bex2	Bex2 Human	Unknown	29.67	0.211
G3	HL43 Bex2	Bex2 Human	Unknown	29.77	0.211
G4	HL44 Bex2	Bex2 Human	Unknown	31.43	0.110
G5	HL44 Bex2	Bex2 Human	Unknown	31.26	0.110
G6	HL44 Bex2	Bex2 Human	Unknown	31.22	0.110
G7	HL47 Bex2	Bex2 Human	Unknown	31.62	0.167
G8	HL47 Bex2	Bex2 Human	Unknown	31.38	0.167
G9	HL47 Bex2	Bex2 Human	Unknown	31.30	0.167
G10	HL49 Bex2	Bex2 Human	Unknown	31.80	0.359
G11	HL49 Bex2	Bex2 Human	Unknown	31.16	0.359
G12	HL49 Bex2	Bex2 Human	Unknown	31.20	0.359
H1	HL52 Bex2	Bex2 Human	Unknown	30.72	0.395
H2	HL52 Bex2	Bex2 Human	Unknown	30.17	0.395
H3	HL52 Bex2	Bex2 Human	Unknown	29.96	0.395
H4	HL54 Bex2	Bex2 Human	Unknown	29	1
H5	HL54 Bex2	Bex2 Human	Unknown	30,03	1
H6	HL54 Bex2	Bex2 Human	Unknown		
H7	HL62 Bex2	Bex2 Human	Unknown	30.95	0.176
H8	HL62 Bex2	Bex2 Human	Unknown	30.60	0.176
H9	HL62 Bex2	Bex2 Human	Unknown	30.72	0.176
H10	Minus RT Bex2	Bex2 Human	Unknown	Undetermined	
H11	Minus RT Bex2	Bex2 Human	Unknown	Undetermined	
H12	Minus RT Bex2	Bex2 Human	Unknown	Undetermined	

3.6 *Real Time PCR Calculations*

The Comparative C_T Method (ΔΔ C_T Method)

The Comparative C_T Method, also referred to as the ΔΔC_T Method ,it uses arithmetic formulas to achieve the result for relative quantitation.

Arithmetic Formula:

The amount of target, normalized to an endogenous reference and relative to a calibrator, is given by:

$$2^{-\Delta\Delta C_T}$$

1. **Calculate the mean and standard deviation values of the replicate sample results.**

Mean C_T values and standard deviations can be calculated in Microsoft® Excel software

2. **Calculate the ΔC_T value.**

The ΔC_T value is calculated by:

$$\Delta C_T = C_{T\,target} - C_{T\,reference}$$

3. **Calculate the standard deviation of the ΔC_T value.**

The standard deviation of the ΔC_T is calculated from the standard deviations of the target and reference values using the formula:

$$s = (s_1 2 + s_2 2)1/2$$

where X1/2 is the square root of X and s= standard deviation

4. Calculate the $\Delta\Delta C_T$ value.

The $\Delta\Delta C_T$ is calculated by:

$$\Delta\Delta C_T = \Delta C_T \text{ test sample} - \Delta C_T \text{ calibrator sample}$$

5. Calculate the standard deviation of the $\Delta\Delta C_T$ value.

The calculation of $\Delta\Delta C_T$ involves subtraction of the ΔC_T calibrator value. This is subtraction of an arbitrary constant, so the standard deviation of the $\Delta\Delta C_T$ value is the same as the standard deviation of the ΔC_T value.

6. Incorporating the standard deviation of the $\Delta\Delta C_T$ values into the fold-difference.

Fold-differences calculated using the $\Delta\Delta C_T$ method are usually expressed as a range, which is a result of incorporating the standard deviation of the $\Delta\Delta C_T$ value into the fold-difference calculation.

The range for target$_N$, relative to a calibrator sample, is calculated by: 2–$\Delta\Delta C_t$ with $\Delta\Delta C_T$ + s and $\Delta\Delta C_T$ – s, where s is the standard deviation of the $\Delta\Delta C_T$ value.

Fold Change Bex1

Table 10

Well	Sample Name	Detector	Ct	StdDev Ct (S_1)	Bex1 mean	Average for controls (HL28, HL33,HL47,HL49)
A1	HL26 Bex1	Bex1	27,59	0,03		
A2	HL26 Bex1	Bex1	27,62	0,03		
A3	HL26 Bex1	Bex1	27,56	0,03	27,59	
A4	HL27 Bex1	Bex1	25,52	0,14		
A5	HL27 Bex1	Bex1	25,25	0,14		
A6	HL27 Bex1	Bex1	25,33	0,14	25,36666667	
A7	HL28 Bex1	Bex1	28,28	0,144		
A8	HL28 Bex1	Bex1	28,05	0,144		
A9	HL28 Bex1	Bex1	28,32	0,144	28,21666667	28,67
A10	HL32 Bex1	Bex1	26,04	0,257		
A11	HL32 Bex1	Bex1	26,33	0,257		
A12	HL32 Bex1	Bex1	26,55	0,257	26,30666667	
B1	HL33 Bex1	Bex1	28,28	0,126		
B2	HL33 Bex1	Bex1	28,12	0,126		
B3	HL33 Bex1	Bex1	28,03	0,126	28,14333333	
B4	HL36 Bex1	Bex1	27,51	0,273		
B5	HL36 Bex1	Bex1	27,22	0,273		
B6	HL36 Bex1	Bex1	26,96	0,273	27,23	
B7	HL38 Bex1	Bex1	27,45	0,156		
B8	HL38 Bex1	Bex1	27,76	0,156		
B9	HL38 Bex1	Bex1	27,66	0,156	27,62333333	
B10	HL42 Bex1	Bex1	25,1	0,253		
B11	HL42 Bex1	Bex1	24,66	0,253		
B12	HL42 Bex1	Bex1	24,66	0,253	24,80666667	
C1	HL43 Bex1	Bex1	28,33	0,671		
C2	HL43 Bex1	Bex1	27,28	0,671		
C3	HL43 Bex1	Bex1	27,07	0,671	27,56	
C4	HL44 Bex1	Bex1	28,05	0,296		
C5	HL44 Bex1	Bex1	27,85	0,296		
C6	HL44 Bex1	Bex1	27,47	0,296	27,79	
C7	HL47 Bex1	Bex1	29,03	0,133		
C8	HL47 Bex1	Bex1	29,25	0,133		
C9	HL47 Bex1	Bex1	29,02	0,133	29,1	
C10	HL49 Bex1	Bex1	29,59	0,359		
C11	HL49 Bex1	Bex1	28,88	0,359		
C12	HL49 Bex1	Bex1	29,19	0,359	29,22	
D1	HL52 Bex1	Bex1	26,87	0,053		
D2	HL52 Bex1	Bex1	26,79	0,053		
D3	HL52 Bex1	Bex1	26,76	0,053	26,80666667	
D4	HL54 Bex1	Bex1	25,37	0,091		
D5	HL54 Bex1	Bex1	25,19	0,091		

D6	HL54 Bex1	Bex1	25,25	0,091	25,27	
D7	HL62 Bex1	Bex1	28,18	0,054		
D8	HL62 Bex1	Bex1	28,07	0,054		
D9	HL62 Bex1	Bex1	28,13	0,054	28,12666667	

ΔCT = CT test sample - Ct calibrator sample (HL28,HL33,HL47,HL49)	±S	ΔCT+S	ΔCT-S	Fold change (ΔCT+S) = $2^{-\Delta CT+S}$
-1,08	0,030	-1,05	-1,11	2,070529848
-3,303333333	0,14	-3,163333333	-3,443333333	8,958972832
-0,453333333	0,144	-0,309333333	-0,597	1,239134966
-2,363333333	0,257	-2,106333333	-2,620333333	4,305955271
-0,526666667	0,126	-0,401	-0,653	1,320
-1,44	0,273	-1,167	-1,713	2,245442844
-1,046666667	0,156	-0,891	-1,203	1,854032671
-3,863333333	0,253	-3,610333333	-4,116333333	12,21289512
-1,11	0,671	-0,439	-1,781	1,355664327
-0,88	0,296	-0,584	-1,176	1,498999602
0,43	0,133	0,563	0,297	0,67689314
0,55	0,359	0,909	0,191	0,532554102
-1,863333333	0,053	-1,810333333	-1,916333333	3,507233135
-3,4	0,091	-3,309	-3,491	9,910789582
-0,543333333	0,054	-0,489333333	-0,597333333	1,403796034

Fold Change Bex2

Table 11

Well	Sample Name	Detector	Ct	StdDev Ct (S_1)	Bex2 mean	Average for controls (HL28, HL33,HL47,HL49)
A1	HL26 Bex2	Bex2	31,25	0,21		
A2	HL26 Bex2	Bex2	30,83	0,21		
A3	HL26 Bex2	Bex2	31,07	0,21	31,05	
A4	HL27 Bex2	Bex2	30,11	0,082		
A5	HL27 Bex2	Bex2	30,19	0,082		
A6	HL27 Bex2	Bex2	30,02	0,082	30,10666667	
A7	HL28 Bex2	Bex2	35,08	0,546		
A8	HL28 Bex2	Bex2	34,18	0,546		
A9	HL28 Bex2	Bex2	34,09	0,546	34,135	32,18458333
A10	HL32 Bex2	Bex2	30,19	0,076		
A11	HL32 Bex2	Bex2	30,34	0,076		
A12	HL32 Bex2	Bex2	30,23	0,076	30,25333333	
B1	HL33 Bex2	Bex2	32,08	0,268		
B2	HL33 Bex2	Bex2	31,55	0,268		
B3	HL33 Bex2	Bex2	31,72	0,268	31,78333333	
B4	HL36 Bex2	Bex2	30,2	0,079		
B5	HL36 Bex2	Bex2	30,36	0,079		
B6	HL36 Bex2	Bex2	30,27	0,079	30,27666667	
B7	HL38 Bex2	Bex2	30,93	0,288		

B8	HL38 Bex2	Bex2	30,36	0,288		
B9	HL38 Bex2	Bex2	30,53	0,288	30,73	
B10	HL42 Bex2	Bex2	29,52	0,098		
B11	HL42 Bex2	Bex2	29,33	0,098		
B12	HL42 Bex2	Bex2	29,38	0,098	29,41	
C1	HL43 Bex2	Bex2	30,08	0,211		
C2	HL43 Bex2	Bex2	29,67	0,211		
C3	HL43 Bex2	Bex2	29,77	0,211	29,84	
C4	HL44 Bex2	Bex2	31,43	0,11		
C5	HL44 Bex2	Bex2	31,26	0,11		
C6	HL44 Bex2	Bex2	31,22	0,11	31,30333333	
C7	HL47 Bex2	Bex2	31,62	0,167		
C8	HL47 Bex2	Bex2	31,38	0,167		
C9	HL47 Bex2	Bex2	31,3	0,167	31,43333333	
C10	HL49 Bex2	Bex2	31,8	0,359		
C11	HL49 Bex2	Bex2	31,16	0,359		
C12	HL49 Bex2	Bex2	31,2	0,359	31,38666667	
D1	HL52 Bex2	Bex2	30,72	0,395		
D2	HL52 Bex2	Bex2	30,17	0,395		
D3	HL52 Bex2	Bex2	29,96	0,395	30,28333333	
D4	HL54 Bex2	Bex2	29	1		
D6	HL54 Bex2	Bex2		1	29	
D7	HL62 Bex2	Bex2	30,95	0,176		
D8	HL62 Bex2	Bex2	30,6	0,176		
D9	HL62 Bex2	Bex2	30,72	0,176	30,75666667	

ΔCT = CT test sample - Ct calibrator sample (HL28,HL33,HL47,HL49)	±S	ΔCT+S	ΔCT-S	Fold change (ΔCT+S) = $2^{-\Delta CT+S}$	Fold change (ΔCT+S) = $2^{-\Delta CT-S}$
-1,134583333	0,210	-0,925	-1,134583333	1,898	2,195551436
-2,077916667	0,082	-1,995916667	-2,159916667	3,988694603	4,468890412
1,950416667	0,546	2,496416667	1,404416667	0,177216315	0,377770862
-1,93125	0,076	-1,85525	-2,00725	3,618144433	4,020151861
-0,40125	0,268	-0,133	-0,669	1,097	1,590
-1,907916667	0,079	-1,828916667	-1,986916667	3,552701965	3,963889283
-1,454583333	0,288	-1,166583333	-1,742583333	2,244794428	3,346338371
-2,774583333	0,098	-2,676583333	-2,872583333	6,39339989	7,323754003
-2,344583333	0,211	-2,133583333	-2,555583333	4,388060246	5,879051164
-0,88125	0,11	-0,77125	-0,99125	1,706747927	1,987906635
-0,75125	0,167	-0,58425	-0,91825	1,499259381	1,889821535
-0,797916667	0,359	-0,438916667	-1,156916667	1,355586023	2,229803635
-1,90125	0,395	-1,50625	-2,29625	2,840706931	4,911793811
-3,184583333	1	-2,184583333	-4,184583333	4,54595478	18,18381912
-1,427916667	0,176	-1,251916667	-1,603916667	2,38157613	3,039674129

Normalization

donor media Bex1	dev st media Bex1	donor media Bex2	dev st media Bex2	
28,82111111	0,590031386	31,53444444	0,216803376	*Table 12*

ΔCt (Bex1-Bex2)	bex1 st dev	bex2 st dev	$s1^2 + s2^2$	dev standard (bex1-bex2)
-2,713333333 donor	0,590031386 donor	0,217 donor	0,39514074	0,628602212
-3,46	0,03	0,21	0,045	0,212132034
-4,74	0,14	0,082	0,026324	0,162246726
-5,918333333	0,144	0,546	0,318852	0,564669815
-3,946666667	0,257	0,076	0,071825	0,268001866
-3,64	0,126	0,268	0,0877	0,296141858
-3,046666667	0,273	0,079	0,08077	0,284200633
-3,106666667	0,156	0,288	0,10728	0,327536258
-4,603333333	0,253	0,098	0,073613	0,271317158
-2,28	0,671	0,211	0,494762	0,703393204
-3,513333333	0,296	0,11	0,099716	0,315778403
-2,333333333	0,133	0,167	0,045578	0,213490047
-2,166666667	0,359	0,359	0,257762	0,507702669
-3,476666667	0,053	0,395	0,158834	0,398539835
-3,73	0,091	1	1,008281	1,004131963
-2,63	0,054	0,176	0,033892	0,1840978

ΔΔCt(ΔCt tr-ΔCt donor)	change fold($2^{-\Delta\Delta Ct}$)	chage fold-dev.stand	change fold+dev.stand
0	1	0,371397788	1,628602212
-0,746666667	1,67791155	1,465779515	1,890043584
-2,026666667	4,07462324	3,912376514	4,236869966
-3,205	9,221490774	8,656820959	9,786160589
-1,233333333	2,351095813	2,083093947	2,619097678
-0,926666667	1,900878955	1,604737098	2,197020813
-0,333333333	1,25992105	0,975720417	1,544121683
-0,393333333	1,313424556	0,985888298	1,640960813
-1,89	3,706352248	3,43503509	3,977669405
0,433333333	0,740548776	0,037155572	1,443941981
-0,8	1,741101127	1,425322723	2,05687953
0,38	0,768437591	0,554947544	0,981927637
0,546666667	0,684600064	0,176897396	1,192302733
-0,763333333	1,697407943	1,298868108	2,095947778
-1,016666667	2,023238881	1,019106917	3,027370844
0,083333333	0,943874313	0,759776513	1,127972113

3.7 Real Time PCR Charts (GraphPad Prism)

Ct values Bex1

Chart 7
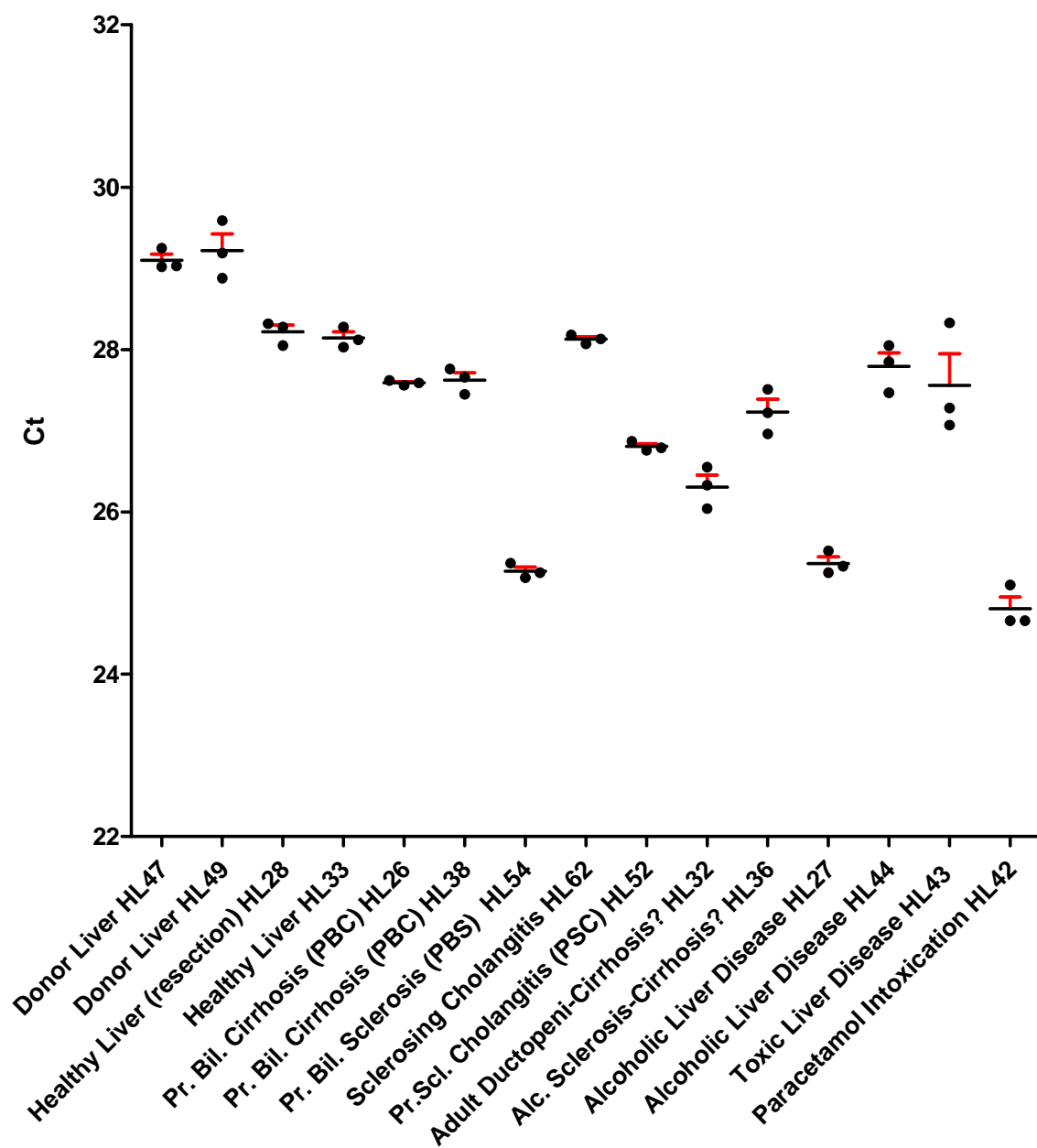
Ct values Bex2
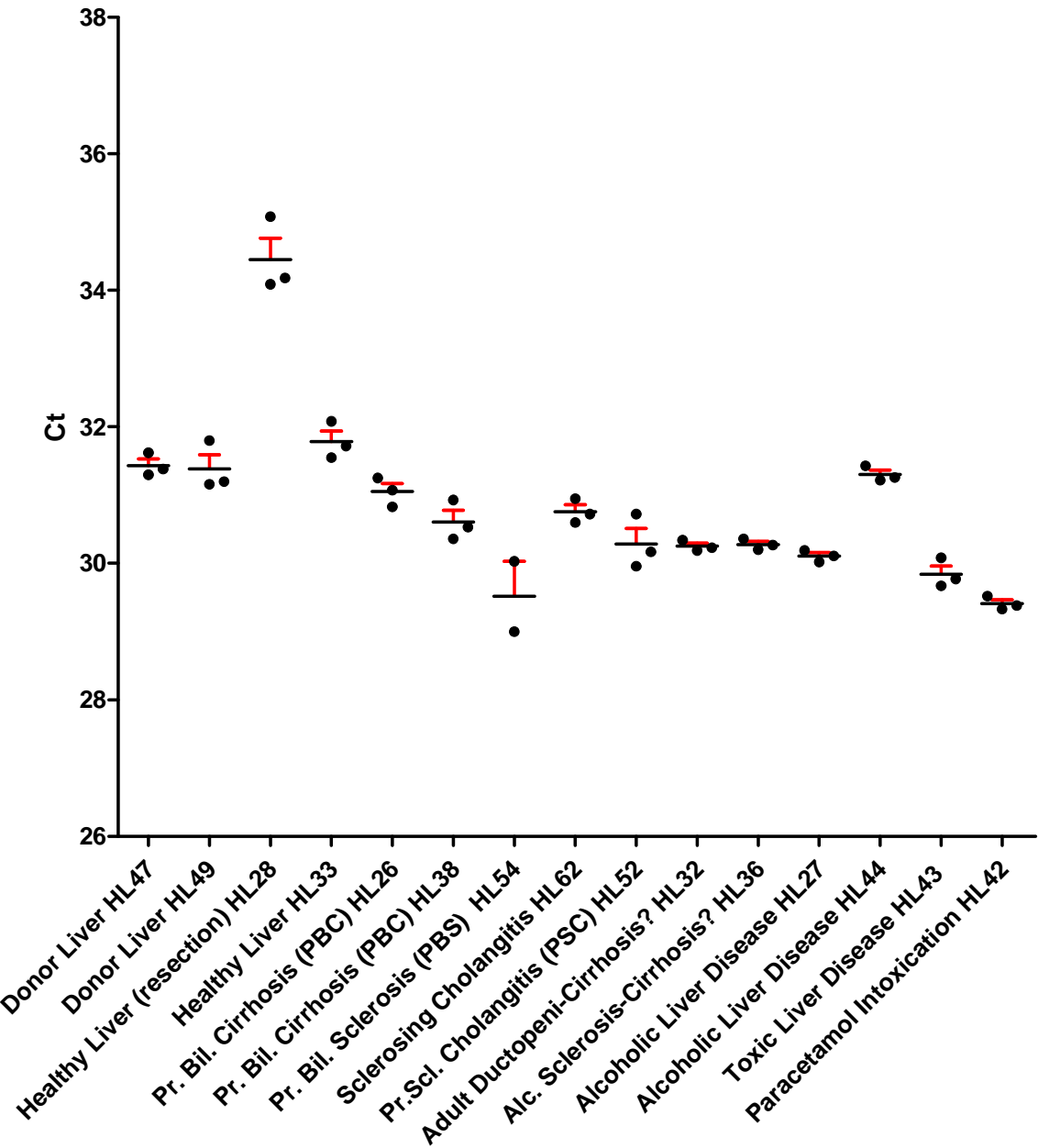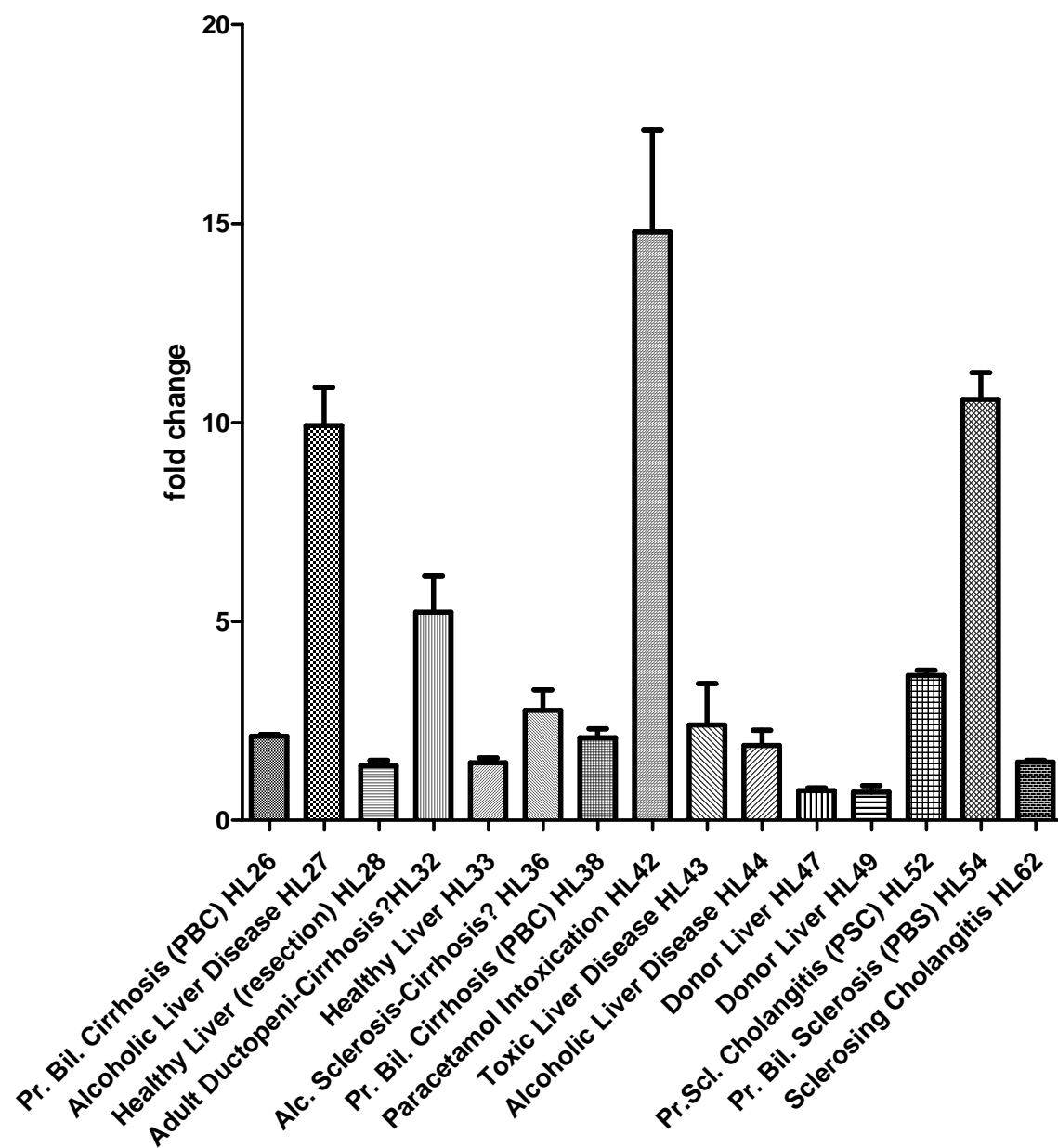
Fold change Bex1

Fold change Bex2
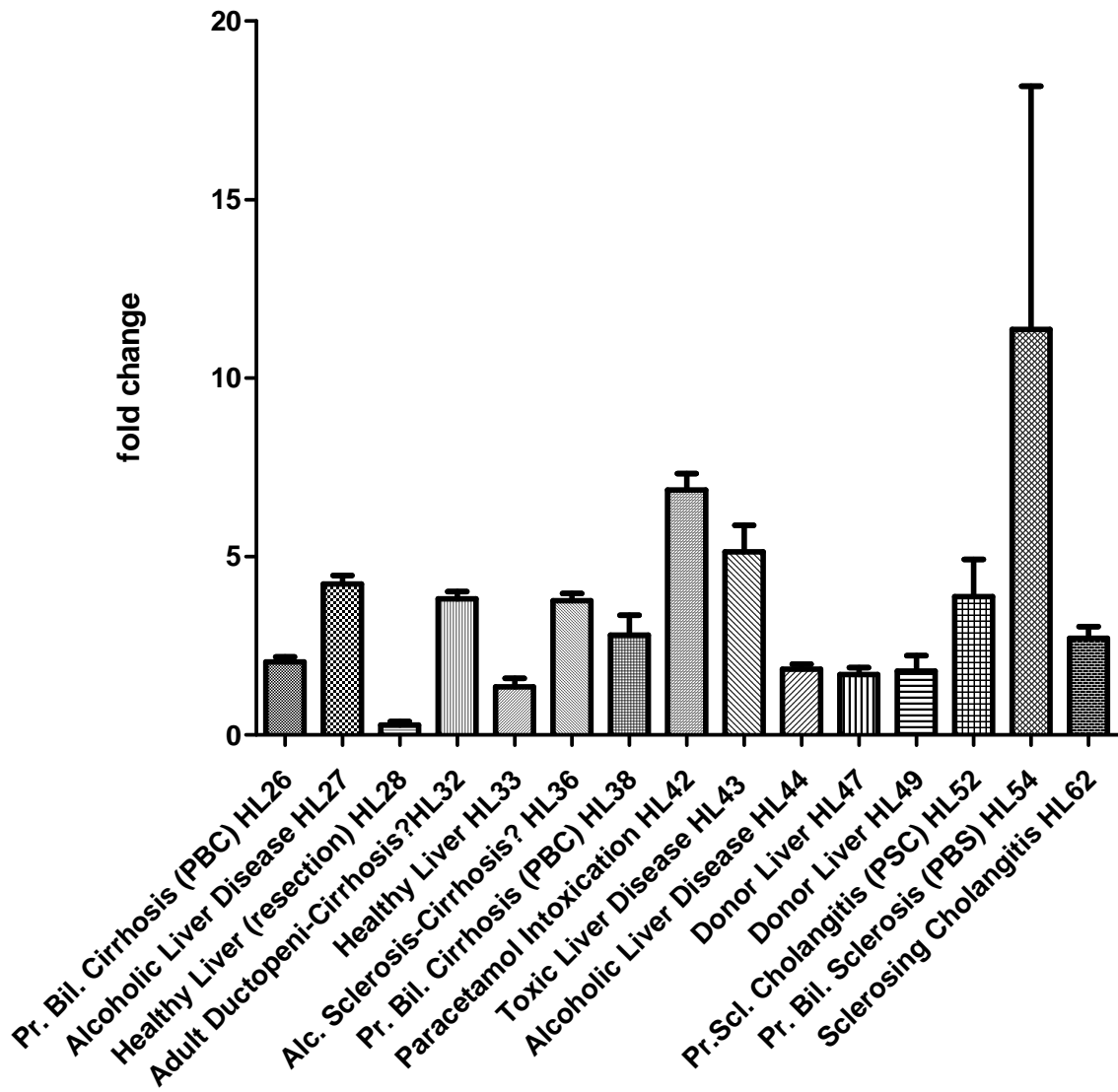
Regression Analysis Correlation between
CK19 and Bex1 in Human livers

Chart 11

Pearson
r = 0,7364
r^2 = 0,5423
P < 0,0017
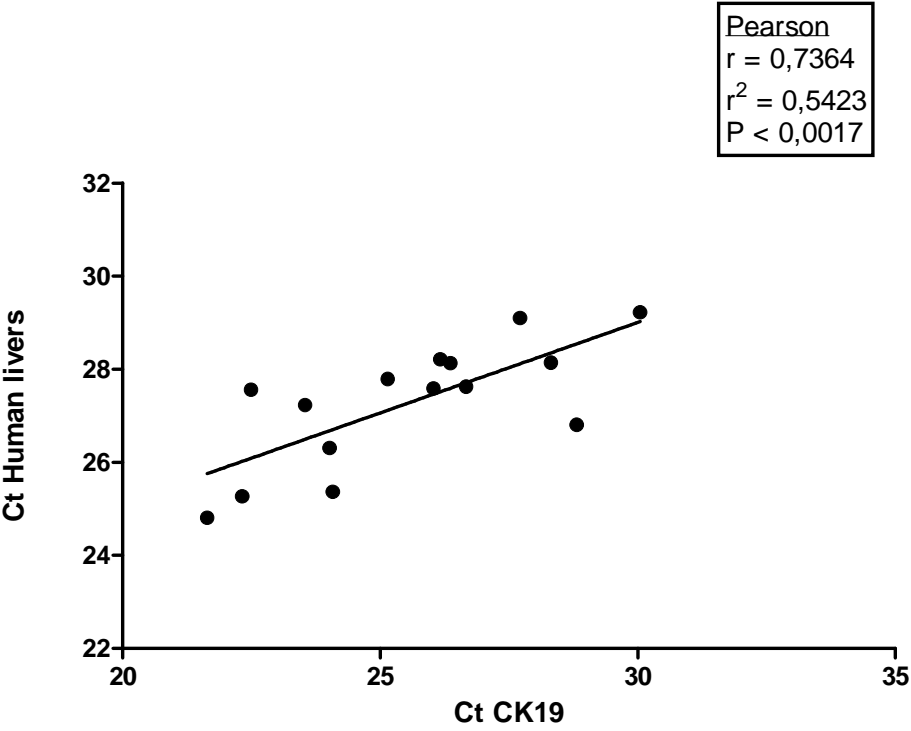
**Regression Analysis Correlation between
CK19 and Bex2 in Human livers**

Chart 12

Pearson
r = 0,5593
r^2 = 0,3129
P < 0,0302
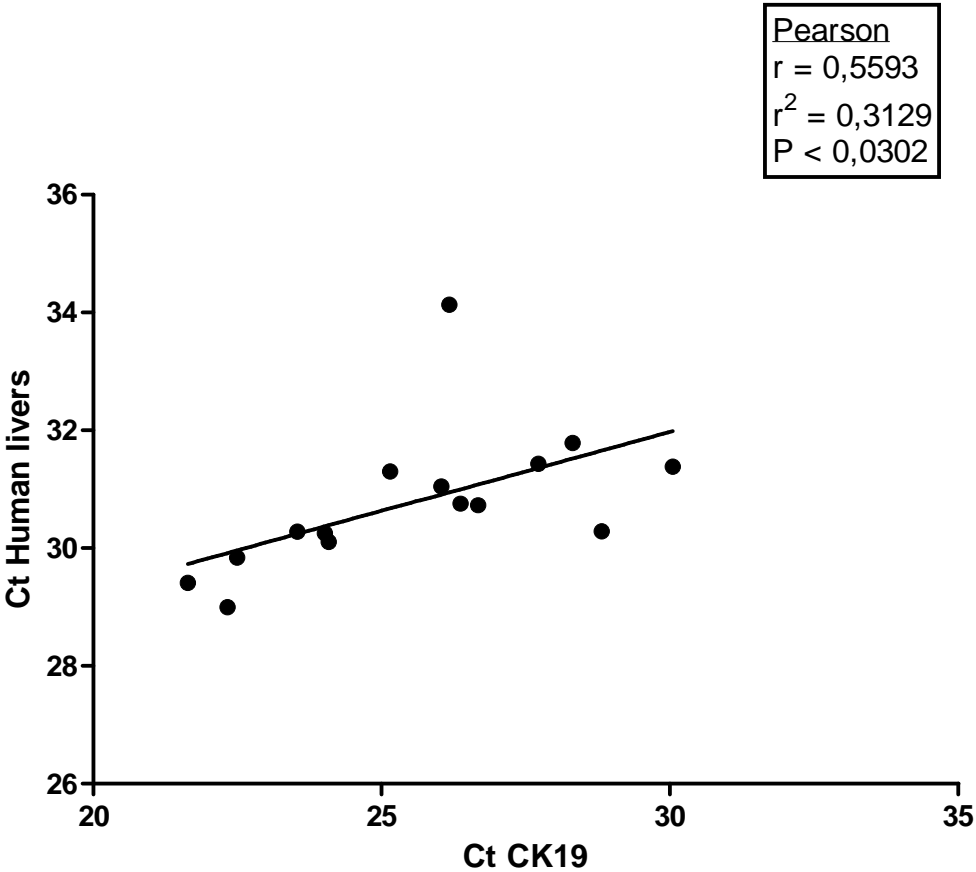
**Regression Analysis Correlation
between Bex1 and Bex2**

Chart 13

Pearson
r = 0,6820
r^2 = 0,4652
P < 0,0051
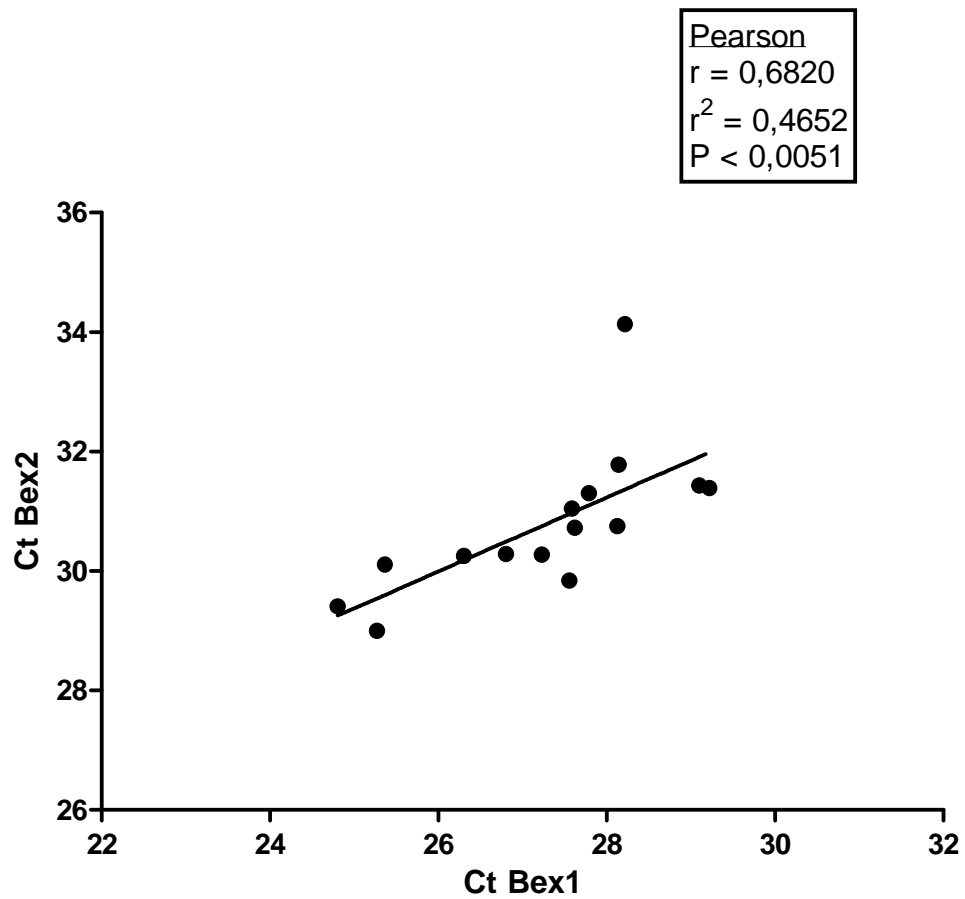
Normalization of Bex1 with Bex2

Chart 14
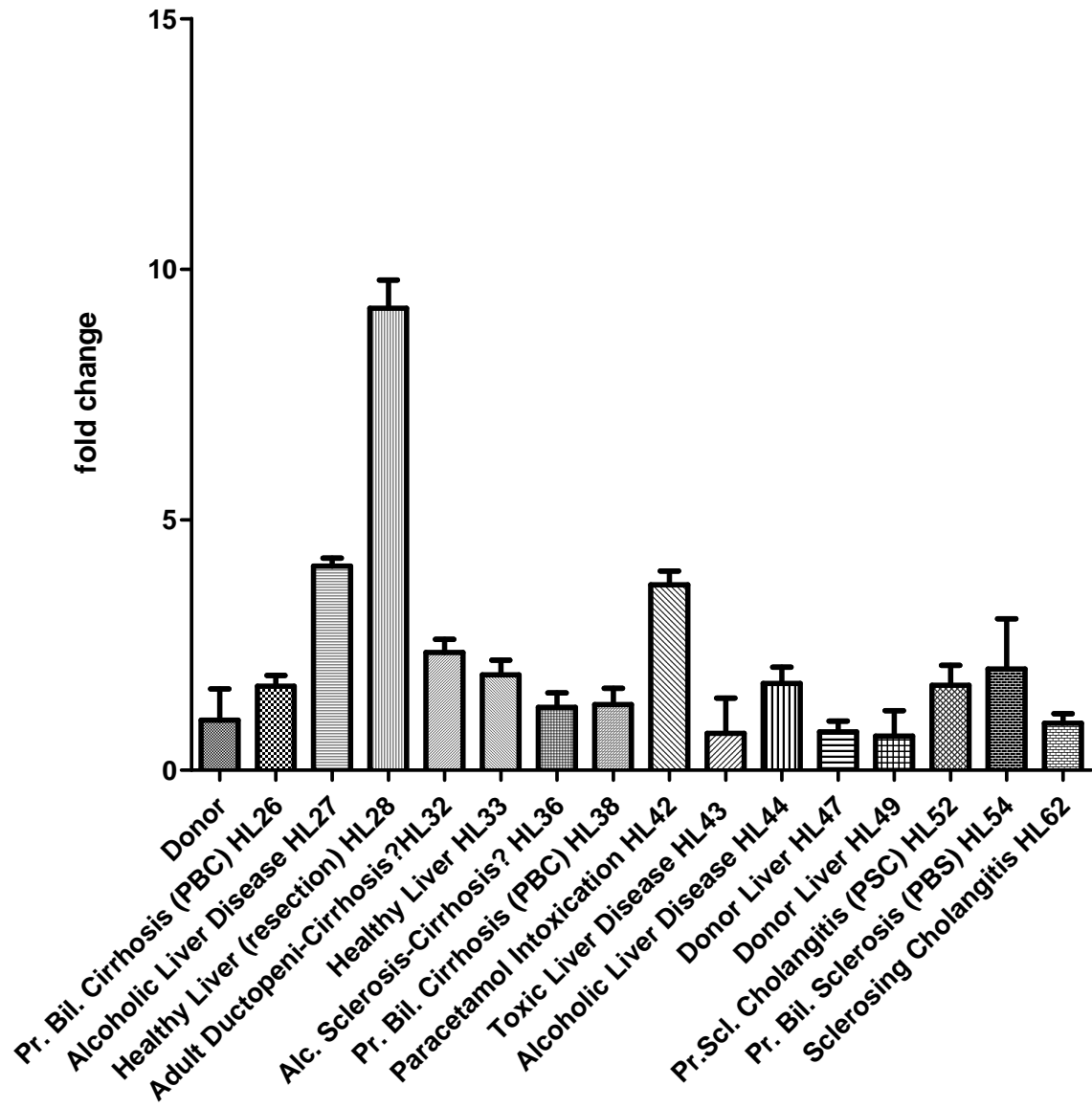
3.8 Antibody Optimization Results

Results Dilution 1:3000:

Table 13

		Bex1
Donor	Heh 9891/05	Good
	Heh 1293/05	Nothing
	Heh 5841/05	Good
	Heh 5927/05	Nothing
PBC	Heh 97-769	Nothing
	Heh 05-8427	Good
	Heh 96-4131	Nothing
	Heh 96-9136	Nothing
PSC	Heh 96-7246	Nothing
	Heh 01-5050	Nothing
	Heh 00-1574	Nothing
	Heh 01-4389	No so good
LDO	Heh 01-9799	Nothing
	Heh 01-8812	Nothing
	Heh 01-10385	Nothing
	Heh 01-7957	Nothing
St.Hep.	Heh 05-11093	Nothing
	Heh 05-9836	Nothing
	Heh 04-10412	Nothing
	Heh 04-12676	Good
Toxic	Heh 98-15474	Good
	Heh 98-6307	Nothing
	Heh 04-1873	Nothing
	Heh 00-3800	Good

Results Dilution 1:1500:

Table 14

		Bex1	**CK19**
Donor	Heh 3318/04	Ok, but not very strong (mediocre)	Ok, but not very strong
	Heh 13988/05	The best	Works very well and strong
	Heh 03-4081	Works very well	Works very well
	Heh 03-10562	Not very good (small tissue)	Not very good (small tissue)
	Heh 03-3979	No	No
	Heh 03-3372	Good (low background)	Good
	Heh 02-10939	Not very good	Not very good
	Heh 9842/05	Good (much background)	Good
	Heh 1763/04	No	No
	Heh 04-11788	Good (much background)	Good
Toxic	Heh 97-10915	Ok, much background	Ok
	Heh 00-3800	No so good, much background	Ok
	Heh 98-6307	No	No
	Heh 04-1873	No	No
PBC	Heh 98-9178	Maybe, much background	Ok
	Heh 98-15479	Ok, much background	Ok
	Heh 96-8703	Ok, much background	Ok
	Heh 99-4107	Ok, much background	Ok
St.Hep.	Heh 05-2939	Ok, much background	Ok
	Heh 04-3811	Ok, much background	Ok
	Heh 05-34	Maybe, much background	Ok
	Heh 05-1535	Ok, much background	Ok
LDO	Heh 03-5226	Ok, much background	Ok
	Heh 03-9034	Ok, much background	Ok
	Heh 03-3935	No	No
	Heh 04-3327	Maybe	Ok

PSC	Heh 00-1574	Ok	Ok
	Heh 02-4674	Ok, nice	Ok
	Heh 02-338	Ok, nice	Ok
	Heh 04-3948	Ok, nice but much background	Ok

Dilution:

For **Bex1**: 1:1500

                1:15000

                1:50000

                1:100000

                1:150000

For **CK19**: 1:50

                1:100

Table 15

Bex1 1:1500	Ok ,not much background
Bex1 1:15000	Ok
Bex1 1:50000	Ok, a bit light
Bex1 1:100000	OK, but very light
Bex1 1:150000	No
CK19 1:50	Ok, perfect
CK19 1:100	Ok

The following pictures shows the results reported in the previous table with four different magnifications.

Fig.22

1:100000

1:50000

1:15000

1:1500

HL49 BEX1 10x pH9 28-06-2011

HL49 BEX1 20x pH9 28-06-2011
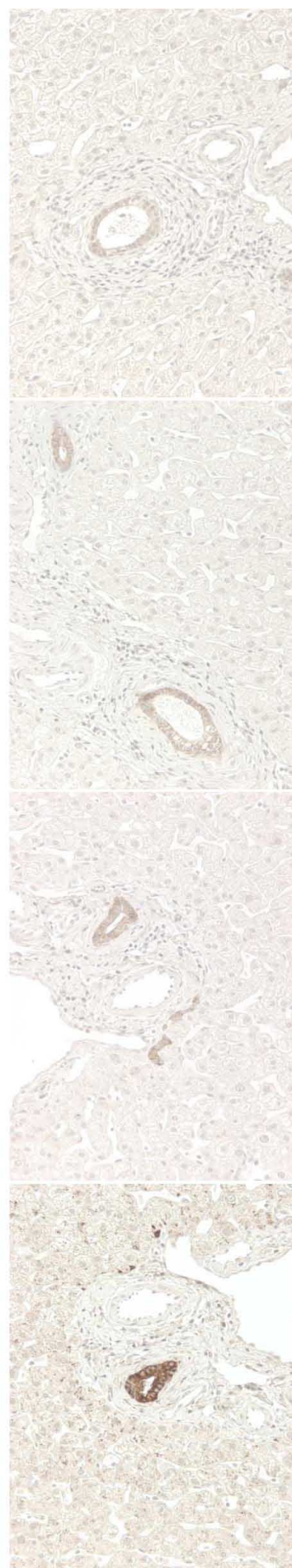
1:100000   1:50000   1:15000   1:1500

HL49 BEX1 40x pH9 28-06-2011
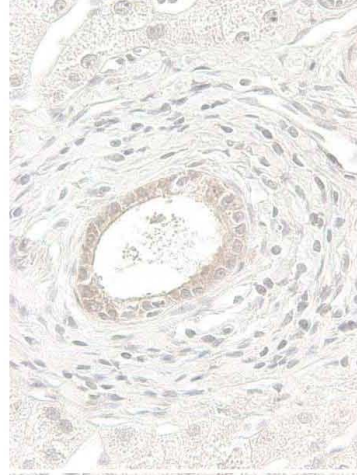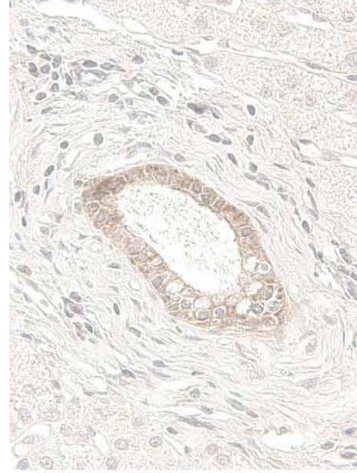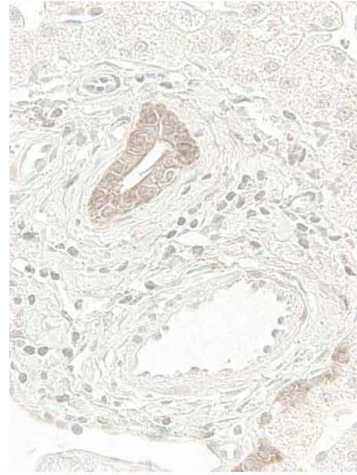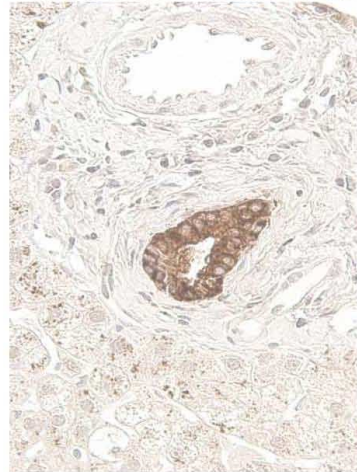
HL49 BEX1 63x pH9 28-06-2011

Fig.23

HL49 CK19 20x pH9 28-06-2011

1:100

1:50

HL49 CK19 63x pH9 28-06-2011

HL49 CK19 10x pH9 28-06-2011

1:100

1:50

HL49 CK19 40x pH9 28-06-2011
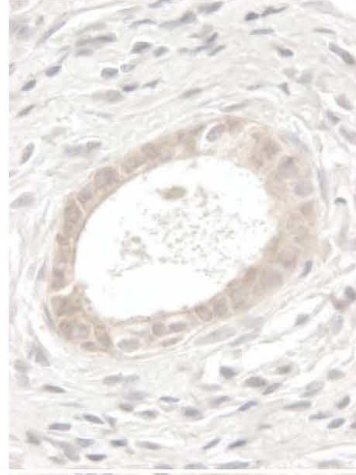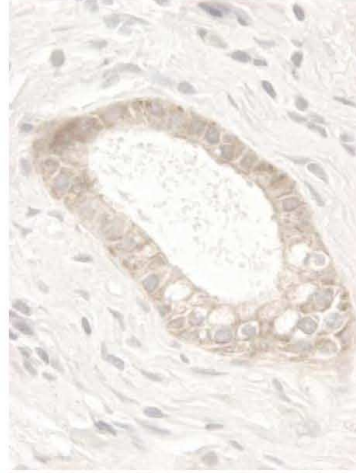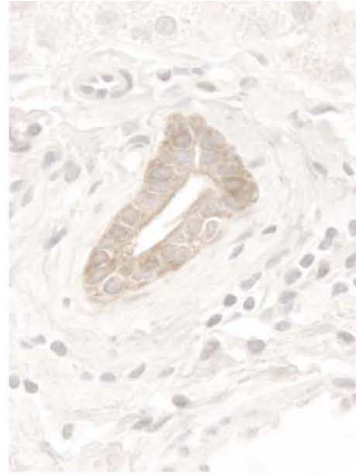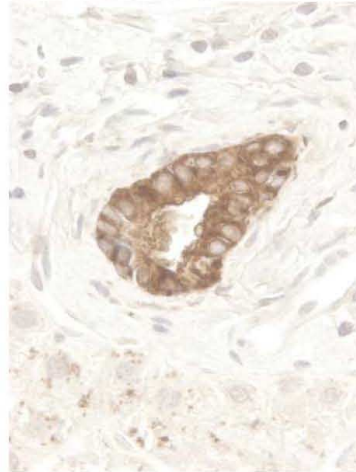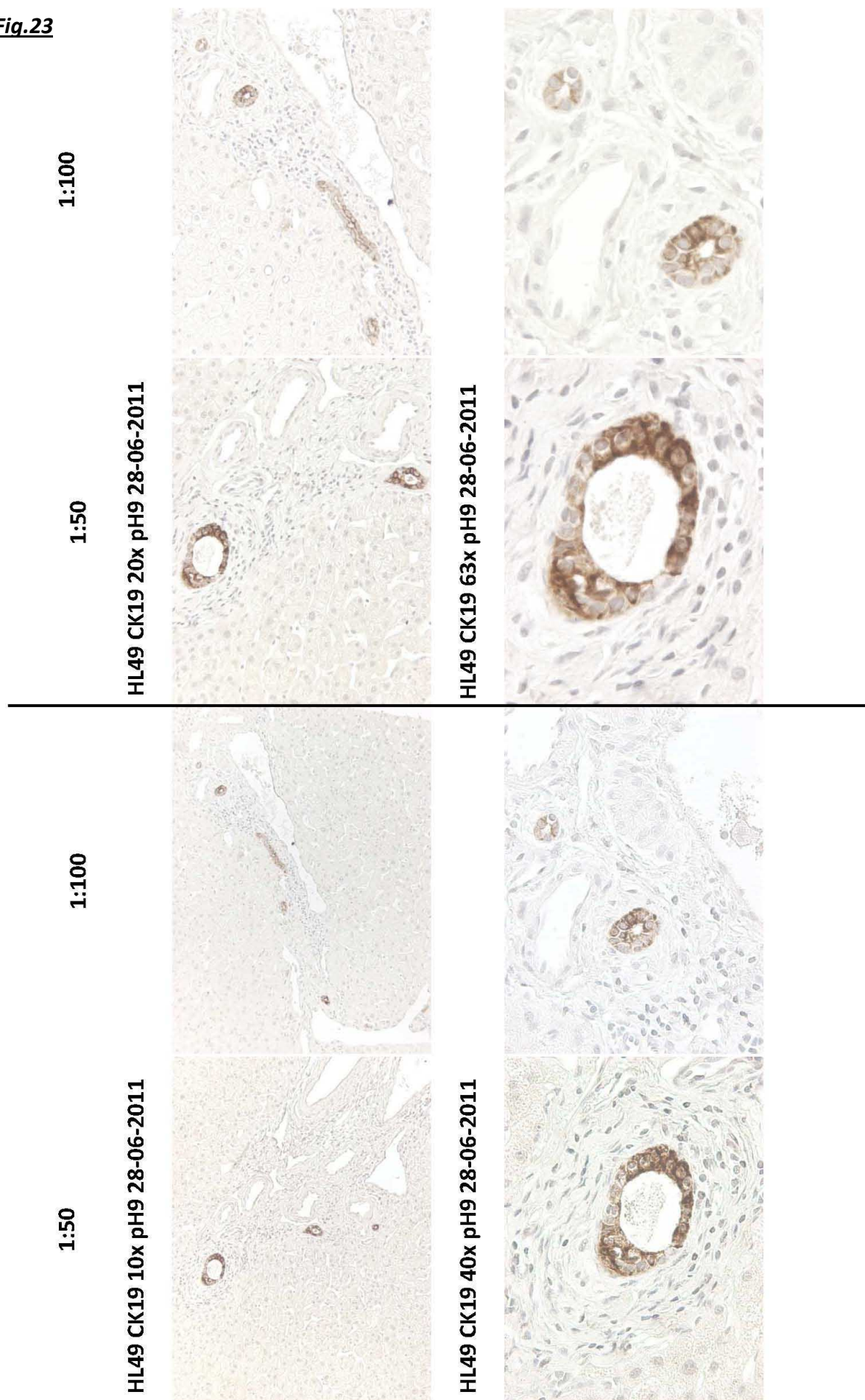
3.9 Bex1 and CK19 Detection Results
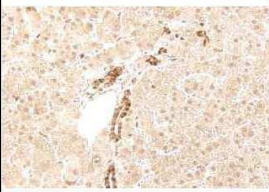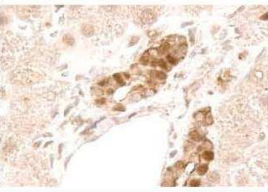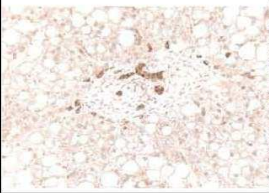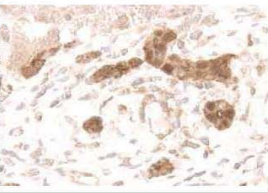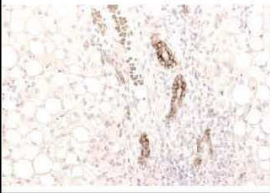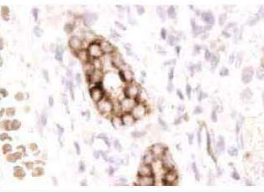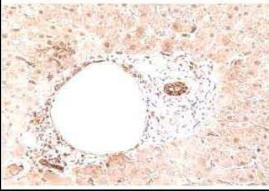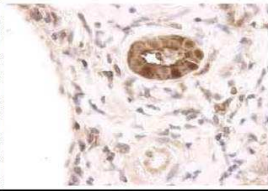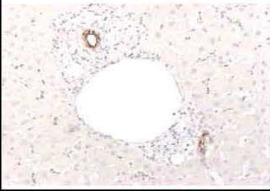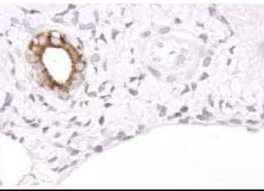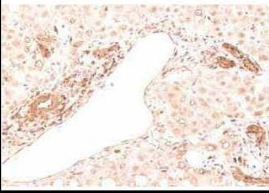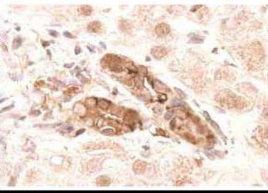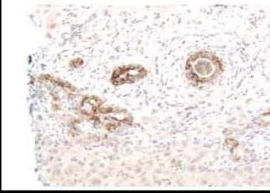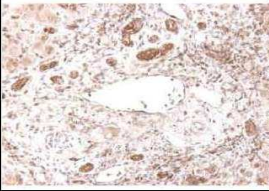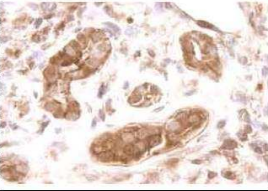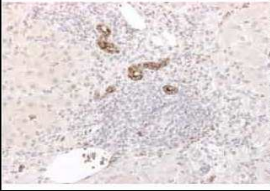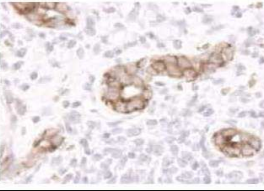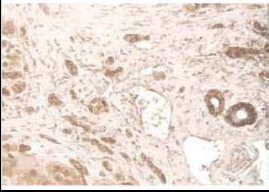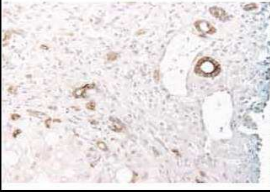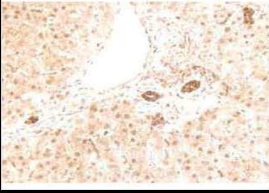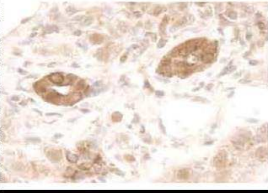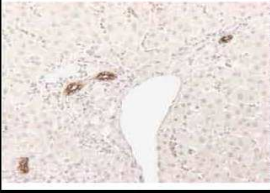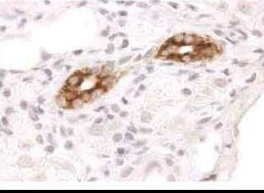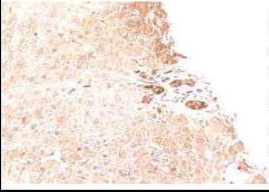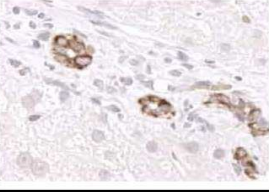
Table 16

		Bex1	**CK19**
HCV	Heh 4901-05	No well	
	Heh 2198-05	No well	
	Heh 1353-05	Ok	Ok
	Heh 6646-05	Ok	Ok
	Heh 3971-05	Ok	Ok
	Heh 11675-05	Ok	Ok
	Heh 9219-05	Ok	Ok
	Heh 14295-05	No well	
	Heh 5918-05	Ok	
HBV	Heh 05-4436	No well	Ok
	Heh 98-3916	No	
	Heh 05-6097	Ok	Ok
	Heh 05-8210	Ok	Ok
	Heh 05-3836	No well	
	Heh 05-2491	Ok	Ok
	Heh 05-2990	No well	
	Heh 00-9555	Ok, much background	
	Heh 00-5451	Ok	Ok
	Heh 01-10245	No	
	Heh 05-11595	Ok	
LDO	Heh 05-7717	Ok	Ok
	Heh 05-13288	Ok	Ok
	Heh 04-3167	Ok	Ok
	Heh 05-7718	No well	Ok
	Heh 03-4558	No	
	Heh 01-2678	No well	Ok

PBC	Heh 97-769	Ok, much background	Ok
	Heh 96-4131	No	
	Heh 05-8427	Ok, much background	
	Heh 03-8518	Ok	Ok
	Heh 04-11276	Ok	Ok
	Heh 99-17753	No well	
Toxic	Heh 98-15474	Ok	Ok
	HL 42 (1)	Ok, much background	
	HL 42 (2)	Ok	
	HL42 (15)		Ok
St.Hep.	Heh 04-10412	Ok, much background	Ok
	Heh 04-8383	Ok	Ok
PSC	Heh 05-3487	Ok	Ok
	Heh 01-5050	Ok	Ok

The following table shows a section for each liver disease with two different magnifications.

Table 17

	Bex1		CK19	
	20x	63x	20x	63x
Donor				
HCV				
HBV				
LDO				
PBC				
St.hep				
Scl Ch				
Toxic				

3.10 Bradford Assay Results

Table 18

595 nm

μg/ml	Standard	Standard	Standard	Standard average		Standard average - blank
20	0,748	0,800	0,789	0,779	20	0,406
10	0,669	0,698	0,700	0,689	10	0,316
5,0	0,588	0,631	0,587	0,602	5,0	0,229
2,5	0,525	0,511	0,606	0,547	2,5	0,174
1,0	0,451	0,446	0,483	0,460	1,0	0,087
0,0	0,361	0,386		0,374	0,0	0,000

Linear regression A=ac+b

a: 0,0181113   b: 0,085425

min: 0,000   Max: 0,406

Standard curve valid for intervals at:

$y = 0,018x + 0,085$

$R^2 = 0,851$

Absorbance minus blank

	Bex1	Bex1	Bex1	Control	Control	Control
1:100	0,405	0,341	0,360	0,490	0,305	0,322
1:100	0,352	0,372	0,431	0,392	0,439	0,373
1:100	0,378	0,394	0,360	0,423	0,244	0,295
1:300	0,213	0,209	0,174	0,231	0,158	0,187
1:300	0,198	0,230	0,149	0,191	0,163	0,189
1:300	0,242	0,273	0,141	0,219	0,128	0,180
1:1000	0,089	0,117	0,041	0,069	0,077	0,129
1:1000	0,082	0,134	0,100	0,053	0,122	0,084
1:1000	0,076	0,083	0,066	0,096	0,080	0,097

HaCaT transfected with pre-miRs

	Bex1	Bex1	Bex1	Control	Control	Control
1:100	0,778	0,714	0,733	0,863	0,678	0,695
1:100	0,725	0,745	0,804	0,765	0,812	0,746
1:100	0,751	0,767	0,733	0,796	0,617	0,668
1:300	0,586	0,582	0,547	0,604	0,531	0,560
1:300	0,571	0,603	0,522	0,564	0,536	0,562
1:300	0,615	0,646	0,514	0,592	0,501	0,553
1:1000	0,462	0,490	0,414	0,442	0,450	0,502
1:1000	0,455	0,507	0,473	0,426	0,495	0,457
1:1000	0,449	0,456	0,439	0,469	0,453	0,470

	Bex1	Bex1	Bex1	Control	Control	Control	
1:100	0,378	0,369	0,383	0,435	0,329	0,330	
1:300	0,217	0,237	0,154	0,213	0,149	0,185	
1:1000	0,082	0,111	0,069	0,072	0,093	0,103	
1:100	1,61	1,56	1,64	1,93	1,34	1,32	Prot. conc. mg/ml
1:300	2,18	2,51	1,14	2,12	1,06	1,65	Prot. conc. mg/ml
1:1000	-0,20	1,40	-0,93	-0,73	0,39	0,96	Prot. conc. mg/ml

	Bex1	Bex1	Bex1	Control	Control	Control	
	1,20	1,82	0,62	1,10	0,93	1,32	Average conc. mg/ml

3.11 Western Blot Result

Fig.24
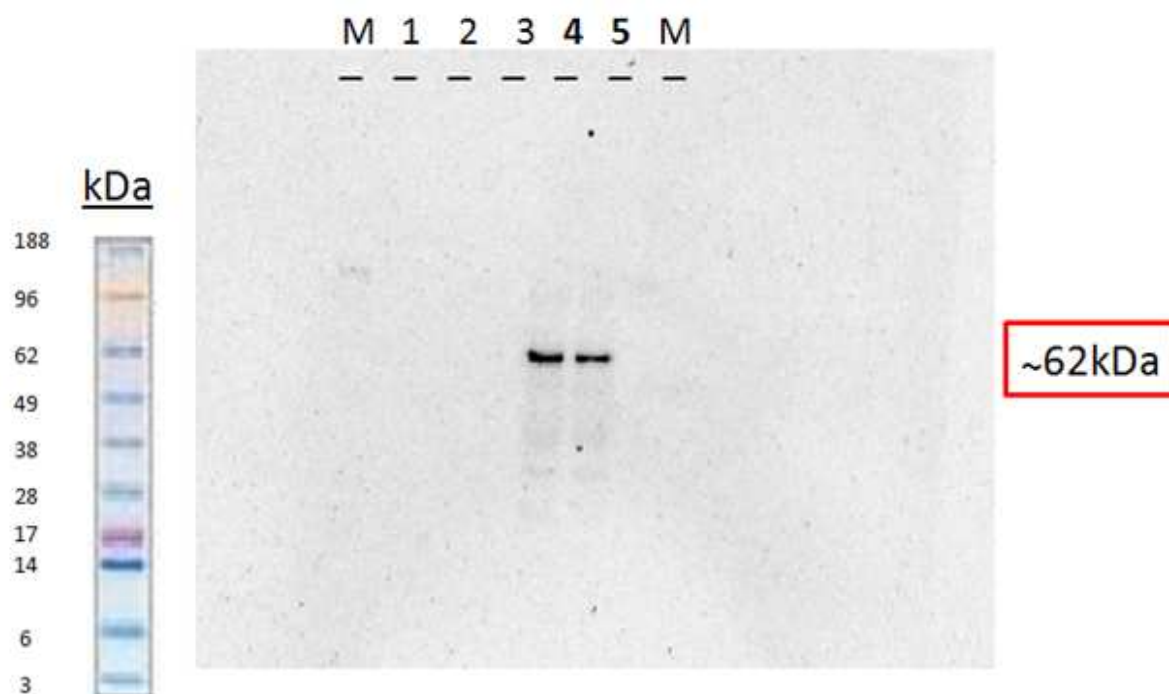
Loaded 12µg of the samples on to the gel.

M: SeeBlue plus pre-stained Standard Marker(LC5925).

1 - 2 - 3: Water.

4: Control (number 3 in Bradford assay, concentration 1,32mg/ml).

5: Bex1(number 2 in Bradford assay, concentration 1,82mg/ml).

4 DISCUSSION

The first aim of this project was to understand if Bex1 and Bex2 are present in healthy and pathological liver tissues and to estimate their levels. Before beginning the Real-Time PCR, we used the Nanodrop technique to evaluate the concentration of RNA in our samples and than we determined the integrity or RNA by the Agilent 2100 Bioanalyzer. In **Fig.21** we can see the electrophoresis of our samples and in **Chart 1** the electropherograms, they show good peaks at 18S and 28S and a RNA Integrity Number (RIN) around. These results prove a good quality of our RNAs that are suitable for the Real Time PCR.

We started with a pilot Real Time PCR on cell lines: WRL68, SK-HEP, HEPG2, Chang, HUH7 and liver tissues: HL28, HL42, HL50 to determine if there is an increase in the levels of Bex1 and Bex2. In **Table 1** and **Table 2** we can see a high level of Bex1 and Bex2 in hepatocellular carcinoma cell lines respect to normal cell and also in pathological liver tissues respect to normal tissues.

After these observations we performed a Real Time PCR on HL42 to determine the Dilution Curves for Bex1 and Bex2. In **Chart 5** and **Chart 6** are shown the Dilution Curves: for Bex1 curve we have m = -3,337 and R^2 = 0,989, for Bex2 curve we have m = -3,317 and R^2 = 0,997. So we have two good m values, very close to   -3,32, that is the value for 100% efficiency of reaction. We also have two good R^2 values, the highest value being 0,999. The R^2 is the correlation coefficient and reflects the linearity of standard curve,.

After this, we performed a Real Time PCR on 15 different liver tissues: HL47, HL49, HL28, HL33 (healthy tissues); HL26, HL27, HL32, HL36, HL38, HL42, HL43, HL44, HL52, HL54, HL62 (pathological tissues). It is very important to notice that in our project we were unable to use a housekeeping gene as endogenous control, because all transcripts currently investigated including GAPDH, actin, TBP, s18 fluctuate during liver regeneration and liver disease. In **Table 8** and **Table 9** the Ct values of Bex1 and Bex2 are reported; in **Table 10** and **Table 11** are shown all the calculations for the Fold Change of Bex1 and Bex2; in **Chart 7**, **Chart 8**, **Chart 9** and **Chart 10** there are the graphical representations of the results obtained by the GraphPad Prism program. An increase of Bex1 can be observed in all pathological liver tissue samples respect to normal tissues; the highest levels are seen for HL54 Primary Biliary Sclerosis

(PBS), HL27 Alcoholic Liver Disease, HL42 Paracetamol Intoxication. Instead the Ct values for Bex2 do not change significantly in the different diseases and also in normal tissues; for this reason we decided to focalize our attention only on Bex1. We also tried to use Bex2 to normalize the results of Bex1, calculations and representation are visible in **Table 12** and **Chart 14**.

The second aim of the project was the immunodetection of Bex1 in healthy and pathological liver tissues. We began with a antibody optimization to determine the best antibody to detect Bex1 with the least possible background.

We decided to use an immunodetection procedure based on Diaminobenzidine (DAB) as chromogen. We started using Bex1 antibody of Abcam (#ab69032) with a dilution of 1:100 on HL42 tissue, but the antibody did not result specific, likely because the dilution was very low. Then, we changed antibody and we used the antibody of Margolis Lab with two dilution of 1:1000 and 1:3000, the first one showed much background, the results of the second dilution are shown in **Table 13**, but they were no so satisfactory and for this reason we decided to change dilution to 1:1500 and determine in the same tissue the presence of CK19 (dilution 1:50), which is a bile duct marker, to understand if the non-presence of Bex1 was attributable to the conservation of samples. The results in **Table 14** show the simultaneous presence or absence of CK19 and Bex1, this proves that the absence of Bex1 was attributable to bad tissue preservation in 4% formaldehyde. For a better optimization we tried five different dilution for Bex1: 1:1500, 1:15000, 1:50000, 1:100000, 1:150000 and two for CK19: 1:50, 1:100. The results in **Table 15**, **Fig.22** and **Fig.23** show that the best dilution for Bex1 is 1:1500 and for CK19 is 1:50. [The possibility to dilute the signal out suggesting that it is a specific reaction (not due to the secondary antibody)].

Over the correct dilution we tried to find the best protocol for an optimal immunohistochemistry. So we tried to boiled the slides with different antigen retrieval buffers: citrate, pH 6, high pH and pH 9 for 10 and 10+10 min; we obtained the best performance with pH 9 buffer for 10+10min. We also decided for an incubation with primary antibody in a moisture chamber at 4°C overnight and for a counterstain in Mayers haematoxylin for 15min.

After obtaining the correct dilutions with the correct protocol, we applied these to all tissues as shown the **Table 16** and **Table 17.** The samples underlined in **Table**

16 and **Table 17** are the best five slides for each disease (only 3 slides for Toxic Hepatitis, because we did not have enough samples) of which we took pictures with the microscope with four different magnifications (10x, 20x, 40x, 63x), using Leica Application Suite – Imaging Software.

We also tried immunofluorescence on frozen sections to detect CK7 and Bex1, but both antibodies for Bex1 (Abcam and Margolis Lab) gave poor results, and for this reason we decided to abandon this technique.

The last step was the silencing of Bex1, with Dharmacon® Accell® siRNA on HuH7 cell line, to investigate the role of our protein in tumor cells and the pathway in which it participates. We decided to use this tecnology because it is independent from viral vectors or lipid-based transfection reagents, it can be employed without significant effects on cell physiology, it provides delivery into difficult-to-transfect cell types and gives a long term gene silencing.

Huh7 cells were grown in tissue culture medium DMEM + GlutaMAX (450ml), 10% FBS (50ml), Gentamicin (2.5ml). Than we transfected part of the cells with siRNA Bex1 SMART Accell, while control cultures not transfected were maintained as control. After transfection we used as a growth mediun a mixture of Accell siRNA and Accell delivery medium, to allow a long term silencing.

After incubation at 37℃ with 5% CO_2 for 72 hours, cells were silenced, harvested, and the protein concentration was determined by theBradford assay at an absorbance of 595nm. **Table 18** shows the concentration of Bex1 in control and silenced samples.

Thereafter, we performed Western Blot to evaluate the level of the silencing. We loaded in well 4 the control with the concentration of 1,32 mg/ml and in well 5 the silenced sample with the concentration of 1,82 mg/ml; we used for the immunodetection the Bex1 antibody of MargolisLab, 1:20000 WB. The result in **Fig.24** shows a clear silencing, because the band in 4 is darker than in 5; but while the bands are found at ~62 kDa, Bex1 was expected at ~23 kDa.

5 CONCLUSIONS

The results of Real Time PCR show that there is an up regulation of Bex1 during liver regeneration in all liver diseases compared to donor liver; instead the concentration of Bex2 remains more or less the same, so we decided to focus our attention only on Bex1. The most significant increase of Bex1 can be seen for: Primary Biliary Sclerosis (PBS), Alcoholic Liver Disease and Paracetamol Intoxication.

These findings open interesting possibilities for exploring Bex1 function in the control of liver regeneration, the same role that has been already described in the regeneration of axon and skeletal muscle (Koo *et al.*, 2005; Khazaei *et al.*, 2010).

Indeed immunohistochemistry studies showed that Bex1 is mostly present in the bile ducts, and in diseased liver tissues we can found the presence of Bex1 also in reactive ductular cells (RDCs) and hepatic progenitor cells (HPC). This confirmed the hypothesis that the up regolation of Bex1 has a role during liver regeneration after tissue damage.

The knock down of Bex1 in Huh7 cell line with Dharmacon® Accell® siRNA yelded unclears result: a clear reduction of our protein was seen as compared to controls, but we expected Bex1 at ~ 23kDa, while the immunoreactive band was found at ~ 62kDa. Further experiments are needed to understand if the antibody recognizes an isoform of Bex in the cell line, or the protein have not been reduced sufficiently, or modifications of the protein are involved.

For the future my aim is to examine the function of Bex1 as tumor suppressor in hepatocellular carcinoma, in line with its role as tumor suppressor in malignat glioma. Bex1 might play an important role in a novel signaling pathway regulating apoptosis in hepatic cancer. Bex1 is already known for being an adapter molecule involved in p75NTR/NGFR signaling, with a role in cell cycle progression and neuronal differentiation; the generation of Bex1 knock out mice migh help understanding its precise role, and in particular its role in liver regeneration.

REFERENCES

1. **Alvarez E**, Zhou W, Witta SE, Freed CR.
    Gene. 2005 Aug 29;357(1):18-28.
    Characterization of the Bex gene family in humans, mice, and rats.

2. **Bernstein SL**, Koo JH, Slater BJ, Guo Y, Margolis FL.
    Mol Vis. 2006 Mar 1;12:147-55.
    Analysis of optic nerve stroke by retinal Bex expression.

3. **Brown AL**, Kay GF.
    Hum Mol Genet. 1999 Apr;8(4):611-9. Erratum in: Hum Mol Genet 1999 May;8(5):943.
    Bex1, a gene with increased expression in parthenogenetic embryos, is a member of a novel gene family on the mouse X chromosome.

4. **Chaisson ML**, Brooling JT, Ladiges W, Tsai S, Fausto N.
    J Clin Invest. 2002 Jul;110(2):193-202.
    Hepatocyte-specific inhibition of NF-kappaB leads to apoptosis after TNF treatment, but not after partial hepatectomy.

5. **Ding K**, Su Y, Pang L, Lu Q, Wang Z, Zhang S, Zheng S, Mao J, Zhu Y.
    Carcinogenesis. 2009 Jan;30(1):35-42. Epub 2008 Nov 21.
    Inhibition of apoptosis by downregulation of hBex1, a novel mechanism, contributes to the chemoresistance of Bcr/Abl+ leukemic cells.

6. **Drozdov I**, Svejda B, Gustafsson BI, Mane S, Pfragner R, Kidd M, Modlin IM.
    PLoS One. 2011;6(8):e22457. Epub 2011 Aug 11.
    Gene network inference and biochemical assessment delineates GPCR pathways and CREB targets in small intestinal neuroendocrine neoplasia.

7. **Foltz G**, Ryu GY, Yoon JG, Nelson T, Fahey J, Frakes A, Lee H, Field L, Zander K, Sibenaller Z, Ryken TC, Vibhakar R, Hood L, Madan A.
Cancer Res. 2006 Jul 1;66(13):6665-74.
Genome-wide analysis of epigenetic silencing identifies BEX1 and BEX2 as candidate tumor suppressor genes in malignant glioma.

8. **Khazaei MR**, Halfter H, Karimzadeh F, Koo JH, Margolis FL, Young P.
J Neurochem. 2010 Nov;115(4):910-20. doi: 10.1111/j.1471-4159.2010.06960.x. Epub 2010 Sep 28.
Bex1 is involved in the regeneration of axons after injury.

9. **Koo JH**, Gill S, Pannell LK, Menco BP, Margolis JW, Margolis FL.
J Neurochem. 2004 Jul;90(1):102-16.
The interaction of Bex and OMP reveals a dimer of OMP with a short half-life.

10. **Koo JH**, Saraswati M, Margolis FL.
J Comp Neurol. 2005 Jun 20;487(1):1-14.
Immunolocalization of Bex protein in the mouse brain and olfactory system.

11. **Koo JH**, Smiley MA, Lovering RM, Margolis FL.
Biochem Biophys Res Commun. 2007 Nov 16;363(2):405-10. Epub 2007 Sep 11.
Bex1 knock out mice show altered skeletal muscle regeneration.

12. **Naderi A**, Teschendorff AE, Beigel J, Cariati M, Ellis IO, Brenton JD, Caldas C.
Cancer Res. 2007 Jul 15;67(14):6725-36.
BEX2 is overexpressed in a subset of primary breast cancers and mediates nerve growth factor/nuclear factor-kappaB inhibition of apoptosis in breast cancer cell lines.

13. **Naderi A**, Liu J, Bennett IC.

    Int J Cancer. 2010 Apr 1;126(7):1596-610.

    BEX2 regulates mitochondrial apoptosis and G1 cell cycle in breast cancer.

14. **Naderi A**, Liu J, Hughes-Davies L.

    Mol Cancer. 2010 May 19;9:111.

    BEX2 has a functional interplay with c-Jun/JNK and p65/RelA in breast cancer.

15. **Naderi A**, Liu J, Francis GD.

    Int J Cancer. 2012 Jan 1;130(1):71-82. doi: 10.1002/ijc.25977. Epub 2011 Apr 20.

    A feedback loop between BEX2 and ErbB2 mediated by c-Jun signaling in breast cancer.

16. **Quentmeier H**, Tonelli R, Geffers R, Pession A, Uphoff CC, Drexler HG.

    Leukemia. 2005 Aug;19(8):1488-9. No abstract available.

    Expression of BEX1 in acute myeloid leukemia with MLL rearrangements.

17. **Riehle KJ**, Dan YY, Campbell JS, Fausto N.

    J Gastroenterol Hepatol. 2011 Jan;26 Suppl 1:203-12. doi: 10.1111/j.1440-1746.2010.06539.x. Erratum in: J Gastroenterol Hepatol. 2011 Jul;26(7):1218.

    New concepts in liver regeneration.

18. **Röhrs S**, Dirks WG, Meyer C, Marschalek R, Scherr M, Slany R, Wallace A, Drexler HG, Quentmeier H.

    Mol Cancer. 2009 Oct 16;8:86.

    Hypomethylation and expression of BEX2, IGSF4 and TIMP3 indicative of MLL translocations in acute myeloid leukemia.

19. **Sánchez A**, Factor VM, Schroeder IS, Nagy P, Thorgeirsson SS.
    Hepatology. 2004 Feb;39(2):376-85.
    Activation of NF-kappaB and STAT3 in rat oval cells during 2-acetylaminofluorene/partial hepatectomy-induced liver regeneration.

20. **Si-Tayeb K**, Lemaigre FP, Duncan SA.
    Dev Cell. 2010 Feb 16;18(2):175-89. Review.
    Organogenesis and development of the liver.

21. **Subrata LS**, Lowes KN, Olynyk JK, Yeoh GC, Quail EA, Abraham LJ.
    Liver Int. 2005 Jun;25(3):633-46.
    Hepatic expression of the tumor necrosis factor family member lymphotoxin-beta is regulated by interleukin (IL)-6 and IL-1beta: transcriptional control mechanisms in oval cells and hepatoma cell lines.

22. **Vilar M**, Murillo-Carretero M, Mira H, Magnusson K, Besset V, Ibáñez CF.
    EMBO J. 2006 Mar 22;25(6):1219-30. Epub 2006 Feb 23.
    Bex1, a novel interactor of the p75 neurotrophin receptor, links neurotrophin signaling to the cell cycle.

23. **Yano Y**, Hayashi Y, Teramoto T, Nakaji M, Nagy P, Ninomiya T, Wada A, Hirai M, Kim SR, Seo Y, Yoon S, Kasuga M.
    J Gastroenterol Hepatol. 2004 Aug;19(8):866-72.
    Apoptotic pathway related to oval cell proliferation.

24. **Zhang L.**
    Biochem Genet. 2008 Jun;46(5-6):293-311.
    Adaptive evolution and frequent gene conversion in the brain expressed X-linked gene family in mammals.

Figure Legends

Fig.1 (Top) The exon–intron gene structure and the chromosomal arrangement of the Bex genes on chromosome X in human. (Bottom) The model of gene conversion explaining the pattern of sequence evolution in Bex. The brackets indicate the portions of Bex involved in gene conversion, and the arrows connect the Bex members involved in gene conversion.
Reference 24

Fig.2 Phylogenetic tree of the human (h), rat (r), and mouse (m) Bex genes.
Reference 1

Fig.3 Eukaryotic Cell
http://vvbiology2.wikispaces.com/Eukaryote

Fig.4 Olfactory marker protein
http://www.antibodies-online.com/antibody/350658/anti-Olfactory+Marker+Protein+OMP/

Fig.5 Binding of nerve growth factor
http://www.nature.com/nrn/journal/v9/n12/fig_tab/nrn2516_F3.html

Fig.6 Cell Cycle
http://www.bdbiosciences.com/research/apoptosis/analysis/index.jsp

Fig.7 Skeletal Muscle Regeneration
http://aohs.web2designer.org/muscle-cell-anatomy

Fig.8 Calmodulin (CaM)
http://zh.wikipedia.org/wiki/File:Calmodulin-Ca.png

Fig.9 Motor Neuron (MN)
http://home.comcast.net/~pegglestoncbsd/brain%20and%20NS.htm

Fig.10 Bex1 expression in axons. MNs from E13-14 mouse embryos were fixed at 3 days in vitro (DIV) and stained with antibodies specific for Bex1 (green), MAP2 (red) and the Tau-1 antibody (blue). The scale bar is 40 µm.

Reference 8

Fig.11 The expression of Bex1 protein, the tissue sections from lumbar-spinal cord of MPZ-KO and MAG-KO mice and mice subjected to sciatic-nerve crush-injury or demyelination were stained with anti Bex1 (green) and anti-non-phosphorylated neurofilament (SMI32; a marker of neurons) (red) antibodies. 4',6-Diamidino-2-phenylindole dihydrochloride hydrate (blue) was used for nuclear staining. Scale bar is 50 µm.

Reference 8

Fig.12 HDAC inhibition

http://www.ifom-ieo-campus.it/research/images/chiocca/fig02.jpg

Fig.13 Overall structure of a portion of a liver

Reference 20

Fig.14 The two levels of liver regeneration

Reference 17

Fig.15 Oval cell proliferation

http://www.medscape.com/viewarticle/463154_3

Fig.16 Protein Bex1 in Donor Liver

My Picture

Fig.17 The direct method of immunohistochemical staining uses one labelled antibody, which binds directly to the antigen being stained for.

http://en.wikipedia.org/wiki/File:Immunohistochemicalstaining1.PNG

Fig.18 The indirect method of immunohistochemical staining uses one antibody against the antigen being probed for, and a second, labelled, antibody against the first.

http://en.wikipedia.org/wiki/File:Immunohistochemicalstaining2.PNG

Fig.19 Experimental workflow for Accell siRNA mediated gene silencing and detection of mRNA knockdown.

http://www.dharmacon.com/uploadedFiles/Home/Support_Center/Application_Notes/gene-silencing-in-sh-sy5y-and-jurkat-cell-lines-using-accell-sirna.pdf

Fig.20 Coomassie Brilliant Blue

http://www.piercenet.com/browse.cfm?fldID=02051005